TECHNO-ECONOMIC EVALUATION OF OFF-GRID HYBRID RENEWABLE ENERGY SYSTEM FOR RURAL RESORT ELECTRIFICATION IN MALAYSIA

MONOWAR HOSSAIN

FACULTY OF ENGINEERING
UNIVERSITY OF MALAYA
KUALA LUMPUR

2017

TECHNO-ECONOMIC EVALUATION OF OFF-GRID HYBRID RENEWABLE ENERGY SYSTEM FOR RURAL RESORT ELECTRIFICATION IN MALAYSIA

MONOWAR HOSSAIN

THIS DISSERTATION IS SUBMITTED IN FULFILLMENT OF THE REQUIREMENTS FOR THE DEGREE OF MASTER OF ENGINEERING SCIENCE

FACULTY OF ENGINEERING
UNIVERSITY OF MALAYA
KUALA LUMPUR

2017

UNIVERSITY OF MALAYA

ORIGINAL LITERARY WORK DECLARATION

Name of Candidate: Monowar Hossain

Matric No: KGA150029

Name of Degree: Master of Engineering Science (M. Eng. Sc)

Title of Dissertation: Techno-economic evaluation of off-grid hybrid renewable energy system for rural resort electrification in Malaysia.

Field of Study: Renewable Energy

I do solemnly and sincerely declare that:

(1) I am the sole author/writer of this Work;
(2) This Work is original;
(3) Any use of any work in which copyright exists was done by way of fair dealing and for permitted purposes and any excerpt or extract from, or reference to or reproduction of any copyright work has been disclosed expressly and sufficiently and the title of the Work, and its authorship have been acknowledged in this Work;
(4) I do not have any actual knowledge nor do I ought reasonably to know that the making of this work constitutes an infringement of any copyright work;
(5) I hereby assign all and every right in the copyright to this Work to the University of Malaya ("UM"), who henceforth shall be an owner of the copyright in this Work and that any reproduction or use in any form or by any means whatsoever is prohibited without the written consent of UM having been first had and obtained;
(6) I am fully aware that if in the course of making this Work, I have infringed any copyright, whether intentionally or otherwise, I may be subject to legal action or any other action as may be determined by UM.

Candidate's Signature Date:

Subscribed and solemnly declared before,

Witness's Signature Date:

Name:

Designation:

ABSTRACT

Energy is considered as a prime driving force for the socio-economic development of a country. Malaysia is one of the developing countries located in Southeast Asia, consisting of two distinct regions namely West Malaysia (Peninsular Malaysia) and East Malaysia (Sabah and Sarawak), divided by the South China Sea, covering an area of 33.27 million hectares. Although the rate of the electrification in urban areas in this country is high, the tourist sites, which are less than 200km^2, located in rural and decentralized islands in the South China Sea, Malaysia (SCSM) mostly depend on diesel generators for 24-hour power supply. The emissions from diesel-based power plants are environmentally risky for tourist spots. Moreover, diesel-based power plants are subjected to many technical and economic problems such as the high operation and maintenance cost, the risk of oil spilling and unpredictable diesel fuel price. Besides the aforementioned problems, an extension of the national electrical grid in these islands is not feasible due to complex terrain.

In this dissertation, a multi-optimal combination of the stand-alone hybrid renewable energy system (HRES) for a large resort center located in Tioman Island in the SCSM has been proposed with detailed techno-economic performance analysis. Hybrid Optimization Model for Electric Renewable (HOMER) software is used for economic and technical analysis of the proposed hybrid renewable energy system. The estimated peak and average load per day for the resort are 1,185 kW and 13,048 kW respectively. Also in this dissertation, novel soft computing methodologies based on the hybrid adaptive neuro-fuzzy inference system (ANFIS) have been developed to predict monthly wind power density for the nearest coastal city of Tioman Island, and then the capability of the proposed hybrid ANFIS models have been examined to extrapolate the wind speed data for Tioman Island as there is no meteorological station in this Island. For these purposes, the standalone ANFIS, ANFIS-PSO (particle swarm optimization),

ANFIS-GA (genetic algorithm) and ANFIS-DE (differential evolution) prediction algorithms have been developed in MATLAB platform.

The best optimized stand-alone hybrid energy system comprises the wind, PV, diesel generator, converter, and the battery. The optimized system resulted in the net present cost (NPC) of $17.15 million, cost of energy (COE) of $0.279/kWh, a renewable fraction (RF) of 41.6%, and CO_2 of 2,571,131 kg/year. Whereas, the diesel only system takes NPC of $21.09 million, COE of $0.343/kWh and CO_2 of 5,432,244 kg/year. The diesel only system has been observed to have the higher NPC, COE and CO_2 emission than the optimized HRES. The designed and analyzed HRES model might be applicable to any tourist locations and decentralized places in the SCSM and around the world with similar climate conditions.

On the other hand, the performance of the proposed hybrid ANFIS models has been determined by computing different statistical parameters such as mean absolute bias error (MABE), mean absolute percentage error (MAPE), root mean square error (RMSE) and coefficient of determination (R^2). The analysis of wind power density prediction result reveals that the ANFIS-PSO and ANFIS-GA enjoy higher performance and accuracy than other models, and they can be recommended for practical application to predict monthly mean wind power density.

ABSTRAK

Tenaga dianggap sebagai penggerak utama untuk pembangunan sosio-ekonomi sesebuah negara. Malaysia adalah salah satu dari negara membangun yang terletak di Asia Tenggara, terdiri daripada dua wilayah berbeza iaitu Malaysia Barat (Semenanjung Malaysia) dan Malaysia Timur (Sabah dan Sarawak), yang dibahagikan dengan Laut China Selatan, yang meliputi kawasan seluas 33.27 juta hektar. Walaupun kadar elektrifikasi di kawasan bandar di negara ini sangat tinggi, tapak-tapak pelancongan, yang kurang daripada jarak 200km^2 bertempat di pulau terletak di luar bandar dan berpusat di Laut China Selatan, Malaysia (SCSM) sepenuhnya bergantung pada penjana diesel untuk bekalan kuasa 24 jam. Pelepasan asap dari loji janakuasa diesel memberi risiko alam sekitar di tempat tumpuan pelancong. Lebih-lebih lagi, loji janakuasa diesel tertakluk kepada banyak masalah teknikal dan ekonomi seperti kos pengendalian dan penyelenggaraan yang tinggi, risiko tumpahan minyak dan harga minyak diesel yang tidak menentu. Selain daripada masalah-masalah tersebut, lanjutan grid elektrik nasional di pulau-pulau ini tidak dapat dilaksanakan kerana kawasan yang kompleks.

Di dalam disertasi ini, gabungan pelbagai optimum sistem tenaga boleh diperbaharui hibrid yang berdiri sendiri (HRES) untuk pusat peranginan yang terbesar terletak di Pulau Tioman di SCSM telah dicadangkan dengan analisis kinerja tekno-ekonomi terperinci. Perisian Model Optimasi Hibrid untuk Peranti Elektrik Boleh Diperbaharui (HOMER) digunakan untuk analisis ekonomi dan teknikal mengenai sistem tenaga solar yang boleh diperbaharui yang dicadangkan. Purata jangkaan dan purata beban harian untuk resort adalah 1,185 kW dan 13,048 kW. Dalam disertasi ini juga, metodologi pengkomputeran lembut baru berasaskan sistem pentadbiran neuro-fuzzy adaptif hibrid (ANFIS) telah dibangunkan untuk meramalkan ketumpatan kuasa angin bulanan untuk bandar pantai Pulau Tioman yang terdekat dan kemudian keupayaan model ANFIS hibrid yang dicadangkan telah diperiksa untuk menyukat data kelajuan angin untuk

Pulau Tioman kerana tiada stesen meteorologi di Pulau ini. Untuk tujuan tersebut, algoritma ramalan berdiri sendiri ANFIS, ANFIS-PSO (pengoktimuman kumpulan partikel), ANFIS-GA (algoritma genetik) dan ANFIS-DE (evolusi pembezaan) telah dibangunkan di platform MATLAB.

Sistem tenaga hibrid berdiri sendiri yang dioptimumkan yang terbaik terdiri daripada PV, angin, penjana diesel, penukar, dan bateri. Sistem yang dioptimumkan menghasilkan kos bersih (NPC) sebanyak $ 17.15 juta, kos tenaga (COE) sebanyak $ 0.279 / kWh, pecahan boleh diperbaharui (RF) 41.6%, dan CO_2 2,571,131 kg / tahun. Sedangkan sistem hanya diesel mengambil NPC sebesar $ 21,09 juta, COE sebesar $ 0.343 / kWh dan CO_2 dari 5,432,244 kg / tahun. Di mana sistem yang hanya mengunakan diesel menghasilkan NPC, COE dan CO_2 yang lebih tinggi berbanding dengan HRES yang dioptimumkan. Model HRES yang direka dan dianalisis mungkin sesuai digunakan di mana-mana lokasi pelancong dan tempat yang dipusatkan di SCSM dan di seluruh dunia yang mempunyai keadaan cuaca yang sama.

Sebaliknya, prestasi model ANFIS hibrid yang dicadangkan telah ditentukan dengan mengira parameter statistik yang berbeza seperti kesilapan ralat mutlak (MABE), kesilapan peratusan mutlak (MAPE), kesilapan akar min (RMSE) dan koefisien penentuan R^2). Keputusan analisis hasil ramalan ketumpatan kuasa angin mendedahkan bahawa ANFIS-PSO dan ANFIS-GA menikmati prestasi dan ketepatan yang lebih tinggi daripada model lain, dan mereka boleh dicadangkan untuk aplikasi praktikal untuk meramalkan kepadatan kuasa angin purata bulanan.

ACKNOWLEDGEMENTS

Foremost, my thanks and praises to the Almighty Allah Subhanahu Wa Taala, for His grace, love, and mercy throughout this work.

I gratefully express my profound gratitude, heartfelt appreciation and indebtedness to my supervisor Prof. Dr. Saad Mekhilef for his interest, scholastic guidance, encouragement and continual efforts towards the successful completion of this dissertation work.

I am also grateful to my parents (Moksed Ali Mondol and Aleya Khatun) and siblings, for their immeasurable sacrifices towards my attainment in life and to my wife (Shahana Nasrin) and son (Ahnaf Hossain), for their help, encouragements and understanding throughout this work and finally, to everyone too numerous to mention that have contributed, in one way or the other, towards completion of this project.

I would like to thank all the member of Power Electronics and Renewable Energy Research Laboratory (PEARL), along with all the staffs of Department of Electrical Engineering, Dean Office, and IPS for their cooperation during my master's candidature.

Monowar Hossain
Department of Electrical Engineering,
Faculty of Engineering, University of Malaya.

TABLE OF CONTENTS

LIST OF FIGURES

LIST OF TABLES

LIST OF SYMBOLS AND ABBREVIATIONS

AD	:	Autonomy day of battery
ANFIS	:	Adaptive neuro-fuzzy inference system
COE	:	Cost of energy
DE	:	Differential evolution
FIM	:	First inter monsoon
GA	:	Genetic algorithm
GHG	:	Greenhouse gas
HOMER	:	Hybrid optimization model for electric renewable
HRES	:	Hybrid renewable energy system
LPSP	:	Loss of power supply probability
MAPE	:	Mean absolute percentage error
MABE	:	Mean absolute bias error
MMD	:	Malaysian meteorological department
NEM	:	North east monsoon
NPC	:	Net present cost
PSO	:	Particle swarm optimization
RF	:	Renewable fraction
RMSE	:	Root mean square error
SCSM	:	South China Sea, Malaysia
SIM	:	Second inter monsoon
SOC	:	State of charge of battery
SWM	:	South west monsoon
WPD	:	Wind power density
R^2	:	Coefficient of determination

$f(V)$	:	Weibull probability density function
$F(V)$	:	Weibull cumulative distribution function
k	:	Weibull shape factor
c	:	Weibull scale factor (m/s)
D_F	:	Derating factor
G_T	:	Solar radiation incident
c_f	:	Wind turbine capacity factor
F_0	:	Fuel curve intercept
F_1	:	Fuel curve slope
m_{fuel}	:	Mass of diesel flow (L/hr.)
$\vec{v}_i$	:	Velocity of particle
$\vec{s}_i$	:	Position of particle
w	:	Inertia weight
u_i^t	:	Mutant individual
y_i^t	:	Trial individual

LIST OF APPENDICES

CHAPTER 1: INTRODUCTION

1.1 Background

Electricity is considered as a prime driving force for the socio-economic development of a country. According to renewable global status report 2015, about 1.1 billion of the world population do not have access to the electricity. Among them, about 87% lived in rural areas whereas, rest 13% lived in urban areas. It is important to note that the lack of electricity in rural areas exacerbates the poverty and seriously hampers health care and educational services (REN21, 2016). On the other hand, about 80.1% of the total world primary energy was generated from the burning of fossil fuels in 2015 whereas, it was 81.1 % in 2014 (IEA, 2016). As a result, the global greenhouse gases (GHGs) emission and temperature of the climate are increasing dramatically. It was accounted that the combustion of fossil fuels and cement production resulted in about 375 Gigaton of carbon ($1GtC=3.66GtCO_2$) between 1750 to 2011 in the world (Stocker et al., 2013). Notably, the world GHG emissions from combustion of fossil fuel were 54 Gt CO_2-eq in 2010, and it will be 70 Gt CO_2-eq in 2050 (Uddin & Kumar, 2014).

Thus, globally there is a growing awareness that increased deployment of renewable energy (RE) is crucial for addressing climate change, creating new economic opportunities, and providing energy access to the billions of people still living without modern energy services. Although discussion is limited to date, renewables also are an important element of climate change adaptation, improving the resilience of existing energy systems and ensuring delivery of energy services under changing climatic conditions. The renewable energy sources such as the wind, hydroelectric, solar, tidal wave and geothermal are often a clean, natural and eco-friendly source of energy. It has been reported that the renewable energy sources contribute 22.8% of global electricity with the domination of the wind, PV, and hydro whereas, the remaining 77.2% comes from fossil fuels and nuclear power plant in 2014 (REN21, 2016).

Malaysia is one of the developing countries located in Southeast Asia, consisting of two distinct regions namely West Malaysia (Peninsular Malaysia) and East Malaysia (Sabah and Sarawak), divided by the South China Sea, covering an area of 33.27 million hectares and a total population of 29.7 million as of 2013. Approximately 71.3% of the Malaysian population is settled in the urban areas as of 2010 whereas, 28.7% lives in the rural areas. In 2010, the rural electrification rate in Sabah and Sarawak was decidedly lower at 84.7% and 72.2% respectively due to the extremely remote, isolated and scattered rural areas and lack of proper infrastructure whereas, it was 98.9% in Peninsular Malaysia (H. Borhanazad et al., 2013).

However, the rural population settled in the remote and rural islands in Malaysia where no accessibility to the national electrical grid due to the high construction cost of the transmission line, relies on the diesel generators for electricity (Basir Khan et al., 2015). Besides, the tourist sectors in these remote islands completely depend on diesel generators for 24-hour power supply (SK A Shezan et al., 2015). But the volatile market price of diesel fuel, CO_2 emission and high operation and maintenance cost of diesel plant make the system environmentally risky and costly (Ashourian et al., 2013; Fadaeenejad et al., 2014). In addition, the diesel price is almost double in these remote islands than on the mainland (Anwari et al., 2012).

These remote islands have an enormous potential of renewable resources such as solar and the wind. Some of them also have micro-hydro potentials. However, a single RE source such as PV or wind does not provide system reliability and cost-effective solution because of their high initial cost, unpredictable and intermittent nature. In recent years, researchers have focused on a more reliable RE system to combine with many sources of renewable energies to form a single system, which is called a hybrid renewable energy system (HRES). Most significant advantages of a HRES are system reliability, reduced cost of energy (COE), flexibility, and higher efficiency. For

example, in a cloudy and windless day, diesel generator and battery combined can meet load demand without the system outages in a PV-wind-diesel-battery hybrid system. Furthermore, when solar panel does not produce any power at night, the wind-diesel-battery system is suitable to support. Again, there is another advantage of storing surplus energy using battery bank for future utilization. Besides, the life time of the battery bank in a HRES can be increased as compared to single renewable energy system (Fadaeenejad et al., 2014).

For the successful installation and implementation of a HRES, proper assessments of renewable sources and planning are required. Besides, the involvement of local community in electrification scheme, training of the operators, commissioning and proper monitoring, and so on all are an important part of successful installation and operation of a HRES (Azad, 2015). Therefore, the techno-economic analysis should be given priority to design and implementation of a HRES.

1.2 Problem statements

Malaysian economy largely depends on tourism sector thus, 24-hour electricity access to those tourist sites is one of the prime needs. Most of the tourism sites and facilities in the South China Sea of Malaysia rely on diesel generators for their electricity supply that results in huge GHG emissions. Furthermore, diesel based power plants are subjected to many other problems including the high and volatile diesel fuel price, transportation problem due to complex terrain, lack of maintenance expert, high operation, and maintenance cost. On the other hand, an extension of the national electric grid is not economically feasible in these places due to the thick jungle and complex terrain. Therefore, standalone hybrid renewable energy system (HRES) can play the most important role to supply reliable electricity to the tourist sectors in these remote and rural islands. Then again, the power output from PV and wind turbine is highly intermittent and unpredictable. Moreover, PV only based large renewable energy

systems are subjected to a rump of PV output, which is not expected to the grid operator. Thus, a single renewable energy source may not supply reliable electricity with cost effective way (Basir Khan et al., 2015). A renewable hybrid system has been described as a cluster of distinct renewable sources, which operate independently and with coordination (C. Wang, 2006). A hybrid energy system that combines two or more energy sources when properly operated will overcome the inherent limitations of each source when considered separately (Bajpai & Dash, 2012). Proper selection of renewable power sources will substantially lower the use of fossil diesel and also increase the sustainability of power supply. Furthermore, conventional sources will complement renewable sources during varying weather conditions, which will definitely improve the consistency of the electric power system (L. Olatomiwa et al., 2015; Lanre Olatomiwa, et al., 2016).

Many researchers have presented the performance and techno-economic analysis of HRES feasible for certain locations around the world. For example, Techno-economic viability of off-grid HRES for remote villages has been reported by many authors (Ajayi et al., 2016; Charfi et al., 2016; Demiroren & Yilmaz, 2010; S Diaf et al., 2008; Himri et al., 2008; Ismail et al., 2013; Nandi & Ghosh, 2010; Rahman et al., 2016; S. M. Shaahid et al., 2014; Shaahid & El-Amin, 2009), whereas, the study on a HRES for hotels and tourist facilities located in remote and rural places are limited (Aagreh & Al-Ghzawi, 2013; Dalton et al., 2008, 2009a, 2009b; Güler et al., 2013; SK A Shezan et al., 2015). Thus, more research can be conducted to understand feasibility and techno-economic performance of HRES for the tourist locations. Among different configurations, the HRES consists of PV, the wind, diesel, micro-hydro (based on available potentiality) and the storage battery, combining with renewable and conventional sources, can be the most effective reliable power supply option for an

isolated load demand such as a resort center application in a decentralized and rural place.

However, the most important and challenging factors for designing a HRES are; accurate modeling and designing of system components such as PV, the wind turbine, diesel generator, battery, converters, etc. Also, the knowledge of other factors associated with HRES such as economic constraints, resource assessment, the market value of system components, load estimation and so on is very important to find the best suitable HRES for a particular region. Another challenge of this research is the development of soft computing methodologies for the prediction of wind power density (WPD) as a part of renewable resource assessment that will eliminate several problems, including complexity, time-consuming etc. of existing numerical methods for WPD prediction.

1.3 Motivation

HRES can be grid connected and off-grid. The off-grid HRES provides greater reliability, higher efficiency, and cost-effective power supply to an isolated load in comparison with a single renewable energy source. Therefore, the main motivation of this work is to design a HRES and analyze the technical and economic aspects to meet an isolated load profile of a selected resort center located in a remote and rural island in the South China Sea called Pulau (Pulau means Island in local language) Tioman, Malaysia. Pulau Tioman is located in the South China Sea along the east coast of Peninsular Malaysia with the geographic location of 2° 47' 47" N, 104° 10' 24" E (Muda et al., 2011). The Island consists of thirteen villages, private and government offices, schools, commercial buildings, mosques, police stations, resort and hotels, hospitals, and an airport. The TNB supplies electricity to this Island with an 8.9 MW diesel power plant at Tekek village and a 500kW mini hydro plant at Juara Village through 11 KV distribution line. However, the TNB is unable to supply electricity to the very big resort

and hotels like Berjaya Tioman Resort (Basir Khan et al., 2015; Berjaya Tioman Resort, 2015). This dissertation aims to investigate the feasibility and techno-economic performance of an off-grid HRES for a large resort center located in Tioman Island for a load demand of 13,048 kWh/day. The proposed HRES is based on solar and the wind as major renewable energy sources, diesel generators as conventional energy back up, and the battery bank as the energy storage device. Another important fact of this research is: there are more than twelve small Islands in the South China Sea surrounding Pulau Tioman named; Pulau Aur, Pemanggil, Sibu, Babi Besar, Tinggi, Rawa, Harimau, Dayang, Tengah, Tulai and Pulau Seri Buat that has more or less same climate conditions as Tioman Island. The monthly average solar radiation (kWh/m^2/day) and wind speed (m/s) for these Islands are presented in Appendix A.1 while monthly average ambient temperature (°C) and clearness index are presented in Appendix A.2. Thus, this analysis can represent any of the off-grid hybrid RE systems for the large resort center located in these Islands.

1.4 Research objectives

The aim of this work is to design and perform techno-economic analysis of a stand-alone HRES for a resort center situated in the remote and rural island in Malaysia that will enable the eco-friendly and reliable power supply to such rural areas. The specific objectives of this research are as follows:

- To predict monthly wind power density for some selected locations named Mersing, Pulau Langkawi, Bayan Lepas and Kuala Terenganu in Malaysia using hybrid adaptive neuro-fuzzy inference system.
- To design a hybrid renewable energy system (HRES) with the optimal sizing of its constituent components capable of providing renewable electricity access to off-grid resort facilities in the South China Sea, Malaysia.

- To perform a techno-economic evaluation of the proposed hybrid renewable energy system.

1.5 Outline of the dissertation

The remaining parts of this dissertation are organized as follows: in Chapter 2, energy status in Malaysia, the share of renewable power generation in national electricity and a review of the applied hybrid renewable energy system in different remote and decentralized areas were presented. A review on different hybrid energy system topologies and optimal sizing of hybrid system approaches were also included here. This chapters also includes a review of the assessment of stand-alone and grid connected hybrid system in different parts of the world (including Malaysia) and renewable energy potential in Malaysia. The potentiality of solar and wind energy, followed by different soft computing techniques for wind power density prediction were discussed. Chapter 3 presents proposed soft computing techniques employed for wind power density prediction and methodologies for techno-economic analysis of proposed hybrid renewable system including site selection, resources assessments, meteorological data collection, load profile estimation, technical and economic modeling of system components, and sensitivity analysis. In Chapter 4, result and discussion of each aspect of methodology were presented. The result and discussion include wind power density prediction, extrapolation of wind speed, techno-economic performance evaluation of the proposed hybrid system, and sensitivity analysis. Finally, Chapter 5 presents conclusions, findings, recommendations and future work of this research.

CHAPTER 2: LITERATURE REVIEW

2.1 Introduction

In this chapter, the energy status in Malaysia with renewable energy resources assessment, current establishment, and future prospects of the hybrid renewable energy system (HRES) are briefly discussed. A short review of solar and the wind energy potentials in Malaysia including a review of wind power density prediction models have been presented in this chapter. The chapter also presents a review on different configurations and topologies of HRES. After that, different methods for optimal sizing of HRES is presented. Finally, a review of the techno-economic analysis of hybrid system is presented.

2.2 Energy status in Malaysia

According to National Energy Balance (NEB) report, the total installed electricity generation capacity in Malaysia was 29,973.8MW in 2014 where the peak demand for Peninsular Malaysia was recorded 16,901MW, Sarawak 2,306MW, and Sabah 908MW. In 2014, gross electricity generation was registered 147,480GWh in Malaysia, an increase of 2.8 percent as compared to 143,497GWh in 2013 (NEB, 2014). Figure 2.1 shows the share of installed electricity generation capacity as of 31st December 2014 in Malaysia. It can be seen from the Figure 2.1 that fuel mix was dominated by natural gas, followed by coal and major hydro.

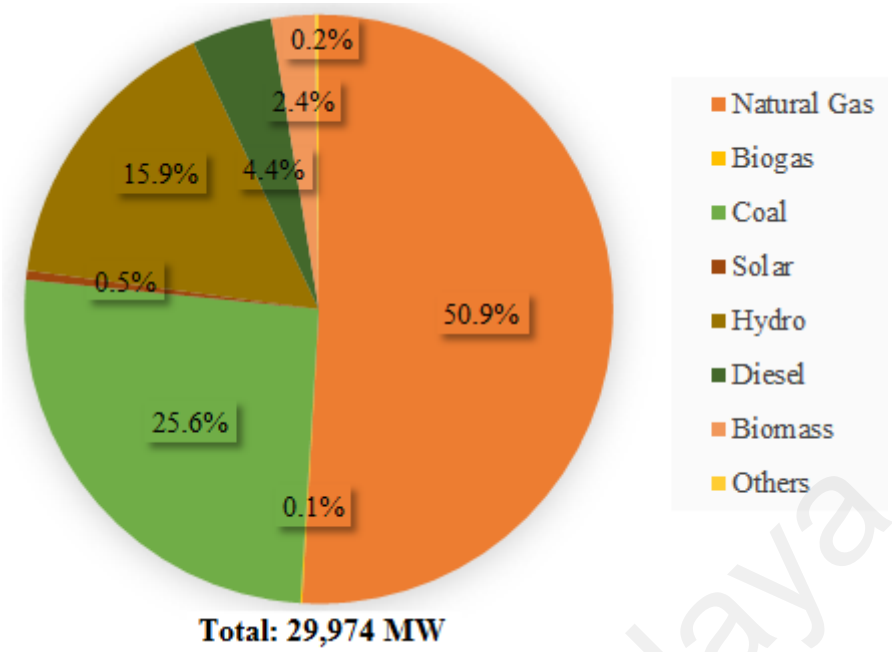

Figure 2. 1: Share of installed electricity generation capacity as of 31st December 2014 in Malaysia (NEB, 2014).

Notably, Malaysia is blessed with vast renewable sources of energy such as biomass, bio gas, solar, the wind, and mini-hydro. The potential for Renewable Energy (RE) is enormous, especially for biomass energy; whereby these resources are not traded and mostly homegrown. The potential of mini-hydro projects especially the run-of-the-river type is also huge, as the energy available from the streams of rivers in the country has been proven to provide a considerable contribution to the supply of electricity in the rural areas. Solar energy is another type of RE resource that is abundant and readily available as Malaysia is geographically located at the equator. On the other hand, the wind speed is comparatively low in Malaysia due to complex terrain (Basir Khan et al., 2015).

However, the installed capacity of renewable power generation was 243MW in Malaysia as of December 2014, which was less than 1% of total fuel mix. According to Eleven Malaysian Plan (RMK11), the installed renewable power generation capacity will be 2080MW in 2020 (RMK11, 2016). Figure 2.2 presents the share of installed and projected RE power generation capacity in Malaysia.

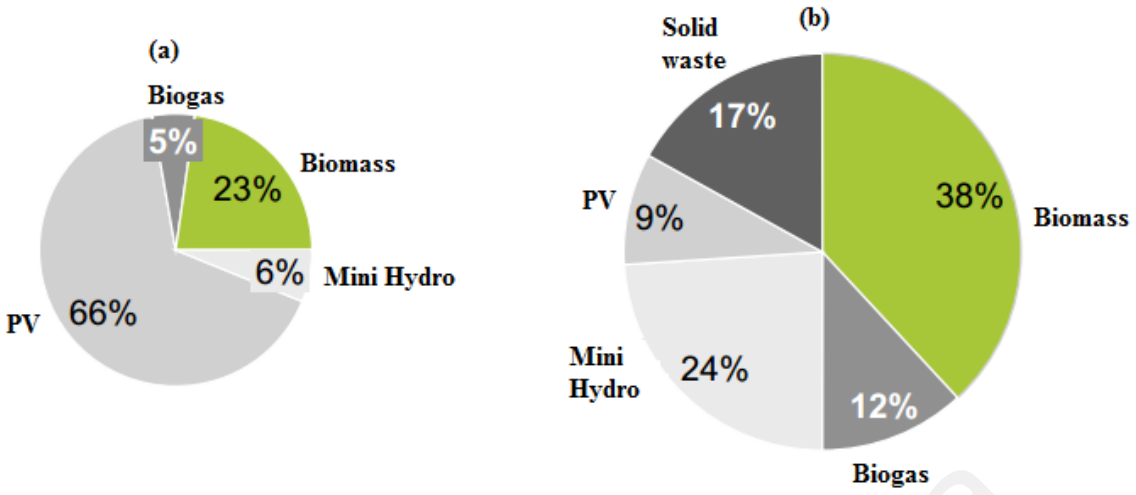

Figure 2.2: the share of (a) installed (b) projected RE generation capacity in 2014 and 2020 respectively in Malaysia (NEB, 2014).

2.3 Renewable energy potential in Malaysia

2.3.1 Solar Energy

Solar energy is renewable, abundant and environmentally friendly. Thus, globally photovoltaic (PV) technology has achieved huge popularity, development, and exploration for both rural and urban electrification (Li et al., 2016). It can be noticed that since 2000, the installed PV system capacity all around the world has reached to 178 GW in 2014 (IEA, 2015). However, Malaysia is situated in the equatorial region and has the climate with high humidity and temperature. The humidity varies from 80% to 90% except for highlands. Throughout the year, the temperature ranges between 22 ºC and 33 ºC (72–91 ºF) and the average daily temperature are 26.5 ºC. Thus, this country has higher solar radiation, which is 400–600 MJ/m^2 per month. This amount of solar radiation indicates that it has a promising potential to establish large-scale solar power installations (Mekhilef et al., 2012). Figure 2.3 shows the average annual solar radiation (MJ/m^2/day) map of Peninsular Malaysia, Sabah and Sarawak whereas, Figure 2.4 presents monthly-daily average solar radiation (kWh/m^2/day) of a particular location having latitude and longitude of 6° 26' 70" N and 100° 12' 30" E respectively in Peninsular Malaysia between the period 1983-2005. Annual average solar radiation of

this place is 4.95 kWh/m^2/day. Solar thermal and PV technologies are two major applications of solar energy in Malaysia. In solar thermal application, solar energy is used for heating purpose whereas, it is converted to direct current in PV application (Saidur et al., 2009).

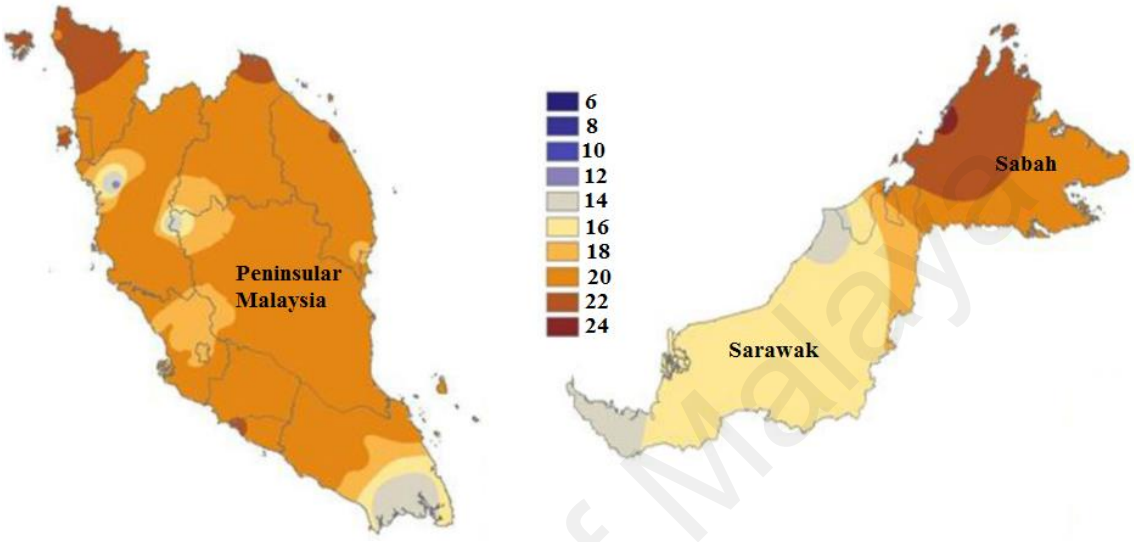

Figure 2. 3: Average annual solar radiation MJ/m^2/day in Malaysia (Mekhilef et al., 2012).

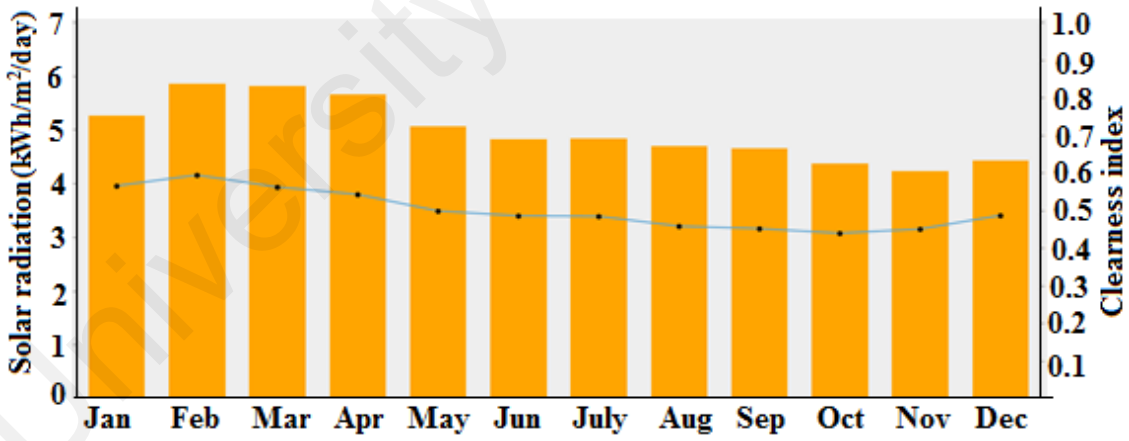

Figure 2. 4: Monthly-daily average solar radiation and clearness index of a particular place in Malaysia.

2.3.2 Wind Energy

The primary energy sources, the fossil fuels will be exhausted, since they are used at a much higher rate than they are found in the earth's crust (Ashourian et al., 2013). Moreover, the price of fossil fuels is highly unstable, and it causes huge greenhouse gases (GHG) emissions and environmental pollutions (Mohammadi et al., 2016). The world GHG emission from combustion of fossil fuel was 54 Gt CO_2-eq in 2010, and it will be 70 Gt CO_2-eq in 2050 as reported by Uddin & Kumar (2014). Notably, around 40% of the world CO_2 emissions come from the power sector and demand for power is increasing radically all over the world (GWEC, 2012). Thus, a dramatic change in the production and consumption of electricity is important to win the fight against global climate change. It is a must to seek renewable energy technologies, which are free from emissions to supply renewable electricity to both developing and industrialized countries (Aquila et al., 2016; GWEC, 2012).

The wind energy is free, environmentally friendly and clean renewable energy (Uddin & Kumar, 2014). Consequently, in the fight of global climate change, wind energy is a major solution (Islam et al., 2011). According to the climate negotiation meeting in Copenhagen, the wind technology is already on track to save 10 billion tons of the world CO_2 emission by 2020, which means that wind energy alone is capable of abating more than 65% of all harmful emissions around the world (GWEC, 2012; Huang & McElroy, 2015). Globally installed wind power capacity has reached at 432.9GW at the end of 2015 where 63GW was in 2015 alone (GWEC, 2015).

Despite good sides of a wind turbine, it has noise and view pollutions. The importance of the noise from wind turbine depends upon the distance between dwellings and turbines and also on wind direction. The noise source from a wind turbine is static and repetitive with a large range of noise frequency (Mohamed, 2016). According to the study by Rogers et al. (2006), noise effects from a wind turbine can be

divided into three general categories: subjective effects, including annoyance and dissatisfaction, disturbance in human activities like sleeping and physiological effects such as anxiety or hearing loss.

The visual pollution from a wind turbine can be subdivided into several negative effects with spatial extents, different causes and possible impacts (Hoen et al., 2011). When the wings of a wind turbine rotate, it reflects the sun by creating flickers of light. This phenomenon attracts attention and adds to the nuisance from the movement effect. The shadow flicker is another visual effect from the wings of a rotating wind turbine. The rotating wings cause flickers of shadow in the immediate surroundings of the wind turbine (Jensen et al., 2014). It is worth mentioning that the noise pollution can be reduced by improved blade design of the wind turbine whereas, the visual effect can be mitigated with the appropriate sitting design of wind farm (Dai et al, 2015).

On the one hand, the impact of intermittent wind generation is a very important issue to consider. The sources of electricity which depend on the meteorological factors such as the wind, solar, tidal and so on has uncontrolled increases or decreases in output are referred to be as intermittent. The intermittency from the wind power plants leads to run fossil fuel based backup generators to ensure system reliability (Goater, May 2014; Green & Vasilakos, 2010).

In Malaysia, little effort has been made to the use of wind energy. The potential for wind energy generation in Malaysia depends on the availability of the wind resource. The wind speed in this country is normally influenced by Northeast (November to March) and Southwest monsoon (late May to September) (Ho, 2016). Several studies have shown that grid connected large-scale wind turbine may not be economically viable due to low wind speed in most of the states in Malaysia. However, small scale off-grid wind turbine can be a good solution for decentralized electrification (Islam et

al., 2011). Figure 2.5 shows monthly-daily average wind speed (m/s) of a particular location (6° 26' 70" N, 100° 12' 30" E) in Malaysia between the period 1983-93.

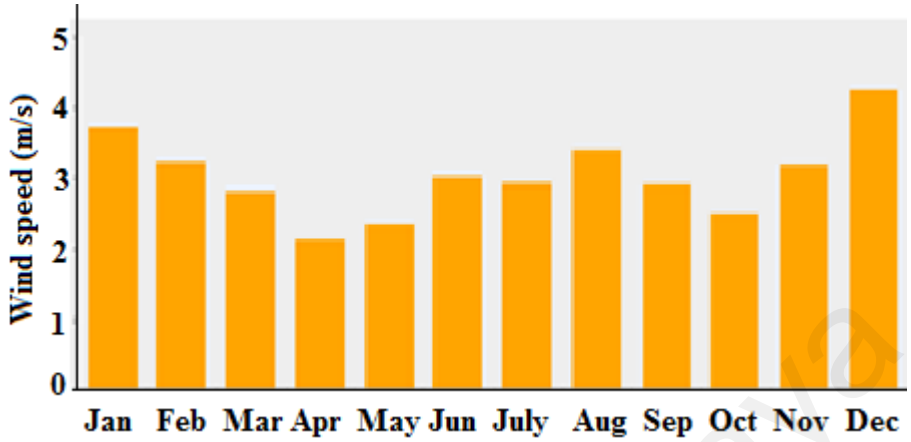

Figure 2. 5: Monthly-daily average wind speed at 50m hub height of a particular place in Malaysia.

2.3.3 Approaches for wind power density prediction

To build a wind farm in any particular location: an analysis of the wind data, estimation of wind power and energy density are essential. The wind power density (WPD) of a particular location is the measure of the potentiality of wind resources and the chance of extracting wind energy at different wind speed from that location (Simons & Cheung, 2016; Xydis, 2015). The knowledge of WPD also helps designer and investor to understand the performance of a wind turbine and to choose the optimal number of a wind turbine with a suitable power rating. The wind power density can be computed from several numerical methods (Islam et al., 2011; Petković et al., 2016).

The problem in numerical methods is that they need high computation time. In the recent years, artificial intelligence (AI) techniques have received overwhelming popularity in the field of the wind energy system as they offer better advantages, including fast computation time, require no knowledge of internal system parameters and compact solutions (Mohammadi et al., 2015; Qazi et al., 2015). In the field of wind energy, ANN method is popularly used by many researchers for the prediction of wind speed and power. Peng et al. (2013) developed an ANN based short term wind power

prediction model that resulted in 10.67% root mean square error (RMSE) in the prediction. Ramasamy et al. (2015) employed an ANN model for the prediction of the wind speed for 11 locations in India where actually measured wind data was not available. The authors used meteorological variables of the target locations from NASA surface meteorology and solar energy database, and the prediction accuracy is compared with measured wind data that was collected from a nearby meteorological station in Hamirpur, India. More literature review regarding the application of the ANN model for the prediction of wind speed and power can be found in (Ata, 2015; Bilgili et al., 2007; Jung & Broadwater, 2014). Furthermore, other AI methods such as ELM model was developed by Mohammadi et al. (2015) to determine the wind power density of a particular location in Iran. The authors compared the WPD obtained from ELM model with that from ANN, GP, and SVM. The results showed that the performance of ELM is higher than other models.

In recent years, ANFIS technique has been employed in many scientific and engineering studies, but limited in wind energy applications (Admuthe & Apte, 2009; Chong et al., 2016; Nikolić et al., 2015; Pousinho et al., 2011). The adaptive neuro-fuzzy inferences system (ANFIS), as a soft computing methodology, is a hybrid intelligent system that merges technique of the learning power of the ANNs with the knowledge representation of fuzzy logic. ANFIS is an adaptable and efficient method in the computational process. The suitability of an ANFIS model to estimate monthly WPD for the location of Aligoodarz, Iran has been shown by Shamshirband et al. (2016). An ANFIS based hybrid model was developed by Pousinho et al. (2011) to forecast the short-term wind power where the authors used historical wind power data as inputs. Petković (2015) predicted Weibull shape factor (k) and scale factor (c) using the ANFIS predictive model. An excellent and precise performance was obtained from this model.

An ANFIS network was constructed by Chong et al. (2016), where the authors showed the performance of the ANFIS to estimate the rotational speed of a vertical axis wind turbine with power augmentation guide vane (PAGV). Again, an ANFIS model was established by Nikolić et al. (2015) for determination of the wind turbine rotor output, torque output, power output and rotational speed of the rotor in regard to wind input speed and diffuser effect. Gnana Sheela & Deepa (2013) applied both ANN and ANFIS models for hourly prediction (1, 3, 6, 12 and 24h respectively) of wind power for a wind farm located in Southern Italy and their prediction accuracy resulted worse when the prediction horizon is increased.

Although ANFIS merges of the learning power of the ANNs with the knowledge representation of fuzzy logic, there are still some difficulties in ANFIS in constructing membership functions (MFs). Therefore, this study proposed hybrid ANFIS such as ANFIS-PSO, ANFIS-GA, and ANFIS-DE to predict wind power density for the four different places in Malaysia namely Mersing, Kuala Terengganu, Pulau Langkawi, and Bayan Lepas. PSO/GA/DE is employed for the tuning of the membership function of ANFIS in order to minimize the prediction error. Besides, this dissertation examined the wind speed prediction capabilities of the proposed models for the locations where measured wind data are not available, and the result of the wind speed extrapolation is compared with the measured wind data collected from the nearby meteorological station.

2.4 Hybrid Renewable Energy System (HRES)

The power delivery system that combines conventional (diesel generator/micro turbine) turbine and renewable energy sources such as wind, PV, and small hydro to supply power to an isolated load is called hybrid renewable energy system (HRES). This is done to reduce CO_2 emission into the surrounding environment and to complement the inherent deficiency of each energy source. The potential of the renewable energy sources in a certain location and the availability of diesel fuel for the conventional source determine the type of hybrid system that will be adopted for certain application for the location. It is noted that the diesel generator is usually used as a backup source in these hybrid systems. Different configurations can be followed in designing hybrid systems to effectively utilize the available renewable energy sources and to serve the load demand at any particular time. Any combination of renewable sources with an optional backup and/or storage device is possible. In order to select the most appropriate configuration for a specific site, a feasibility study based on metrological data and life cycle cost analysis has to be done. In addition, technical and sociocultural considerations have to be taken into account while making the decision process.

The hybrid system employs the best features of each of complementary energy resources on the system. For instance, the hybrid systems having solar, the wind, diesel generators, and storage device are highly reliable power supply option to the isolated load due to complementary nature of the wind and solar resources (Zhou et al., 2010). The wind turbine can supply electricity to the days characterized by windy, cold and cloudy and normal days while PV supplies electricity on sunny and partially cloudy days. The diesel generator and storage devices can work as a system load back up. Therefore, a HRES is highly reliable, cost-effective, and eco-friendly mode of

electricity supply. Table 2.1 presents the advantages of HRES over single source based RE and conventional system.

Table 2.1: Comparison of a hybrid, single RE based and conventional system.

Criteria	**Single source (Conventional)**	**Single source (RE)**	**HRES**
Capital cost/kW	Low	High	Moderate
O & M cost	High	Low	Moderate
Load Demand	Appropriate for consistently high kWh/day	Most Appropriate for low kWh/day	Appropriate for all kinds of kWh/day load.
Fuel	Relative to load requirement	No fuel	Less fuel need due to complementary nature
Schedule of repair & maintenance	Frequent	Less frequent	low
Reliability	Dependent on fuel and repair expert	Dependent on natural resources	Highly reliable due to complementary nature of natural resources
Negative environmental impact	High	low	moderate
Dependency on natural resources	Independent	Very high	Partial

In this dissertation, a hybrid system that comprises of PV, wind, diesel, and battery will be investigated. The PV and the wind have been chosen because of the enormous potential in the selected case study as earlier discussed. Also because they are primary sources that take full advantages of renewable energy (Nehrir et al., 2011). The battery serves as energy storage for compensating fast transient and ripple power. The diesel engine is employed as a generator with constant power for strong and reliable backup. There are three general categories of the hybrid system described below:

2.4.1 DC coupled hybrid system

In a DC coupled HRES, different distributed generation systems are connected to the DC bus through an appropriate power electronics converter. DC energy source or load can be connected to the DC bus either directly or via proper DC/DC boost converter to achieve the required voltage level. This system can deliver power to the AC load and

utility (or take) via an appropriate bi-directional converter. Figure 2.6 shows a DC coupled hybrid energy system. Some advantages of this configuration are simple, require no synchronization, fewer transmission losses, and single-wired approach. Some disadvantages of this configuration include the problem with voltage compatibility and failure of the DC/AC converter leads to no power supply to the load, hence entire system failure.

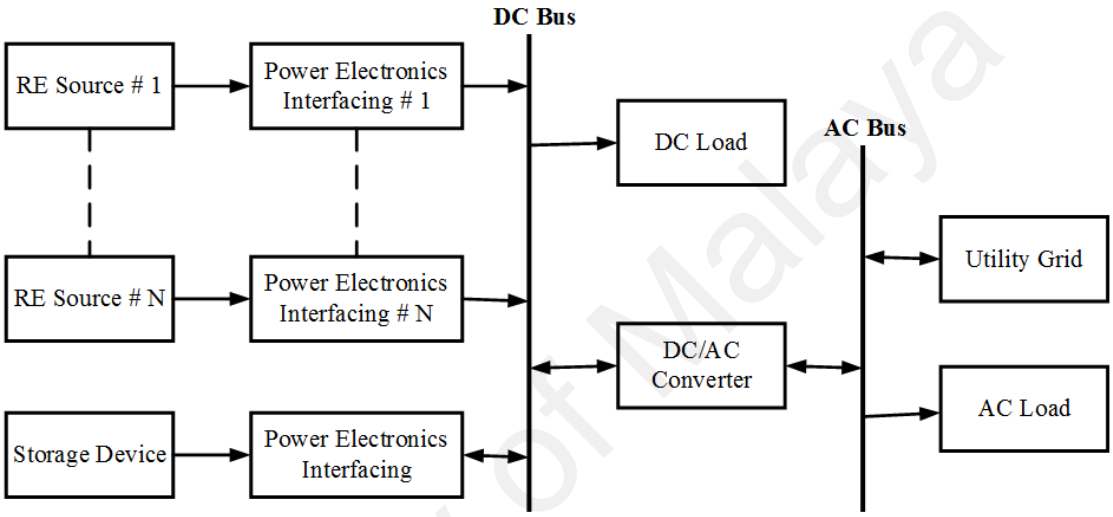

Figure 2. 6: A DC coupling: hybrid renewable energy system.

2.4.2 AC coupled hybrid system

In an AC coupled HRES, different distributed generation systems are connected to the AC bus through an appropriate power electronics converter. DC load can be connected to the system via an appropriate AC/DC converter and a DC bus. Figure 2.7 shows an AC coupled hybrid energy system. These system configurations have some advantages including modularity of structure, highly reliable, support multi-voltage and terminal matching. On the other hand, it has some disadvantages as well including unsuitable for distance transmission, power factor and harmonics correction necessary, and synchronizing necessary to add generators to the AC bus.

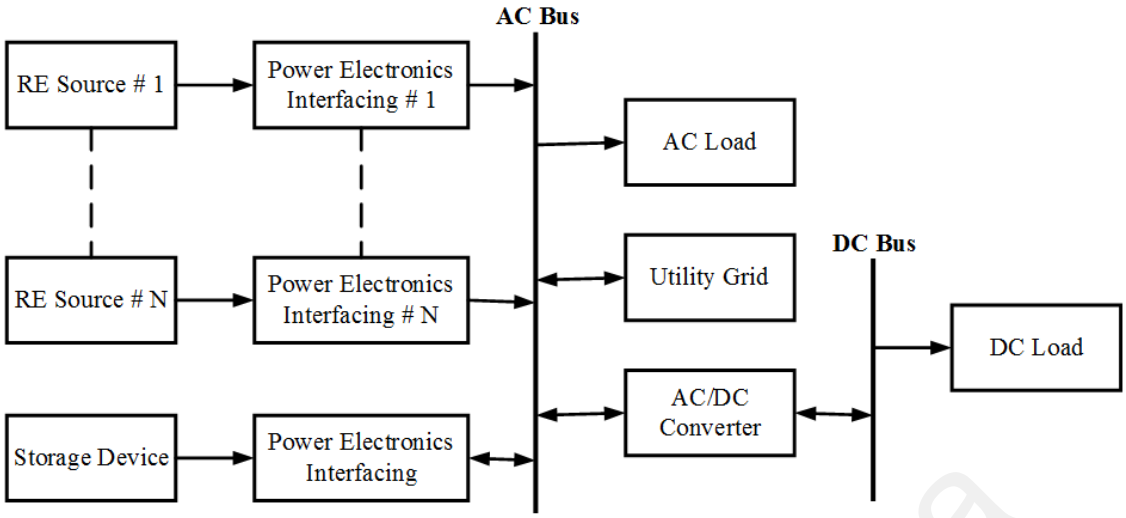

Figure 2.7: An AC coupled: hybrid renewable energy system.

2.4.3 AC-DC coupled hybrid system

In an AC-DC coupled HRES, different distributed generation systems are connected to a DC bus and/or an AC bus through an appropriate power electronics converter. Figure 2.8 shows an AC-DC coupled hybrid energy system where distributed generators are connected to the AC bus and/or DC bus. In this configuration, different energy sources can be connected directly to the bus without extra interfacing devices. The AC-DC coupled hybrid systems are more efficient and cost-effective and have low conversion losses. On the other hand, an AC-DC hybrid system needs complex control and more accurate power management scheme.

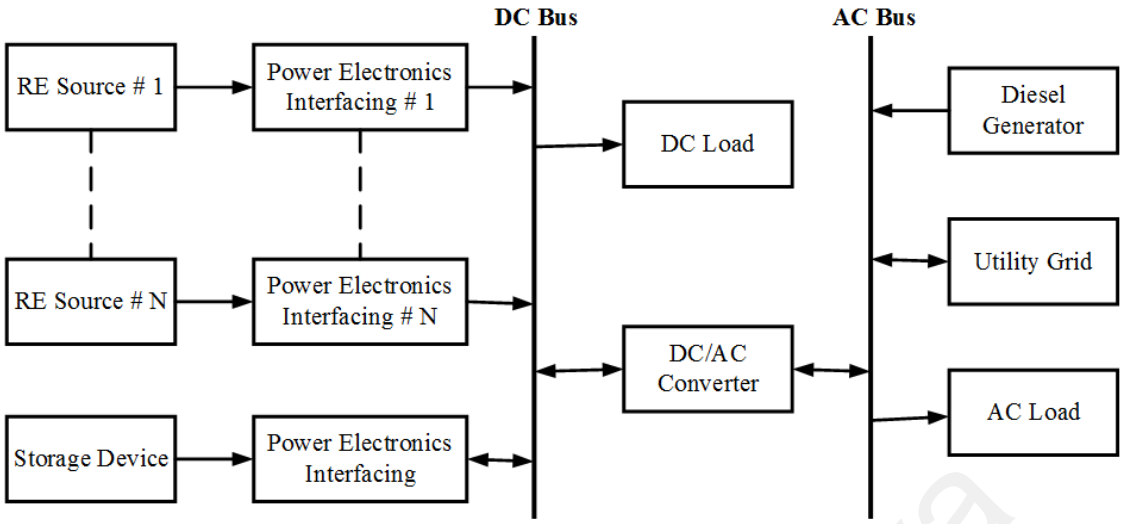

Figure 2.8: An AC-DC coupled: hybrid renewable energy system.

2.5 Applied HRES in Malaysia

In Malaysia, to accelerate the rural electrification program and as a fuel diversification strategy after the 1970 oil-price escalation, high priority was assigned to the development of the RE resources. Under the 4th (1981-85) to 11th Malaysian Plan (2016-20) as a part of rural electrification, the emphasis was given to the development of the solar hybrid system (SHS) consisting of PV, the wind, diesel, mini hydro and battery (RMK 1-11, 2016; List of environmental issues, 2012). The potential for small hydropower plants in East and West Malaysia has been investigated in a number of studies (Ibrahim Hussein & Nathan Raman, 2010; Khan et al., 2014; Raman et al., 2009). In Malaysia, Tenaga Nasional Berhad (TNB), Sarawak Energy Berhad (SEB) and Sabah Electricity Sendirian Berhad (SESB) are the three major power companies. TNB and SEB are responsible for the generation, transmission, and distribution of the electricity in Peninsular Malaysia and Sarawak respectively. SEB is wholly owned by the state government of Sarawak. On the other hand, SESB is responsible for the electricity supply in Sabah and Federal Territory of Labuan.

In 2002, a PV–wind–diesel hybrid system was installed in an Orang Asli village of Kampung Denai in Rompin, Pahang by TNB. At the same year, a PV–diesel hybrid system was launched with two 8kW PV and two 48kW diesel generator to power a cable car office in Gunung, Langkawi island. To provide energy access and modern education facility to the rural schools, Ministry of Education (MoE), Malaysia established 19 solar hybrid systems in Pahang, Johor, Kelantan, and Perak in 2012.

In 2008, 11 solar hybrid power systems were established by TNB in different rural villages in Perak, Johor, Kelantan, Pahang (Phase 1 & 2). Besides, TNB electrified 16 rural villages consists of 276 houses located in RPS Kemar, Gerik, Perak with a PV-diesel-battery hybrid system having the capacity of 850kW PV, 2 diesel generators (350 &450kW) and a battery bank of 4800kWh in 2012. Between 2008-09, several solar hybrid systems were established in remote villages and schools in Sabah to provide electricity access and thereby, enlighten their way of life.

The rural and remote islands in the South China Sea, Malaysia are full of renewable energy resources. In 2004-2005, eight solar hybrid system (SHS) was established by TNB in five different islands situated in the South China Sea, Malaysia. These SHS are operated in Pulau Besar (45kW), Pulau Pemanggil (50kW), Pulau Sibu (100kW), Pulau Aur (50kW) and Pulau Tinggi (50kW) (H. Borhanazad et al., 2013). Again in 2007, the Malaysian government in collaboration with TNB implemented a hybrid renewable energy system (HRES) in Perhentian Island, which comprised of 100 kW PV array, two 100 kW wind turbine, one 100 kW diesel generator and a battery bank of 480 kWh, 240 Volt (DC) (Darus et al., 2009). The aforementioned hybrid power systems are briefly presented in Table 2.2.

Table 2. 2: Established solar hybrid system (SHS) in different remote locations in Malaysia (H. Borhanazad et al., 2013; Darus et al., 2009; Khairul, 2014; Sopian et al., 2005; TNBES, 2016).

	Project Location	Project Capacity	Owner	Completion Date
1.	SHS at Gunung Machincang, Langkawi island.	Two 8kW PV and 2×48kW diesel generator (DG) to serve cable car office	LADA	2002
2.	SHS Kg. Denai, Rompin, Pahang.	10 kW PV with DG to supply 20 houses	KKLW	2002
3.	SHS Mersing islands, Johor (Phase 1)	6 SHS, 65 kW peak of solar power to supply 215 houses	KKLW	2005
4.	SHS Mersing islands, Johor (Phase 2)	1. 2 SHS 2. 30 kW peak of solar power to supply 60 houses	KKLW	2006
5.	SHS Perhentian island	100 kW PV and 2×100kW wind turbine with 100kW DG power to serve: • 280 domestics customers • 3 commercial customers and • 22 chalet operators	KKLW	2007
6.	SHS Kapas island	50 kW PV and 25kW DG to supply 8 resorts (116 rooms)	KKLW	2007
7.	SHS Org Asli Perak, Johor, Kelantan, Pahang (Phase 1 & 2)	11 SHS, 176 kW peak of solar power to supply 744 houses	KKLW	2008
8.	SHS Banggi island	200 kW peak of solar power to supply 402 consumer inclusive houses, mosque, government office, clinic and schools	KKLW	2008
9.	SHS for remote schools, Sabah	4 SHS, 80 kW peak of solar power to supply 4 schools	KKLW	2008
10.	SHS Sabah	6 SHS, 105 kW peak of solar power	KKLW	2009
11.	SHS Kalabakan	250 kW peak of solar power to supply 591 houses	KKLW	2009
12.	SHS remote schools in Perak, Kelantan, Pahang, and Johor	19 SHS, 735 kW peak of solar power to supply 19 schools	MoE	7/2012
13.	SHS RPS Kemar, Gerik, Perak	850 kW PV with DG of 350 & 450 kW to supply 342 consumer inclusive houses, mosque, government office, clinic, and schools	KKLW	11/2012

Currently, there are more than 58 mini scale hydro power stations in Malaysia but all are not in operation. Table 2.3 presents the name and installed capacity of mini hydro that is run by TNB, SEB and SESB whereas, Table 2.4 shows cumulative installed capacity of mini hydro that is run by feed in tariff (FiT) holder, independent power producer (IPP) as well as TNB, SEB and SESB as of National Energy Balance (NEB) report 2014. From Tables 2.3 and 2.4, we can see that the total installed capacity of mini hydro in Malaysia was 72.2 MW with total generation 1,82,063MWh in 2014 contributing by TNB 9.327MW, SEB 7.297MW, SESB 8.0MW, mini hydro FiT holder 15.7MW, mini hydro IPP 20MW, and others 11.90MW (NEB, 2014).

Table 2. 3: Installed capacity of mini hydro power stations in Malaysia run by TNB, SEB, and SESB as of December 2014 (I. Hussein & N. Raman, 2010)

Station	**Capacity (MW)**	**Station**	**Capacity (MW)**
Kedah		**Sabah**	
1. Sg Tawar Besar	0.540	1. Kedamaian (Kota Belud)	2.103
2. Sg Mempalam	0.397	2. Malangkap (Kota Belud)	1.000
3. Sg Mahang	0.483	3. Sayap (Kota Belud)	1.000
Perak		4. Bombalai (Tawau)	1.100
1. Sg Tebing Tinggi	0.178	5. Merotai (Tawau)	1.100
2. Sg Asap	0.110	6. Kiau (Kota Belud)	0.375
3. Sg Kinjang	0.349	7. Naradau (Ranau)	1.760
4. Sg Bil	0.258	8. Pengapuyan	4.830
5. Sg Kenas	0.532	**Subtotal**	**13.043**
6.Sg Chempias	0.120	**Sarawak**	
7. Sg Temelong	0.872	1. Sg Pasir	0.760
Terengganu		2. Penindin	0.352
1. Sg Brang	0.270	3. Sebako	0.333
2. Sg Cheralak	0.50	4. Lundu	0.352
Pahang		5. Kalamuku 1	0.500
1. Sg Sempam G2	1.245	6. Kalamuku 1	0.500
2. Sg Pertang	0.492	7. Sg Keijin	0.500
3. Sg Perdak	0.364	8. Sg Kota 1	2.000
4. Sg Sia	0.548	9. Sg Kota 2	2.000
Kelantan		**Subtotal**	**7.297**
1. Sg Renyok G1	0.800		
2. Sg Renyok G2	0.800		
3. Sg Sok	0.588		
4. Sg Rek	0.270		
Subtotal	**9.327**		
Grand Total	**(9.327+13.043+7.297)**		**29.667**

Table 2. 4: Electricity generation and installed capacity of small hydro energy by public and private licensees by region, 2014.

Region	Type of scheme	Installed capacity (MW)	Unit generated (MWh)
Peninsular Malaysia	Mini hydro-FiT	9.20	41,976
	Mini hydro-IPP	20.00	52,880
	Mini hydro-Cameron highlands scheme	11.90	30,321
	Mini hydro-TNB	9.3	8,753
Sabah	Mini hydro-SESB	8.00	19,943
	Mini hydro-FiT	6.50	16,650
Sarawak	Mini hydro-SEB	7.3	11,540
Grand Total		**73.68**	**1,82,063**

2.6 Assessment of stand-alone and grid connected HRES

Renewable energy (RE) resources assessment is the precondition to build an RE system for various applications around the world. An RE system which is planned and designed properly, provides consistent and excellent energy delivery to the customers (Dihrab & Sopian, 2010; Hiendro et al., 2013). The solar and wind are most commonly available RE sources around the world and hence, they are commonly explored. A comprehensive study of available long-term solar radiation data and the wind regime in a specific location is, therefore, a vital for the designing and prediction of energy output of their respective energy conversion devices. An in-depth knowledge of the solar radiation data and the wind regime will help in determining their suitability for any specific applications.

In literature, researchers have explored the potentiality of the RE resources for different part of the world. A research was conducted to supply electricity to Gokceada Island, Turkey and the researchers considered different scenarios such as stand-alone PV and wind turbine, grid connected PV and wind turbine, diesel only and PV-wind-diesel hybrid system. Among them, the stand-alone PV with the wind provided the most economical electricity supply for the island (Demiroren & Yilmaz, 2010). Techno-economic viability of a stand-alone HRES, grid-connected RE system and grid-only

system for a large and medium hotel located in the sub-tropical coastal area of Queensland was studied by focusing on NPC and payback period (Dalton et al., 2008, 2009b). Economic assessment of a PV-diesel-battery hybrid system was conducted for Northern Province of Saudi Arabia showed that 45% and 21% of total energy remained unused with PV penetration of 69% and 51% respectively (S. M. Shaahid et al., 2014). For a North American off-grid community, a PV-wind-diesel-battery system was analyzed by Rahman et al. (2016), considering seven renewable scenarios. A techno-economic feasibility study was conducted to provide renewable electricity to a small hotel in Ajloun city located in the north part of Jordan. This study found that grid connected small scale wind turbine is the most economical way for renewable energy access to the hotel based on net present cost (NPC) and payback period (Aagreh & Al-Ghzawi, 2013).

In Malaysia, several studies of HRES were conducted based on the performance evaluation, optimal sizing, technical and economic analysis, but with no particular study of HRES for remote tourist facilities located in the remote islands of the South China Sea, Malaysia. An off-grid wind-diesel-battery system for two residential hotels in Cameron Highland, Malaysia with a peak load of 8.7 kW was reported by SK A Shezan et al. (2015). The authors showed that 15 wind turbines (each 10kW), 1 diesel generator (4kW) and 2 lead acid battery can supply reliable electricity to the hotels with the cost of energy (COE) 0.199/kWh and NPC of $77,019. A hybrid system consists of PV-diesel-battery was suggested by Ismail et al. (2013), for supplying 63.58 kWh/day to an isolated house in Langkawi Island, Malaysia. N. Izadyar et al. (2016) identified most potential rural areas in Malaysia for the application of HRES and an economic evaluation was conducted. The performance evaluation of a standalone PV-wind-diesel-battery system was carried out for a small community located at Selangor, Malaysia by Sk A. Shezan et al. (2016). The authors showed that reliable electricity can be supplied

to this community for $1.877/kWh. An optimal combination of the PV-diesel-micro hydro-battery system has been proposed to supply reliable electricity to Tekek Village in Tioman island by Basir Khan et al. (2015). The authors showed that the net present cost (NPC) of the proposed HRES would be $31.9 million with COE of $0.142/kWh. An optimal green energy system consists of PV-wind-fuel cell-battery was proposed by Ashourian et al. (2013) for Juara Village in Tioman island. The authors showed that their proposed system can supply green electricity for $1.10/kWh without any unmet electrical load. The techno-economic feasibility of several HRES was presented in Ngan & Tan (2012) for four stores building in University Technology Malaysia (UTM). This study found that PV-wind-diesel-battery and PV-diesel-battery systems are more economical and environmentally friendly than diesel only system when the price of diesel fuel increase from the base value.

2.7 Optimal sizing of the hybrid system

Over sizing of a hybrid system components leads to increasing the overall system cost while under sizing leads to unreliable power delivery of the system. Thus, the optimal sizing of the constituent generating units and other associating components is the vital importance when designing and planning the hybrid system for economic and efficient utilization of the available RE resources. There are two general criteria namely power supply reliability and system economic minimization to select optimal system components that will meet the load demand with reliably and cost effectively.

2.7.1 Power supply reliability

The production of electricity from RE resources such as solar and the wind is highly dependent on weather conditions. Thus, the power supply reliability assessment is a desperate need when planning and designing a hybrid RE system. There is a number of methods to determine the reliability of the system among them the loss of power supply probability (LPSP) criteria is the most popular one (Zhou et al., 2010).

2.7.1.1 Loss of power supply probability (LPSP)

The LPSP is the probability that an insufficient power supply results when the hybrid system is not able to satisfy the load demand. The reliability of an off-grid PV-wind hybrid system can be obtained considering LPSP as a key design parameter. The chronological simulations and probabilistic techniques are two approaches for the application of LPSP when designing a reliable standalone PV-wind system. The first approach has disadvantages such as computationally burdensome and requires time series data. On the other hand, the probabilistic approach incorporates the fluctuating nature of the resource and the load, thus eliminating the need for time-series data (Zhou et al., 2010). The mathematical representation of LPSP is as following (Heydari & Askarzadeh, 2016):

$$LPSP = \frac{\sum_{t=1}^{T} LPS(t)}{\sum_{t=1}^{T} P_L(t) * \Delta t} \qquad (2.1)$$

where $LPS(t)$ and $P_L(t)$ are loss of power supply and load demand at hour t. In a PV-wind-diesel-battery hybrid system loss of power supply at any hour t can be calculated as:

$$LPS(t) = \left[P_L(t) - \left(P_{PV}(t) + P_{WT}(t) + P_{DG}(t) + P_{batt\_dch}(t)\right)\right] \qquad (2.2)$$

where, $P_{PV}(t)$, $P_{WT}(t)$ and $P_{DG}(t)$ are power output from the PV, wind and diesel generator respectively, while $P_{batt\_dch}(t)$ is the discharge capacity of the battery.

2.7.1.2 Loss of load probability (LOLP)

This is a measure of the probability that the load demand will exceed the capacity of the hybrid system. This is also known as expected energy not supplied and measured in kWh, and can be computed as (Ould Bilal et al., 2010):

$$LOLP = \sum_{t=1}^{8760} L_d * D \qquad (2.3)$$

where, L_d and D are annual average load demand (kW) and duration of time (h) for which load not to be met respectively.

2.7.1.3 Level of autonomy (LA)

This represents the fraction of time under which the load is not met. This is the ratio between duration of unmet electric load (H_{LOL}) to total number of hours (H_{Total}) of the system operation which is expressed by following equation (L. Olatomiwa, 2016):

$$LA = \frac{H_{LOL}}{H_{Total}} \qquad (2.4)$$

2.7.2 System economic optimization

An economic analysis is essential to suggest an optimal combination of the components in a HRES. The following are the major economic criteria:

2.7.2.1 Net present cost (NPC)

This is comprised of capital, replacement, operation and maintenance cost of the system components over total project life span. NPC is also known as life cycle cost and given as (Sinha & Chandel, 2015b):

$$C_{npc,tot} = \frac{C_{ann,tot}}{CRF(i,R_{proj})} \qquad (2.5)$$

where, $C_{ann,tot}$ is the total annualized cost ($/year), i is the annual real interest rate (%), R_{proj} is the project lifetime (year), CRF represent capital recovery factor. The CRF and $C_{ann,tot}$ are given by the following equations (Lanre Olatomiwa et al., 2015):

$$CRF(i,N) = \frac{i(1+i)^N}{(1+i)^N - 1} \qquad (2.6)$$

$$C_{ann,tot} = C_{ann.cap} + C_{ann.rep} + C_{ann.O\&M} \quad (2.7)$$

where N and i are the number of years and annual real interest rate respectively. On the other hand, $C_{ann.cap}$, $C_{ann.rep}$ and $C_{ann.O\&M}$ are the annual capital, replacement, operation and maintenance cost respectively. Hybrid optimization model for electric renewable (HOMER) software, used in this study, does not use nominal interest rate in the computations but real interest rate which is computed from nominal interest rate using following equation (Ramli et al., 2015):

$$i = \frac{i\prime - f}{1+f} \quad (2.8)$$

In equation (2.8), f is the annual inflation rate and i′ is the nominal interest rate.

2.7.2.2 Cost of energy (COE)

The price of per kWh of electricity is called the cost of energy (COE) (Park & Kwon, 2016). The COE is computed by dividing the total annualized cost by annual electricity served to load which is defined as follows (Sinha & Chandel, 2015a):

$$COE = \frac{C_{ann,tot}}{L_{ann.load}} \quad (2.9)$$

From the above discussion, it is clear that the optimal sizing of the hybrid system is important both for the economic and technical issues of the system. The optimal sizing includes the optimal number and the capacity of system components like a wind turbine, PV panel, batteries and much more. In literature, the researchers mostly have used NPC, COE, and LPSP for the optimal sizing of a HRES.

2.7.3 Methodologies for optimal sizing of HRES

In literature, different methods employed for optimizing the size of a HRES. For example, the numerical algorithms (Kellogg et al., 1998), probabilistic approach (Borowy & Salameh, 1996), deterministic method (El-Hefnawi, 1998), graphical

construction method (Karaki et al., 1999), linear programming techniques (Chedid & Rahman, 1997), artificial intelligence techniques (Hanieh Borhanazad et al., 2014 Modiri-Delshad, & Mirtaheri, 2014; Shadmand & Balog, 2014; J. Wang & Yang, 2013; L. Wang & Singh, 2009) and software tools (Bahramara et al., 2016; Dalton et al., 2008; Sinha & Chandel, 2014) are employed for optimal sizing of the hybrid system that are summarized in Fig 2.9.

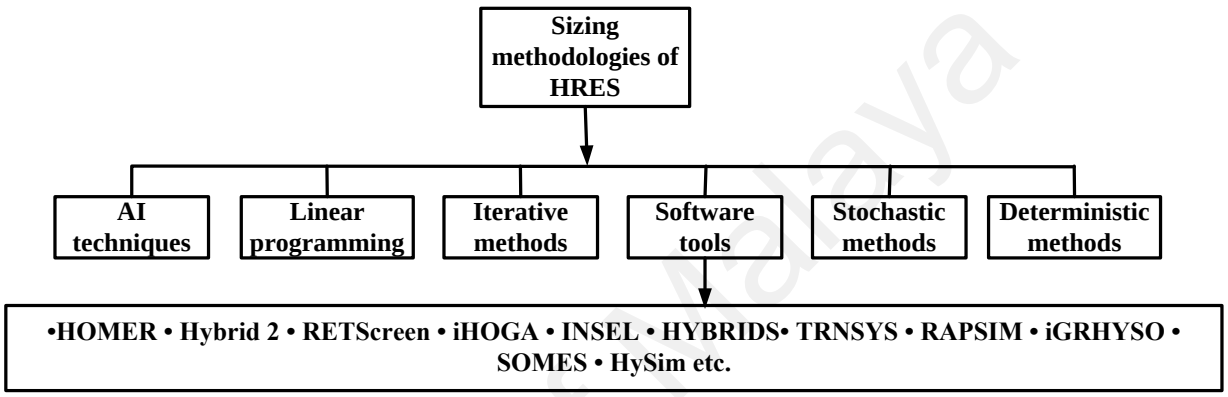

Figure 2. 9: Methodologies for optimal sizing of HRES.

As presented in Fig 2.9, there are different computer software tools for optimum sizing of a Hybrid RE system such as HOMER (Hybrid Optimization Model for Electric Renewable), Hybrid 2, RETScreen, iHOGA (Improved Hybrid Optimization by Genetic Algorithm), INSEL (Integrated Simulation Environment Language), HYBRIDS, TRNSYS (Transient Energy System Simulation Program), RAPSIM (Remote Area Power Simulator), iGRHYSO (Improved Grid Connected Renewable Hybrid System Optimization), SOMES (Simulation and Optimization Model for Renewable Energy Systems), and HySim (Hybrid Energy Simulation). Among them, HOMER is widely used, user-friendly software tools for designing and analysis of the hybrid system (Sinha & Chandel, 2014).

HOMER is a computer model developed by the U.S. National Renewable Energy Laboratory (NREL) in 1993 to assist in the design of micro power systems and to

facilitate the comparison of power generation technologies across a wide range of applications. HOMER models a power system's physical behavior and its life-cycle cost, which is the total cost of installing and operating the system over its life span. HOMER allows the modeler to compare many different design options based on their technical and economic merits. It also assists in understanding and quantifying the effects of the uncertainty or changes in the inputs (Lambert et al., 2006).

Figure 2.10 shows a typical architecture for the HOMER Pro micro grid analysis tool of version 3.3.3. It is vivid that seven significant steps necessary to design a HRES in HOMER model. These steps include: the meteorological resources input (solar, the wind and temperature, etc.), selection of system control (economic, fuel and weight minimization), project economics (discount and inflation rate, project lifetime, etc.) and dispatch strategy selection (load following and cycle charging), load and components modeling and finally sensitivity input selection. On the other hand, the output of HOMER model would be the net present cost (NPC), cost of energy (COE), a renewable fraction (RF), excess electricity (EE), emissions and much more.

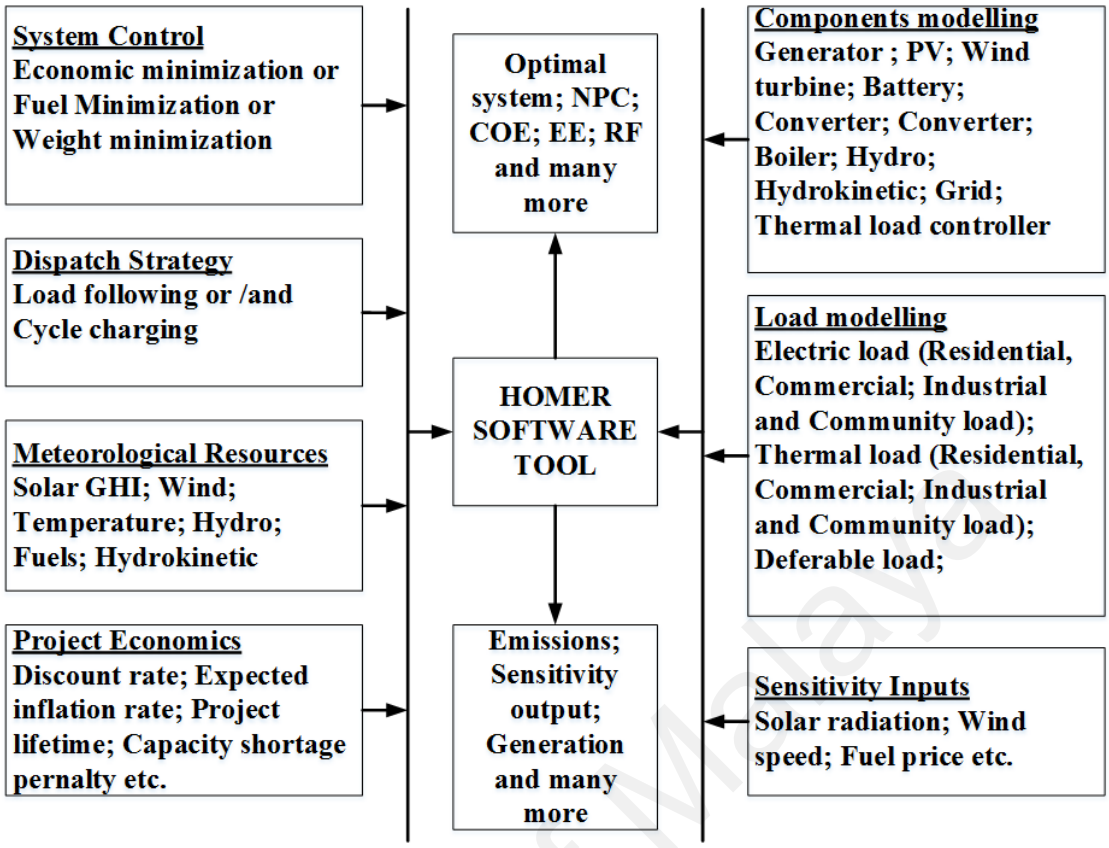

Figure 2.10: A typical architecture for HOMER micro grid analysis tool.

In this study, design and techno-economic analysis of the proposed off-grid PV-wind-diesel-battery hybrid system have been carried out with HOMER software. The results and analysis of this study will be useful in planning, feasibility study and decision-making purposes of a proposed hybrid system for the rural and remote resort facilities.

2.8 Summary

This chapter first addressed the energy status in Malaysia, followed by a review of different hybrid renewable energy system (HRES) and its topologies, assessment of solar and the wind potentials, and a review on the stand-alone and grid-connected HRES carried out by different researchers, with discovery that there is no particular study on the techno-economic performance analysis of HRES for tourist facilities located in rural and remote islands in the South China Sea, Malaysia. The hybrid

renewable system offers a lot of advantages over the single renewable source and conventional fuel based power system due to intermittent nature of renewable sources, high, volatile diesel fuel price and much more. Besides, among different hybrid systems, the hybrid AC-DC coupling system is considered the best configuration to provide the rural and decentralized electricity access. In this chapter, different methodologies for the hybrid system reliability analysis including the loss of power supply probability (LPSP) and the loss of load probability (LOLP) are presented. This chapter also presents the economic optimization methodologies including the net present cost (NPC) and the cost of energy (COE) methods. Among them, the LPSP and the NPC are commonly and popularly used methods for reliability and economic minimization of the hybrid system respectively. A brief review on the optimal sizing of the hybrid system is presented in this chapter. It is observed that there are different software tools in literature for optimum sizing and designing of a HRES and among them, HOMER (hybrid optimization model for electric renewable), developed by the U.S. National Renewable Energy Laboratory (NREL), is found to be the most popular, user-friendly and enriched software tool for this purpose. Thus, HOMER has been considered for the designing, optimal sizing, techno-economic and environmental analysis of the proposed hybrid renewable system.

CHAPTER 3: METHODOLOGY

3.1 Introduction

In this study, a complete design and the techno-economic analysis of a standalone hybrid PV-wind-diesel-battery system is proposed for the application in a remote and rural resort facilities where an extension of the national electric grid is not economically viable. A detailed methodology of this work is presented in the following flowchart:

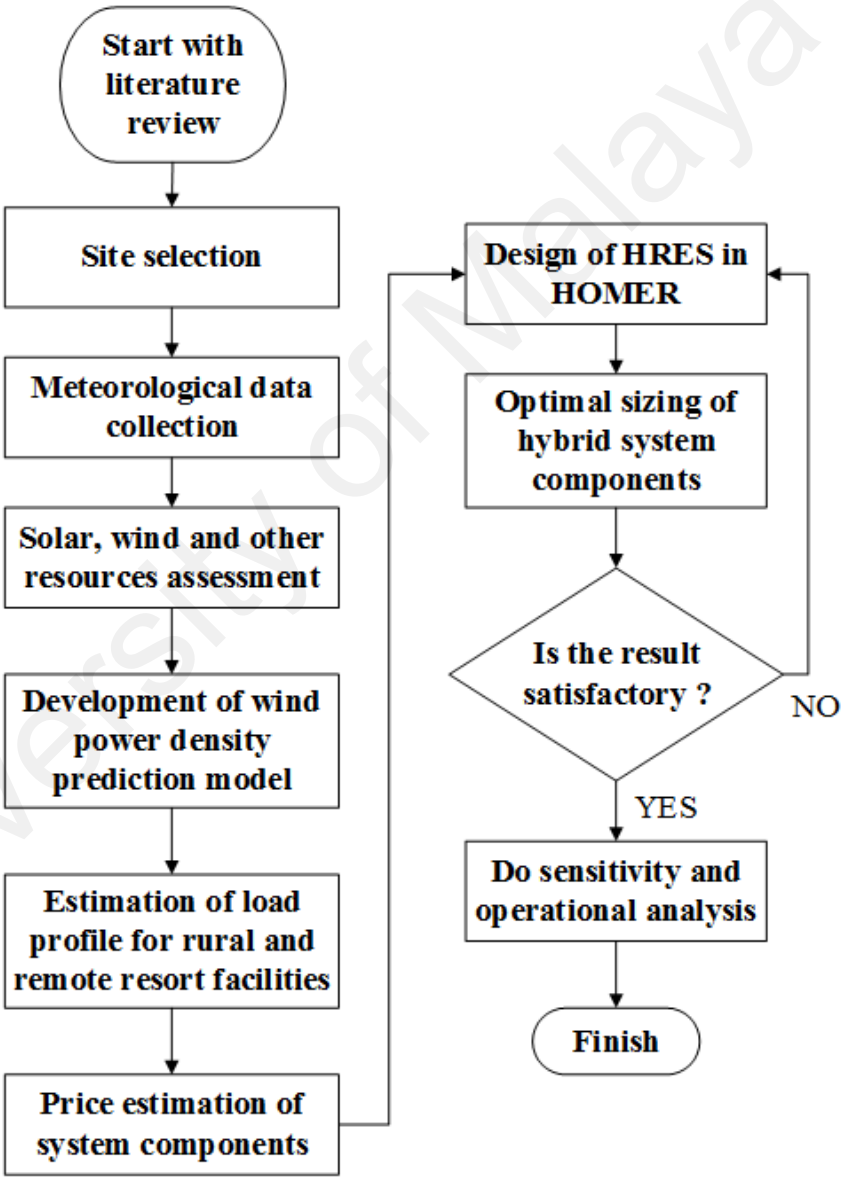

Figure 3. 1: Flowchart of the entire methodology.

3.2 Site selection, data collection and resources assessment

The Berjaya Tioman Resort (BTR), a big chalet style hotel and resort located in Tioman Island, was selected in this study for techno-economic design and analysis of the proposed hybrid RE system. The geographical location of the resort is 2° 48' 30" N, 104° 8' 29" E, as shown in Fig. 3.2. The resort is powered by the diesel generators installed at the resort. The resort is a chalet style architecture with 268 rooms and suites, two restaurants (Sri Nelayan and Natahari), 2 bars (beach bar and sunken pool bar), one ball room (Shahzanhall, I & II) which can accommodate approximately 400 guests, and 4 other separate meeting rooms (Mukut, I & II and Tioman, I & II) (Berjaya Tioman Resort, 2015).

Figure 3. 2: Location of BTR in Tioman Island [Source: Google map and then edited].

However, this island does not have any meteorological stations. The nearest meteorological station that collects wind data is the coastal station at Mersing, which is 32 km from the island. On the other hand, Hospital Kota Tinggi is the nearest station that collects solar radiation, which is 150km from the Tioman island (Basir Khan et al., 2016a). Basir Khan et al. (2015) proposed a HRES for Tekek Village in Tioman island

using solar data from the NASA surface meteorology and the wind data from Mersing station whereas, Ashourian et al. (2013) used both solar and wind data from NASA surface meteorology and solar energy database for optimal planning a hybrid RE system in Juara Village, Tioman island. Thus, this study has considered the case: designing the proposed hybrid system using the wind and solar data collected from meteorological station at Mersing and NASA surface meteorology and solar energy database respectively. It is important to note that the previous researchers have shown the capability of the meteorological data collected from NASA surface meteorology and solar energy database to model hybrid renewable energy system in places where measured data are not available. For example, the design and techno-economic feasibility studies of the HRES conducted in Ref. (Abdilahi et al., 2014; Adaramola, 2014; Adaramola et al., 2014; Fyrippis et al., 2010; N. Izadyar et al., 2016; L. Olatomiwa et al., 2015) used meteorological data from NASA surface meteorology and solar energy database. Monthly average global solar radiation for the period of July 1983 to June 2005 that was collected from NASA surface meteorology and solar energy database for Tioman Island is shown in Fig.3.3. Annual average solar radiation in Tioman Island is 5.21kWh/m^2/day.

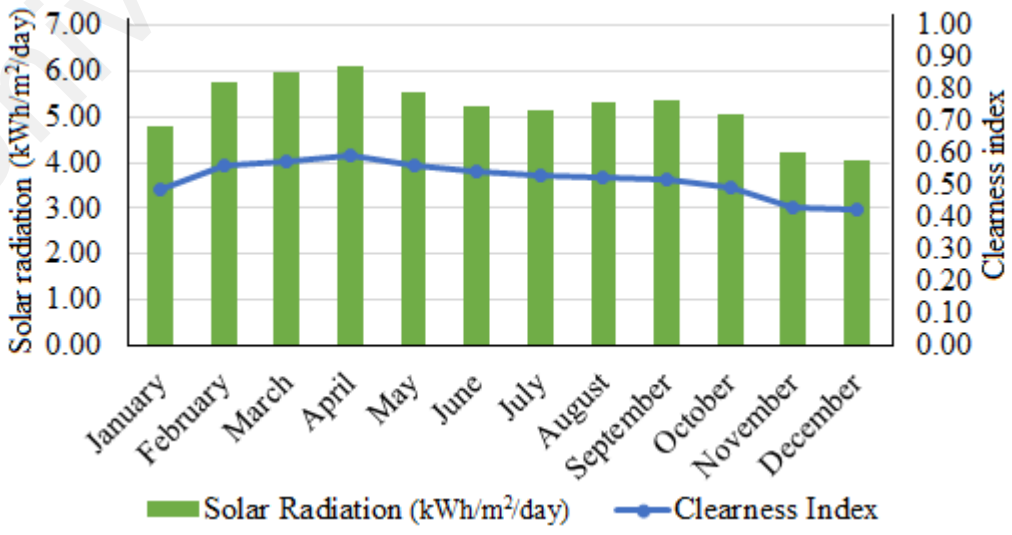

Figure 3. 3: Monthly average daily solar radiation and clearness index at Tioman Island.

On the other hand, the wind speed data of eleven years (2004-2014) that was obtained from MMD at Mersing. Daily average wind speed for the site is shown in Fig. 3.4 starting from 1 January 2004 to 30 December 2014. At this station, for the measurement of wind speed and wind direction, a rotating cup type anemometer and a wind vane were used at the height of 43.6m from sea level. The wind power law is used frequently to adjust wind speed data at various turbine hub heights (Ohunakin et al., 2011; Ramli et al., 2016).

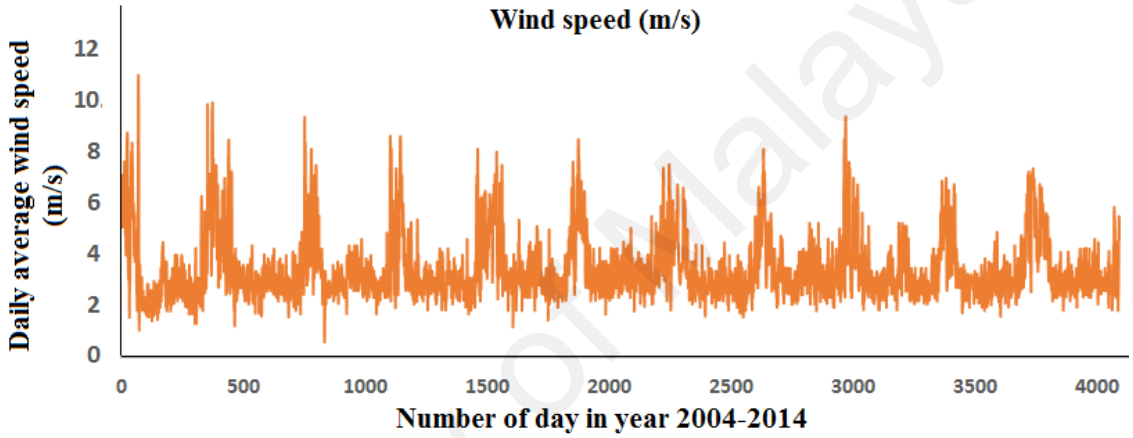

Figure 3. 4: Monthly daily wind speed of Tioman Island in 2004-2014.

3.3 Wind power density prediction

The aim of this dissertation is to predict wind power density of Mersing station, a coastal city situated in Southern part of Malaysia, which is 32km from the Tioman Island. Again, the prediction capabilities of proposed models will be validated by predicting monthly wind power density of three additional cities situated under three distinctive locations in Malaysia that are shown in Table 3.1.

Table 3.1: Location and description of the sites.

Locations	State	Location of meteorological stations		Measured height of wind speed (m)
		Latitude	Longitude	
Mersing	Johor	2° 27' N	103° 50' E	43.6
Kuala Terengganu	Terengganu	5° 23' N	103° 60' E	5.2
Pulau Langkawi	Kedah	6° 20' N	99° 44' E	6.4
Bayan Lepas	Pulau Penang	5° 17' N	100° 16' E	2.46

For this purpose, the data of wind speed was collected from Malaysian Meteorological Department (MMD) situated in the respective locations during the period of 2004-2014. As presented in Table 3.1, the wind data were measured at different heights above sea level by a rotating cup type anemometer. Those are 43.6m, 5.2m, 6.4m and 2.46m for Mersing, Kuala Terengganu, Pulau Langkawi, and Bayan Lepas respectively. It is important to mention that the wind data recorded in different heights need to adjust to the same height because of the various characteristics of wind speed with altitudes. The wind shear, which is the variation of wind velocity with altitudes, is most pronounced near the surface (sea and land). Due to the drag of surface and viscosity of air, the wind blows faster at higher altitudes.

Typically, the variation of wind speed at daytime follows the $1/7^{th}$ power law whereas, when the temperature become stable or better at night time, the wind speed close to the ground usually subsidies and at turbine altitudes, it does not decrease that much or may even increase. Thus, the daily average wind speed data was collected from the meteorological station and then adjusted at turbine hub height of 50m using power law. The power law for wind speed adjustment at different hub heights is defined as (Islam et al., 2011):

$$\frac{v}{v_o} = \left(\frac{h}{h_o}\right)^{\alpha} \qquad (3.1)$$

where v is the wind speed at the desired height h and v_o is the wind speed at measured height h_o. While α is power law coefficient. The exponent (α) is an empirically derived coefficient that varies depending upon the stability of the atmosphere. For neutral stable conditions, it is approximately 1/7, or 0.143, which is commonly assumed to be constant in the wind resource assessments. This is because the differences between the two levels are not usually so great as to introduce substantial errors into the estimation (usually<50m). The value of the coefficient varies from less than 0.10 for very flat land, water or ice to more than 0.25 for heavily forested landscapes and the typical value of α is 0.14 for low roughness surfaces. The value 0.143 for the coefficient has been chosen for this assessment (Islam et al., 2011; Justus, 1978; Ramadan, 2017).

3.3.1 Computation of wind power density

The wind power density (WPD) is an essential indicator to estimate the wind potentiality in a specific location. The computation methods of WPD include the application of measured wind data and the use of Weibull distribution function. The power in the wind at a measured wind speed v passing through a blade sweep area can be expressed as (Mohammadi et al., 2016; Mohammadi & Mostafaeipour, 2013):

$$\bar{P} = \frac{1}{2n} * \rho * \sum_{i=1}^{n} v^3 = \frac{1}{2} * \rho * \overline{v^3} \left(\frac{W}{m^2}\right) \qquad (3.2)$$

where n is the number of data points over a time period, $\overline{v^3}$ is the mean of cube of wind speed and ρ is the air density (kg/m^3) which is taken 1.175 kg/m^3 in this study (Akorede, Rashid, Sulaiman, Mohamed, & Ab Ghani, 2013). As presented in (Akdağ & Dinler, 2009; Justus, 1978), the 2-parameters Weibull distribution function is the most appropriate, recommended and accepted for the wind potentiality analysis.

In Weibull distribution, the probability distribution function (PDF) determines the probability of the wind at a given velocity V and PDF is expressed as (Arslan, 2010; Malik, 2011; Phuangpornpitak & Kumar, 2011):

$$f(V) = \left(\frac{k}{c}\right)\left(\frac{V}{c}\right)^{k-1} exp\left[-\left(\frac{V}{c}\right)^{k}\right] \qquad (3.3)$$

On the other hand, the cumulative distribution function (CDF) of wind speed V indicates the probability that the wind velocity is equal to or lower than Vor within a given wind speed range and the CDF is expressed as (Manwell et al., 2010; Ohunakin et al., 2011):

$$F(V) = 1 - exp\left[-\left(\frac{V}{c}\right)^{k}\right] \qquad (3.4)$$

where V is wind speed (m/s), k (dimensionless) is shape factor and c (m/s) is scale factor.

As earlier mentioned, the k and c (m/s) can be computed by several empirical methods. Commonly used is the standard deviation method. In this method, k and c are defined as follows (Islam et al., 2011):

$$k = \left(\frac{\sigma}{\bar{v}}\right)^{-1.086} \qquad (3.5)$$

$$c = \frac{\bar{v}}{\Gamma\left(1+\frac{1}{k}\right)} \qquad (3.6)$$

where $\bar{v}$ is the average wind speed (m/s), σ is standard deviation and $\Gamma(x)$ is the gamma function which is defined as (Jowder, 2009; Ohunakin et al., 2011):

$$\Gamma(x) = \int_0^\infty t^{x-1}e^{-t}\,dt \qquad (3.7)$$

Another empirical method is the power density or energy pattern factor method. In this method, E_{pf} is needed to be estimated to compute the shape factor k and scale

factor c (m/s). The E_{pf} is known as wind pattern factor which is used for wind turbine aerodynamic design and it is defined as follows (Akdağ & Dinler, 2009; Mohammadi & Mostafaeipour, 2013):

$$E_{pf} = \frac{\frac{1}{n}\sum_{i=1}^{n} v_i{}^3}{\left(\frac{1}{n}\sum_{i=1}^{n} v_i\right)^3} = \frac{\overline{v^3}}{\bar{v}^3} = \frac{\Gamma\left(1+\frac{3}{k}\right)}{\Gamma^3\left(1+\frac{1}{k}\right)} \qquad (3.8)$$

In simple word, E_{pf} is the ratio of mean of cube wind speed to cube of mean wind speed. When E_{pf} is known then shape factor k can be easily estimated by following formula (Akdağ & Dinler, 2009):

$$k = 1 + \frac{3.69}{(E_{pf})^2} \qquad (3.9)$$

The wind power density on the basis of Weibull probability density function is estimated using the following equation (Mohammadi et al., 2016):

$$\bar{P} = \frac{1}{2}\,\rho \int_0^{\infty} v^3 f_w(v)\, dv = \frac{1}{2}\rho\, c^3 \Gamma\left(1+\frac{3}{k}\right)\ (W/m^2) \qquad (3.10)$$

3.3.2 Development of the Prediction models

As mentioned in section 3.3, to accomplish the study objective, 11 years (2004-2014) long term wind speed data measured by a rotating cup-type anemometer were collected from the four different locations in Malaysia namely Mersing, Kuala Terengganu, Pulau Langkawi, and Bayan Lepas. The raw data was thereafter adjusted to turbine hub height of 50m. Afterward, the monthly mean wind speed at 50m and the corresponding wind power density from measured data were applied on the developed standalone ANFIS and hybrid ANFIS models. The proposed stand-alone ANFIS and hybrid ANFIS prediction models were developed on the MATLAB platform.

3.3.2.1 ANFIS (Adaptive neuro-fuzzy inference system)

The term adaptive neuro-fuzzy inference system (ANFIS) was first introduced by Jang in 1993. ANFIS is a hybrid intelligent scheme that merges the learning power of ANNs with the knowledge representation of fuzzy logic to produce a powerful processing tool (Jang, 1993). The fuzzy inference system (FIS) is the core of ANFIS. The FIS is based on expertise expression in terms of 'IF–THEN' rules, thus it can be used to predict the behavior of many uncertain systems. One of the advantages of FIS is that it does not require knowledge of the main physical process as a pre-condition for operation. Thus, ANFIS integrates FIS with a back propagation learning algorithm of a neural network. These techniques provide a method for the fuzzy modeling procedure to learn from available data set, in order to compute the membership function parameters that best allow the associated fuzzy inference system to track the given input/output data as shown in Fig.3.5. For one input, two fuzzy 'IF–THEN rule are generated for the maximum equal to 1 and minimum equal to 0.

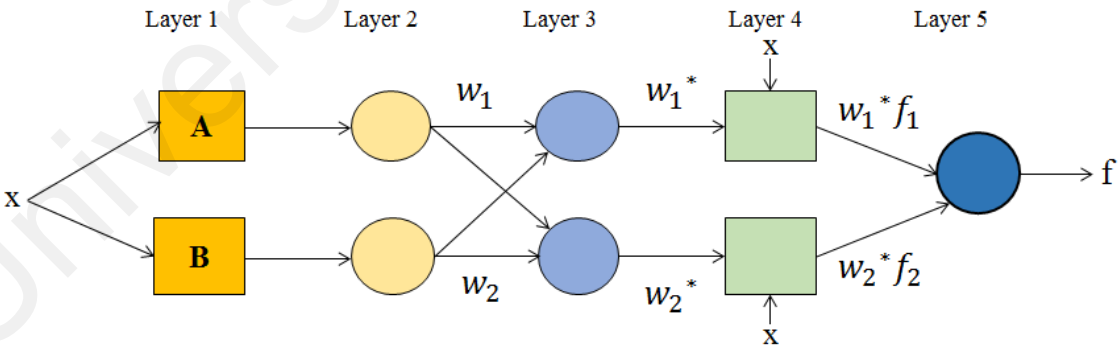

Figure 3. 5: ANFIS structure.

The fuzzy inference system employed in this study uses one input x and one output f. A first-order Sugeno fuzzy model with two fuzzy if-then rules is used as follows (Thakagi & Sugeno, 1983) :

Rule 1: $if\ x\ is\ A\ \ then\ f_1 = p_1 x + t_1$ (3.11)

Rule 2: $if\ x\ is\ B\ then\ f_2 = p_2 x + t_2$ (3. 12)

Fig. 3.6 represents the bell-shaped membership function (MF) with three parameters. The bell-shaped MFs is presented in Eq. 3.13, for which the lowest and highest amounts are 0 and 1, respectively.

$$f(x; a, b, c) = \frac{1}{1+\left(\frac{x-c}{a}\right)^{2b}} \quad (3.\ 13)$$

The function is subject to the following parameters, namely *a*, *b* and *c*. Each of these parameters defines as follows: *a* is half width of the curve; *b* defines the gradient together with *a*, and *c* is the midpoint of the membership function.

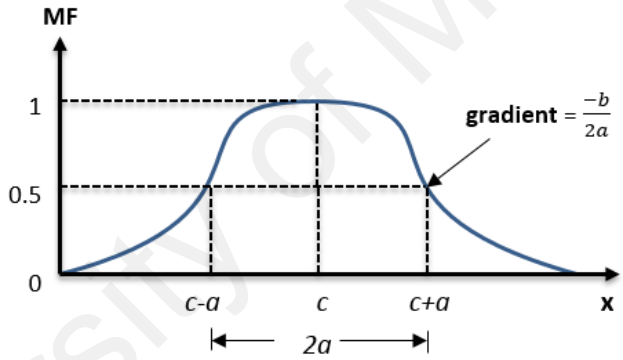

Figure 3. 6: Three parameters in bell membership function; a, b and c.

On the other hand, the formulation of each layer of ANFIS model shown in Figure 3.5 is summarized in Table 3.2.

Table 3. 2: The formulation of each layer of ANFIS model.

Layer	Formulations	Remarks
Layer 1	$O_{1,i} = \mu_{Ai}(x) \ \ for\ i = 1,2$ $where$ $\mu_{Ai}(x) = \frac{1}{1 + \left(\frac{x-c}{a}\right)^{2b}}$	Consists of membership functions (a, b), where the fuzzification process takes place. Every node in this layer is an adaptive node.
Layer 2	$O_{2,i} = w_i = \mu(x)_i \cdot \mu(x)_{i+1},$ $for\ i = 1,2$	This is a product layer, it multiplies the incoming signals from layer 1 to generate an output which is a linear combination of the inputs multiplied by the normalized firing strength, w_i . Each node in this layer is a fixed node.
Layer 3	$O_{3,i} = w_i^* = \frac{w_i}{w_1 + w_2},$ $i = 1,2$	In this layer, the normalization process takes place to scale the firing strengths. It also has the fixed nodes. The rule's firing strength to the sum of all rule's firing strength is calculated for the corresponding node.
Layer 4	$O_{4,i} = w_i^* \cdot f = w_i^*(p_i x + t_i)$	This is a defuzzification layer. It delivers the output values resulting from the inference of rules, based on the consequent parameter, where every node *i* is an adaptive node.
Layer 5	$O_{5,i} = \sum_i w_i^* . f_i \ = \frac{\sum_i w_i . f_i}{\sum_i w_i}$	This is the output layer. It combines all inputs from the defuzzification layer and transforms the fuzzy classification leading to a crispy output. The node in this layer is non-adaptive and estimates the overall output of all incoming signals.

Three optimization techniques namely the PSO, GA, and DE were employed to adjust the ANFIS membership function parameters. The main benefit of combining these three techniques with ANFIS is to reduce the error rates by tuning and optimizing the membership functions.

3.3.2.2 ANFIS-PSO

PSO is an approach for optimizing "continue" and "discontinue" decision-making functions, which was developed by Dr. Kennedy and Dr. Eberhart in 1995 (Eberhart & Kennedy, 1995). PSO has been used to model animals' sociological and biological behavior (like groups of birds searching for food) (Bashir & El-Hawary, 2009). The PSO has also been employed in population-based search approach, in which a particle of a population is present for each individual potential solution or swarm. In this method, the position of each particle is changed constantly in a search space until getting to the optimum solutions and computational limitations are reached (Shoorehdeli et al., 2009).

In PSO, swarm starts with a group of random solutions, each of which is called a particle, and $\vec{s}_i$ represents the particle's position. Likewise, a particle swarm moves in the problem space, where $\vec{v}_i$ expresses the particle's velocity. A function f is evaluated at each time step through input $\vec{s}_i$. Every particle records its best position related to the best fitness gained to this point, in $\vec{p}_i$ vector. $\vec{p}_i{}^g$ tracks the most appropriate position identified by any neighborhood member. In universal form of PSO, $\vec{p}_i{}^g$ represents the best appropriate position in the entire population. A new velocity is achieved for any particle i in each iteration according to the best positions of individual, $\vec{p}_i(t)$ and $\vec{p}_i^g(t)$ neighborhood. The new velocity can be presented by:

$$\vec{v}_i(t+1) = w\vec{v}_i(t) + c_1\overrightarrow{\emptyset_1}.\left(\vec{p}_i(t) - \vec{x}_i(t)\right) + c_2\overrightarrow{\emptyset_2}.\left(\vec{p}_i^{\,g}(t) - \vec{x}_i(t)\right) \qquad (3.14)$$

In Eq. (3.14), w represents the inertia weight. The positive acceleration coefficients are shown by c_1 and c_2. $\overrightarrow{\emptyset_1}$ and $\overrightarrow{\emptyset_2}$ represent uniformly-distributed random vectors in [0,1], in which a random value is tried for every dimension. $\vec{v}_i$ limit in the [$-\overrightarrow{v_{max}}$, $\overrightarrow{v_{max}}$] range is reliant on the problem. Provided that the velocity exceeds the mentioned limit, in some cases it is rearranged within its suitable limits. The position of every particle alters depending upon the velocities as follows:

$$\vec{s}_i(t+1) = \vec{s}_i(t) + \vec{v}_i(t+1) \qquad (3.15)$$

According to Eq. (3.14) and (3.15), the particles incline to gather around the best.

Fig. 3.7 depicts the diagram of the sequential PSO and ANFIS combination (Juang, 2010).

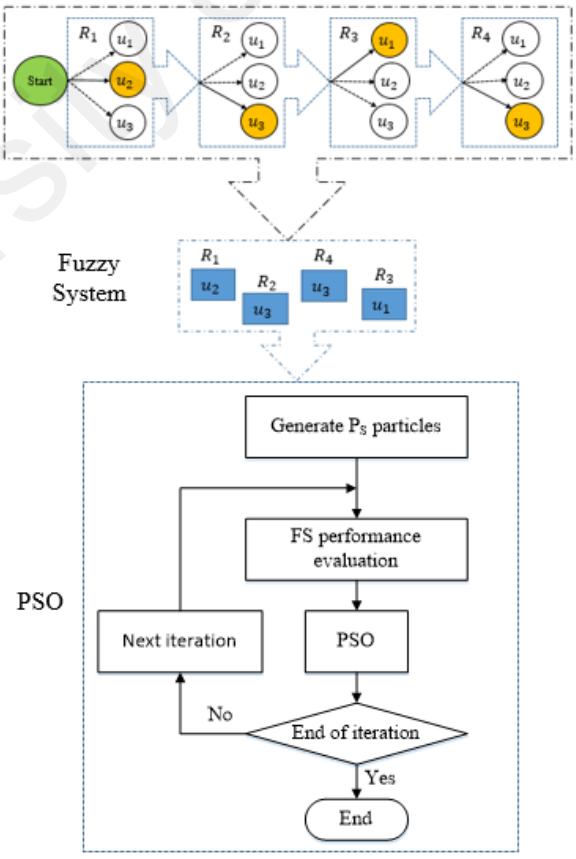

Figure 3. 7: Diagram of the sequential combination of PSO and ANFIS.

The PSO used for the designing a fuzzy system (FS) or parameter optimization is expressed as:

$$R_i: if\ x_1(k)\ is\ A_{i1}\ And\ \dots And\ x_n(k)\ is\ A_{in}\ , Then\ u(k)\ is\ a_i \qquad (3.16)$$

Here, a_i is a crisp value, k represents the time step, the input variables are $x_1(k), \dots, x_n(k)$, A_{ij} is a fuzzy set $and\ u(k)$ signifies the system output variable.

For the FS in Eq. (3.16) which comprises r rules and n input variables, its free parameters are defined through a position vector:

$$\vec{s} = [m_{11}, b_{11}, \dots, m_{1n}, b_{1n}, a_1, \dots \dots, m_{r1}, b_{r1}, \dots, m_{rn}, b_{rn}, a_r] \in \Re^D$$

(3. 17)

$$m_{rj} = x_j(k), b_{rj} = b_{fix},\ j = 1, \dots, n \qquad (3.18)$$

According to Eq. (3.17) and Eq. (3.18), the ith solution vector $\overrightarrow{s_i}$ is created as:

$$\overrightarrow{s_i} = [s_{i1}\ s_{i2} \dots\ s_{iD}] = [m_{11} + \Delta m_{11}^i, b_{fix} + \Delta b_{11}^i, \dots, m_{1n} + \Delta m_{1n}^i, b_{fix} + \Delta b_{1n}^i, a_1, \dots, m_{r1} + \Delta m_{r1}^i, b_{fix} + \Delta b_{r1}^i, \dots, m_{rn} + \Delta m_{rn}^i, b_{fix} + \Delta b_{rn}^i, a_r]$$

(3. 19)

In the Eq. (3.19), Δm_{ij} and Δb_{ij} represent small random numbers, a_i designates a random number distributed arbitrarily and homogeneously in the FS output range. The f (evaluation function) for $\overrightarrow{s_i}$ is calculated based upon the FS performance.

PSO looks for the best originator part parameters. P_s represents the population size. Eq. (3.17) sets the elements in position $\vec{s}$. When $t = 0$, the $\overrightarrow{s_1}(0), \dots, \overrightarrow{s_p}(0)$ or initial positions are created arbitrarily according to the best-performing FS found in PSO

($\vec{s}_{PSO}$). $\overrightarrow{s_1}(0)$ is considered similar to $\vec{s}_{PSO}$. The left $P_s - 1$ particles, $\overrightarrow{s_2}(0), \dots, \overrightarrow{s_{p_s}}(0)$, are created by addition of uniformly-distributed random numbers to $\vec{s}_{PSO}$ shown as:

$$\overrightarrow{s_i}(0) = \vec{s}_{PSO} + \overrightarrow{w_i},\ i = 2, \dots, P_s \qquad (3.20)$$

Here, $\overrightarrow{w_i}$ represents a random vector. The primary speed values of all particles, $\overrightarrow{v_i}(0)$, $i = 1, \dots, P_s$, are generated randomly. Each particle's performance is evaluated according to the FS. The f is described as the $E(t)$ or error index mentioned above.

The best position ($\overrightarrow{p_i}$) of each particle and the best particle $\overrightarrow{p_g^i}$ in the whole population is obtained according to f. Eq. (3.14) and (3.15) overhaul the velocity and position of each particle. The whole learning procedure is accomplished as soon as a pre-defined paradigm is obtained (Juang, 2010). There are five PSO main parameters used during conducting experiment as shown in Table 3.3, which are maximum number of iterations, population size of the domain, inertia weight, damping ratio, global and personal learning coefficient. For this case study, we determined these parameter's optimum values by trial and error procedure.

Table 3.3: Parameter characteristics for ANFIS-PSO.

Population Size	Iterations	Inertia Weight	Damping Ratio	Learning coefficient	
				Personal	Global
100	500	1	0.99	2	2

3.3.2.3 ANFIS-GA

Genetic Algorithm is a global search heuristics technique which is popularly used to find solutions for optimization and to solve highly complex search problems. It is a particular class of the evolutionary computing that is inspired from the idea of natural selection evolutionary process. The GA performs inheritance, mutation, selection, and recombination (Mitchell, 1998). In ANFIS-GA hybrid approach, GA is combined with

ANFIS to extend its prediction proficiency. More precisely, GA is implemented to improve the performance of the ANFIS by tuning and optimizing the membership functions of a Sugeno type fuzzy inference system. Later, the ANFIS-GA forecast allows reforming of the upcoming behavior of the wind power density and therefore, determines the viability of the wind power plants from any location. The hybrid ANFIS-GA model used in this study shown in Figure.3.8.

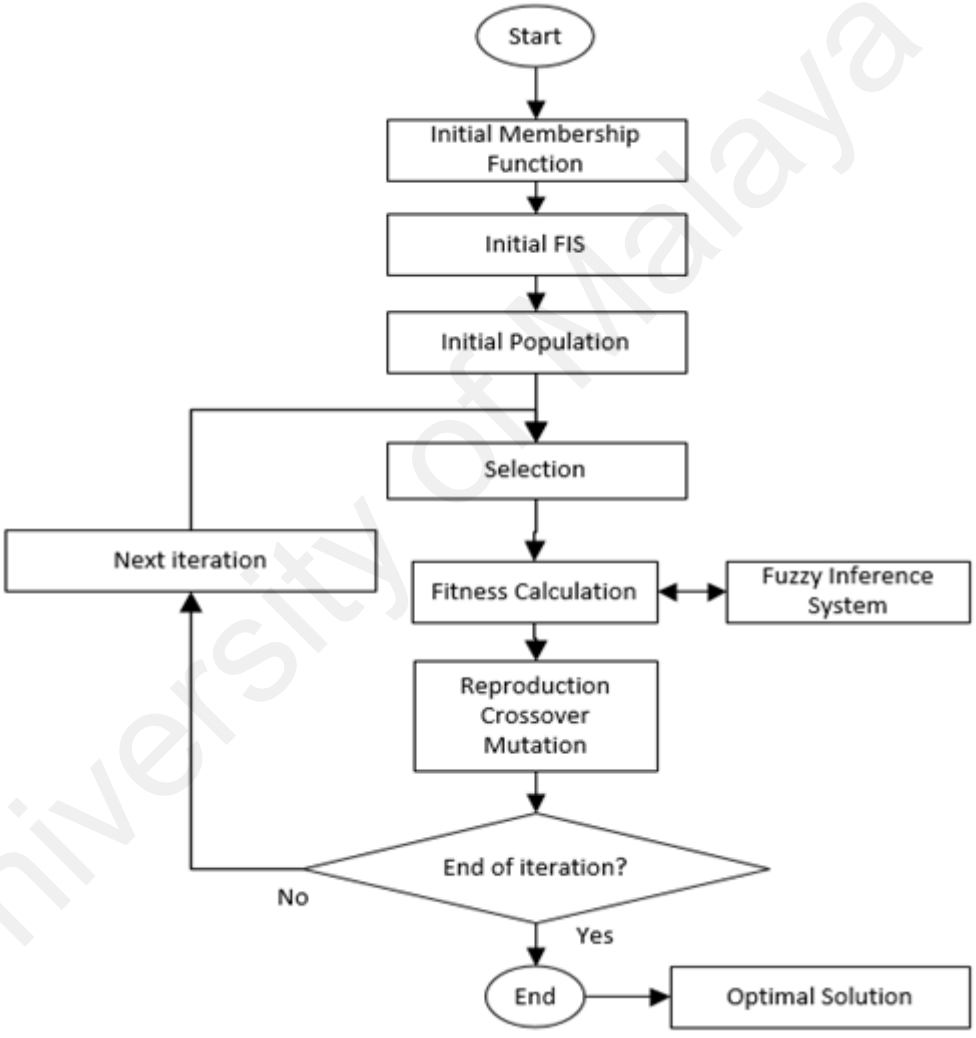

Figure 3. 8: ANFIS-GA Model.

GA model begins with a set of solutions (referred to as chromosomes) represented as population. A new population is drawn from the completion of a previous population. New solutions that formed from selected solution (offspring) are designated according to their fitness. This process is repeated until some condition occurs. For example, the

number of populations or improvement of the optimal solution is fulfilled. To achieve this, ANFIS algorithm plays an important role as part of the fitness function, $f(x)$. The fitness function with the intervention of ANFIS fitness function can be stated as:

$$f_1(x) = \frac{1}{m}\sqrt{\sum_{i=0}^{m}(d_i - a_i)^2} \qquad (3.21)$$

Where *m* is the number of feature attributes, a_i is the output derived through ANFIS, d_i is the desired wind power density.

The next fitness function can be presented as Eq. (3.22).

$$f_2(x) = \frac{1}{n-m}\sqrt{\sum_{i=m}^{n}(d_i - a_i)^2} \qquad (3.22)$$

Where, *n* is total number of input features, d_i is set to minimum, a_i is actual value of wind power density and $n - m$ represents remaining undesired features. The final equation is minimized $f(x)$, describe as,

$$f(x) = \frac{f_1(x)+f_2(x)}{2} \qquad (3.23)$$

For this case study, we determined specific parameters initialization for the genetic algorithm. These include a number of iterations, population size, mutation and crossover percentage. The selection of these parameters decides, to a great extent, the ability of the designed controller. The range of the tuning parameters is listed as follows in Table 3.4.

Table 3.4: Parameter characteristics for ANFIS-GA.

Population Size	Number of Iterations	Crossover Percentage	Mutation Percentage	Mutation Rate	Selection Pressure	Selection Function
100	500	0.8%	0.3%	0.02	8	Roulette Wheel

After the fitness function $f(x)$ of each chromosome *x* in the population is evaluated, a new population is created and following steps are repeated until it is completed. The better fitness gives a bigger chance to the parent chromosomes to be selected from a population. Then it is cross over the parents to form a new offspring with the crossover probability. The next mutation probability mutates new offspring at each position in the chromosome. As the solution goes under reproduction, crossover and mutation with parameters setting, the best solution in current population is returned if end condition is satisfied. The optimal solution calculated will help GA to search for optimized membership function.

3.3.2.4 ANFIS-DE

The differential evolution (DE) is first introduced as a heuristic method by Storn & Price (1997) to solve the problems which involve the global optimization, nonlinear and non-differentiable continuous space functions. Since both DE and GA are part of evolutionary computing, a method of DE's functioning is alike to GA's approach. The different in DE is using actual real numbers in the strict mathematical sense which can be applied to real-valued problems over a continuous space. As a result, the designs of crossover and mutation are significantly different. The idea behind the method of DE is that the difference between two vectors produces a difference vector which is used with a scaling factor to traverse the search space (Hegerty, 2009).

In ANFIS-DE hybrid approach, DE is combined with ANFIS to improve the performance of ANFIS prediction proficiency. The DE initializes with a population size of individual solutions which can be represented as $x_i^t = 1,2,\dots,popsize$ for each individual where *i* represents the population and t_{th} represents the generation to which the population belongs. Then the algorithm depends on the operation of three main operators namely mutation, crossover, and selection which are briefly described below and is shown in Figure 3.9.

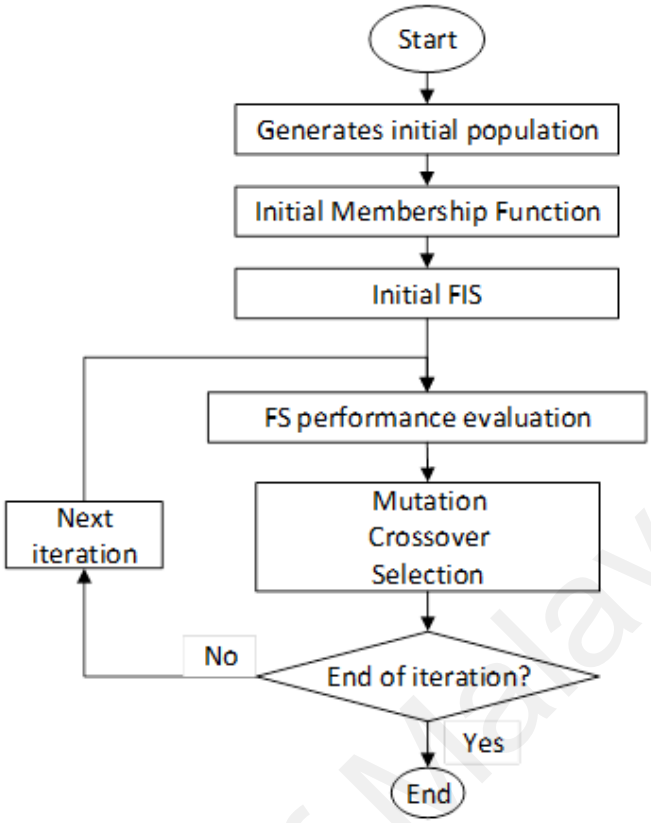

Figure 3. 9: ANFIS-DE Model.

The mutation operator is the main operator of DE which differs from other EAs. We implemented DE/rand/1 mutation strategy as described in Eq. 3.24.

$$u_i^t = x_{r_1}^t + F.(x_{r_2}^t - x_{r_3}^t) \qquad (3.24)$$

where, u_i^t is the mutant individual for x_i^t and r_1, r_2, r_3 are randomly selected and satisfy individuals. Moreover, they are not equal to running index (*i*) and mutually different. *F* is control parameter in the range of [0, 2]. The process crossover is carried out after the mutation phase is completed and can be described as,

$$y_{id}^t = \begin{cases} u_{id}^t & if\ rand \le C_R, \\ x_{id}^t & otherwise, \end{cases} \qquad (3.25)$$

where, y_i^t is the trial individual, d represents the d_{th} component of individuals. The *rand* and crossover rate C_R are parameters in the range of [0, 1].

The selection operation in DE is also different from other evolutionary algorithms. Once all *pop size* of the trial individuals is generated, the selection operation is processed as follows:

$$x_{id}^{t+1} = \begin{cases} y_i^t \text{ if fitness } (y_i^t) \leq \text{fitness } (x_i^t), \\ x_i^t \qquad\qquad \text{otherwise,} \end{cases} \qquad (3.26)$$

where fitness(x) is the fitness function. Table 3.5 shows our initial parameters for ANFIS-DE.

Table 3.5: Parameter characteristics for ANFIS-DE

Population Size	No. of Iterations	Crossover Percentage	Lower bound of scaling factor	Upper bound of scaling factor
100	500	0.2%	0.2	0.8

3.3.3 Statistical indicators model performance evaluation

The performance of the proposed system can be checked by computing several statistical parameters. The most popular statistical error indicators are the mean absolute bias error (MABE), mean absolute percentage error (MAPE), root mean square error (RMSE), and coefficient of determination (R^2). The MABE is the average quantity of the summation of all absolute bias error between the predicted and measured value which is represented as:

$$MABE = \frac{1}{N}\sum_{i=1}^{N}\left|\left(V_{i,P} - V_{i,M}\right)\right| \qquad (3.27)$$

The MAPE is the mean absolute percentage difference between the predicted and measured wind power density. The equation for MAPE is as follows:

$$MAPE = \frac{1}{N}\sum_{i=1}^{N}\left|\left(\frac{V_{i,P} - V_{i,M}}{V_{i,M}}\right)\right| \times 100 \qquad (3.28)$$

The RMSE presents the accuracy of the model by comparing the deviation between predicted and measured wind power density. The value of RMSE is always positive. It is defined as:

$$RMSE = \sqrt{\frac{1}{N}\sum_{i=1}^{N}\left(V_{i,P} - V_{i,M}\right)^2} \qquad (3.29)$$

The coefficient of determination (R^2) indicates the strength of the linear relationship between the predicted and measured wind power density. The R^2 is obtained by:

$$R^2 = 1 - \frac{\sum_{i=1}^{N}\left(V_{i,P} - V_{i,M}\right)^2}{\sum_{i=1}^{x}\left(V_{i,M} - V_{M,avg}\right)^2} \qquad (3.30)$$

In the Eq. (3.27-3.30), $V_{i,P}$ and $V_{i,M}$ are wind power density estimated from developed prediction models and measured data respectively.

3.4 Load estimation for the resort facilities

The resort is powered by diesel generators installed at the resort, but hourly load data was not available at the resort. Thus, hourly load profile of one year for the resort was estimated. The list of electric appliances employed, and their power rating is shown in Table 3.6, while the estimated daily average load profile for the resort is shown in Fig. 3.11 for different seasons. All the electric appliances and its numbers are computed based on the available information from the resort (Berjaya Tioman Resort, 2015).

Table 3.6: Load estimation of the resort based on the available information from the resort (Berjaya Tioman Resort, 2015).

Load description		Power rating (Watt)	Quantity (no.)	Running hour/day	Total power (kW)
Category	Appliances				
All 268 Rooms in chalets	Air conditioning	1,500	268	10	4020.0
	Cable TV	150	268	5	201.0
	Tube light	25	804	12	241.2
	Table light	18	536	5	48.24
	Ceiling fan	80	536	4	171.52
	Fridge	400	268	18	1929.6
	Hair dryer	2,500	268	2	1340.0
	Coffee maker	1,500	268	2	804.0
Conference room that accommodate 400 guests	Air conditioning	1,500	10	3	45.0
	Tube light	25	50	3	3.75
	CFL bulb	40	10	3	1.2
	Overhead projector	300	1	2	0.60
	Slide projector	200	1	2	0.40
	Microphone	10	5	1	0.05
	Desktop computer	120	1	3	0.36
	Laptop computer	80	1	2	0.16
4 meeting rooms	Air conditioning	1,500	8	4	48.0
	Tube light	25	15	4	1.5
	CFL bulb	40	15	4	2.4
	Slide projector	200	1	2	0.4
	Microphone	10	4	1	0.04
	Laptop computer	80	1	2	0.16
2 Bars & 2 Restaurants	Air conditioning	1,500	12	8	144
	Cable TV	150	4	5	3.0
	Refrigerator	400	8	12	38.4
	Tube light	25	30	8	6.0
	CFL bulb	40	20	8	6.4
	Ceiling fan	80	8	6	3.84
	Freezer	400	4	12	19.2
Resort Office	Air conditioning	1,500	2	10	30.0
	Tube light	25	5	5	0.625
	CFL bulb	40	5	5	1.0
	Desktop computer	120	1	10	1.2
	Refrigerator	400	2	8	6.4
	Printer	100	2	4	0.80
	Scanner	10	2	2	0.04
	Oven	3,000	1	2	6.0
Total					**9126.49**

The electrical load in this resort varies seasonally due to variation in tourist presence. The duration of northeast monsoon (NEM), the first inter-monsoon (FIM), the southwest monsoon (SWM), and the second inter-monsoon (SIM) are November-February, March-April, May-August, and September-October respectively that control the climate and weather in Tioman Island (Basir Khan et al., 2015). In NEM season, high wind speed and heavy rainfall affect the tourism business significantly. Consequently, the load profile of this resort is high during SWM, FIM, and SIM seasons and slightly low in NEM season as shown in Figure. 3.10.

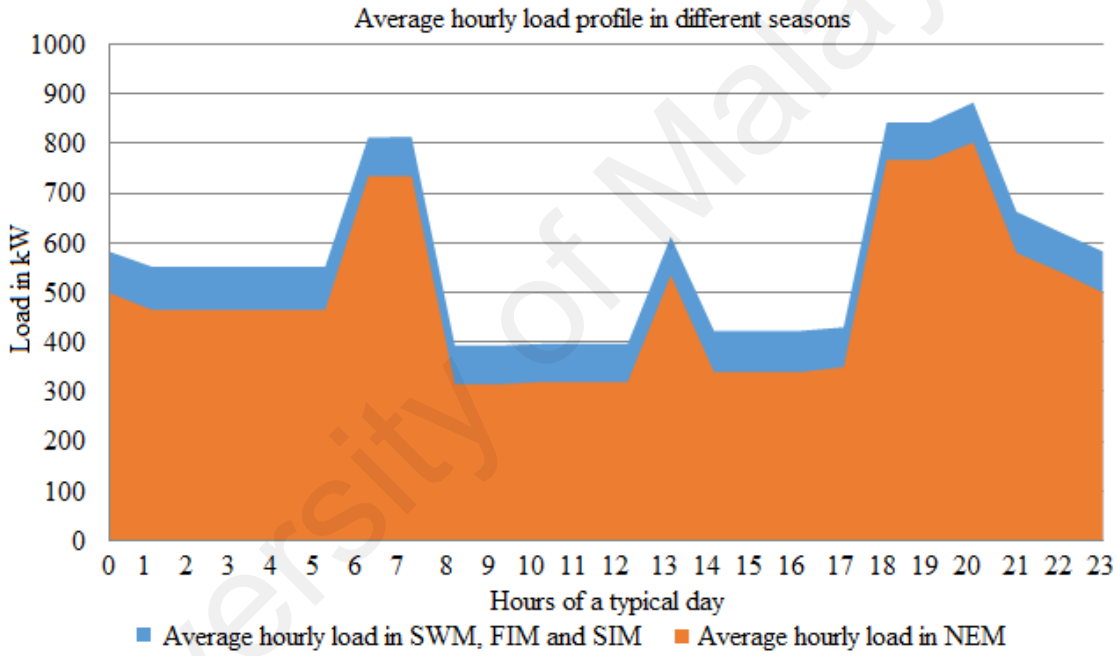

Figure 3. 10: Hourly average load profile of a typical day in different seasons for the resort.

Estimated hourly load data for one year served as input in HOMER taking a day to day load variance of 10% and a time step of 15%, which is presented in Figure. 3.11. Estimated peak load and average load per day were 1,185kW and 13,048kW respectively.

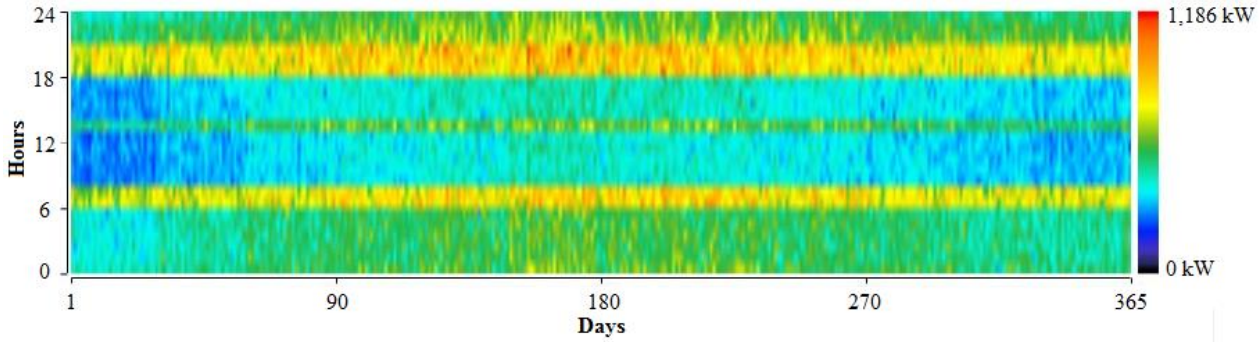

Figure 3. 11: Hourly average load profile in different days in a year considering a day to day variability 10% and a time step of 15%.

3.5 Modelling of HRES

The proposed HRES was primarily designed with the solar, wind, battery, converter, diesel generator and ac load profile as shown in Figure 3.12. The inputs of HOMER model were estimated hourly load profile data for one-year, monthly average wind speed, ambient temperature and solar irradiance, technical and economic data of system components and equipment characteristics. The diesel fuel price was considered $0.80/L which is 1.25 times over the diesel price forecasted in August 2014 by the Malaysian government for the mainland. The price of diesel for Malaysian Island is considered higher than the mainland price because of additional transportation and labor cost (Anwari et al., 2012).

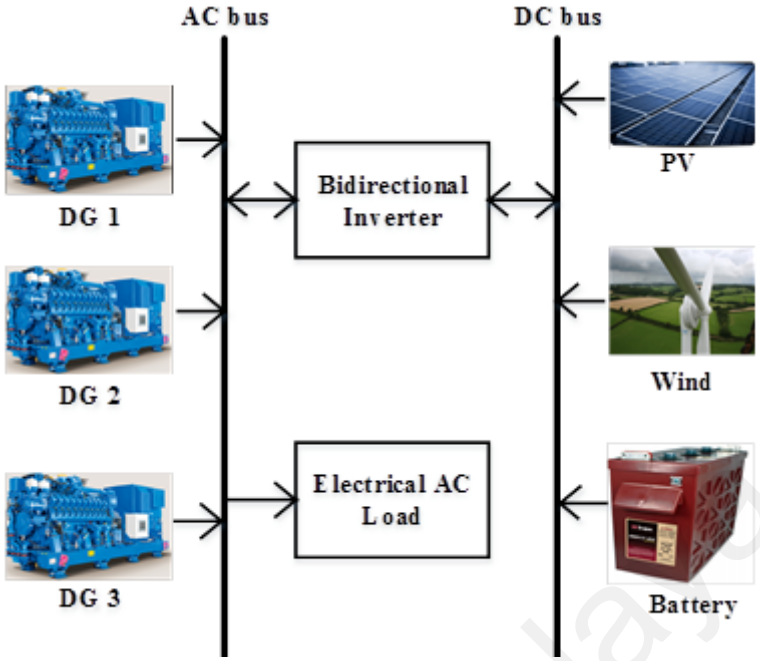

Figure 3. 12: HOMER model of the proposed hybrid renewable energy system.

3.5.1 Photovoltaic (PV)

Accurate modeling of the PV is important to get maximum power output from it and the output of a PV system varies for a different day and different seasons of the year due to the change in local meteorological conditions. Therefore, adequate information on the daily and seasonal pattern of the meteorological data will enable energy planners to have a better understanding of the performance of a PV system (L. Olatomiwa, 2016). Derating factor, temperature coefficient, azimuth and panel slope are important issues to consider while modeling a PV in HOMER. In this study, PV was designed using HOMER that uses following equation to calculate output power from PV panel:

$$P_{out,pv} = C_{R,PV} D_F \frac{G_T}{G_{T,STC}} \left[1 + \alpha_P \left(T_C - T_{C,STC}\right)\right] \qquad (3.31)$$

where, $C_{R,PV}$ is the rated capacity of the PV array (kW), D_F is derating factor, G_T and $G_{T,STC}$ are the solar radiation incident on the PV panel in the current time step (kW/m^2) and at standard test conditions (1kW/m^2) respectively, α_P is the temperature co-efficient of power (%/℃), T_C and $T_{C,STC}$ are PV cell temperature in current time step (℃) and

standard test conditions (℃) respectively. The PV size considered in this study ranged 0-1000 kW with step size of 50 kW. The temperature co-efficient, derating factor, operating temperature considered for the PV panel were -0.5/℃ , 80% and 47℃ respectively. The efficiency of the PV module at standard test condition was assumed 13%. The ground reflectance of 20%, default panel slope (2.79º), and azimuth (West to South) were considered for modeling of the PV panel. The tracking of the PV was not considered in this study. The capital and replacement cost of the PV were assumed $2000/kW with operation and maintenance cost of $10/kW/year.

3.5.2 Wind turbine (WT)

To extract maximum power from a wind turbine in any particular location, it is important to choose and design the wind turbine with favorable rated power, cut-in wind speed. Also, the wind speed that gives rated power based on the wind resources of the site is another factor to consider. HOMER calculates the power output of the wind turbine in each time step. This entails a three-step process. Firstly, HOMER adjusts the wind speed of measured height to given hub height of wind turbine. Secondly, it computes the power output at that height using the standard air density. Finally, HOMER adjusts the power output value for the actual air density.

In this study, EWT Direct Wind 52/54 wind turbine is selected for the site. The nominal output power of the turbine is 250 kW, with rated power output at 8 m/s and cut in wind speed 2.5 m/s. The hub height of 50m is considered for the turbine and power law as in Equation 3.1 is used to adjust measured wind speed to turbine hub height. The power curve with respect to the wind speed is very important when selecting a wind turbine for a particular location. The power curve for the selected wind turbine is shown in Figure 3.13 that was collected from manufacturers. Once HOMER determines the wind speed at hub height, it refers to the wind turbine's power curve to

calculate the power output at that wind speed under standard conditions of temperature and pressure. If the wind speed is below or above the cut-in and cut-out wind speed respectively, the turbine produces no power. After that, HOMER determines the output power at actual air density using following equation:

$$P_{out} = \left(\frac{\rho}{\rho_0}\right) * P_{out.STP} \qquad (3.32)$$

where, P_{out} and $P_{out.STP}$ are power output of the wind turbine at actual air density and at standard temperature and pressure (STP) respectively whereas, $\frac{\rho}{\rho_0}$ is the ratio of air density of the site at actual conditions to STP.

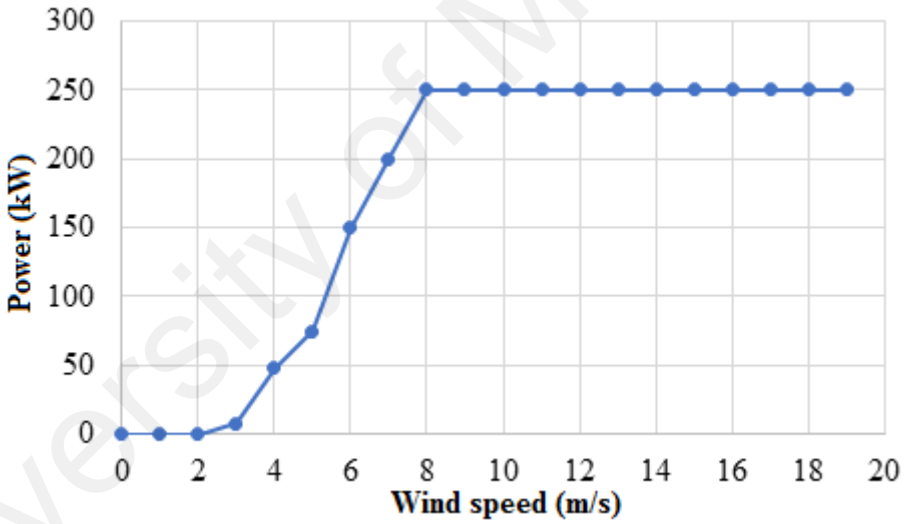

Figure 3. 13: Wind speed vs power curve of EWT DW 52/54 wind turbine.

The life time and capital cost of the turbine are considered 20 years and $375,000/unit respectively. On the other hand, replacement cost and operation-maintenance cost are considered 70 % (per unit) and 2% (per year) of the capital cost respectively. The performance of turbine can be examined by computing capacity factor of the wind turbine which is the ratio between mean power output to the rated electrical power output of the wind turbine given as (Mathew, 2006):

$$c_f = \frac{P_{e,avg}}{P_{eR}} = \frac{e^{-\left(\frac{v_c}{c}\right)^k} - e^{-\left(\frac{v_r}{c}\right)^k}}{\left(\frac{v_c}{c}\right)^k - \left(\frac{v_r}{c}\right)^k} - e^{-\left(\frac{v_f}{c}\right)^k} \qquad (3.33)$$

where, $P_{e,avg}$ and P_{eR} are average power output and rated the electrical power of the wind turbine respectively, while v_c , v_r and v_f are cut-in, rated and cut-off wind speed of the turbine provided by the manufacturers and besides, *k* and *c* are the Weibull shape and scale parameter that can be computed using equations 3.5 and 3.6 respectively. The capacity factor should not be less than 0.25 for cost effectiveness of wind power generation (Mathew, 2006). Thus, the resultant energy output from a wind turbine can be computed from following equation (L. Olatomiwa, 2016):

$$E_{out} = C_f * E_{rated} \qquad (3.34)$$

3.5.3 Diesel generator

Renewable energy sources are intermittent in nature and therefore, a combination of conventional energy sources with renewable ensure the steady and reliable power supply in a hybrid RE system. Diesel generator (DG) is commonly used in the hybrid system as the backup power source, especially when RE sources along storage battery are unable to supply load demand. Moreover, the output of PV is subjected to a ramp, which is not expected to the grid and thus, integrating diesel generators with PV for mitigating fluctuations has gained popularity. In HOMER, when designing a diesel generator several parameters are very important such as fuel type and price, fuel and efficiency curve, fuel properties, minimum load ratio and running hour, schedule maintenance, fuel measuring unit and so on. In this study, three diesel generators of Cummins brand with step size 50kW are designed having a maximum capacity of 0-1000kW (DG 1) and 0-500kW (DG 2 & 3) and minimum load ratio is considered 25% for all units. Diesel fuel ($/L) is chosen as fuel type that has following properties

described in Table 3.7 and Figures. 3.14 and 3.15 describe the fuel curve and efficiency curve.

Table 3.7: Diesel fuel properties and expected emissions.

Properties	**Quantity**	**Emissions (gm/L of fuel)**	**Quantity**
Lower heating value (MJ/kg)	43.2	Carbon Monoxide	6.5
Density (kg/m^3)	820	Unburned hydrocarbon	0.72
Carbon content (%)	88	Particulate matter	0.49
Sulfur content (%)	0.33	Nitrogen oxide	58
		Proportion of fuel sulfur converted to PM	2.2

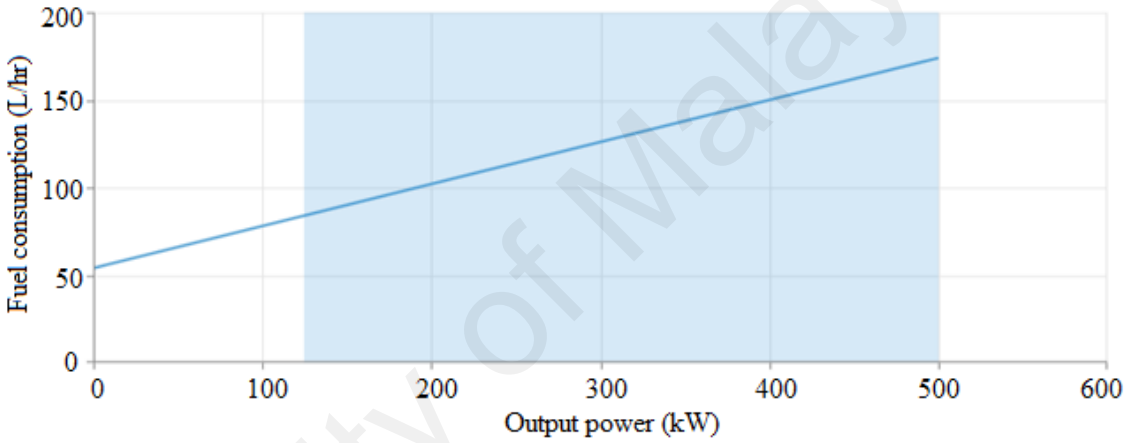

Figure 3. 14: Fuel curve of 500kW diesel generator generated in HOMER.

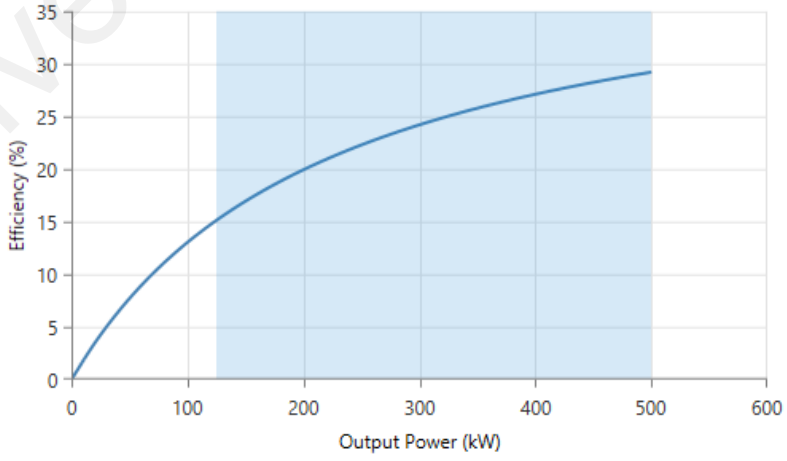

Figure 3. 15: Efficiency curve of a 500kW diesel generator generated in HOMER.

HOMER generates the fuel curve based on the following equation:

$$F = F_o Y_{gen} + F_1 P_{gen} \qquad (3.35)$$

where, F_o and F_1 are fuel curve intercept coefficient (L/hr./kW) and fuel curve slope (L/hr./kW) respectively while, Y_{gen} and P_{gen} are rated capacity of the generator (kW) and electrical output (kW) of the generator respectively. In this study, slope of 0.24 L/hr./kW and intercept coefficient of 0.108 L/hr./kW are used for 500kW reference diesel generator. The efficiency curve is generated based on the following relationship:

$$\eta_{gen} = \frac{3.6\, P_{gen}}{m_{fuel}\, LHV_{fuel}} \qquad (3.36)$$

where, m_{fuel} is the mass flow rate (L/hr.) of fuel which is defined as equation (3.37) and LHV_{fuel} is the lower heating value (MJ/L) which is a measure of energy content of the fuel.

$$m_{fuel} = \rho_{fuel}\left(\frac{F}{1000}\right) = \frac{\rho_{fuel}(F_o Y_{gen} + F_1 P_{gen})}{1000} \qquad (3.37)$$

In this study, the capital, replacement and O & M cost of diesel generators is considered \$220/kW, \$200/kW and \$0.03/hr. respectively. The diesel fuel price is considered \$0.80/L which is 1.25 times over the diesel price forecasted in August 2014 by the Malaysian government for the mainland. The price of diesel for Malaysian Island is considered higher than the mainland price because of additional transportation and labor cost (Anwari et al., 2012).

3.5.4 Battery energy storage

Due to random behavior of renewable energy sources, the battery capacity changes constantly. In every time step, HOMER calculates how much power can be absorbed or discharged by the battery bank based on the state of charge (SOC) of the previous time

step. When the output power from PV and wind turbine greater than the load demand, the storage battery goes through charging process if the SOC of the battery below the maximum allowable charging state. The battery charge capacity at this period can be described as (S. Diaf et al., 2007):

$$C_B(t) = C_B(t-1).(1-\sigma) + \left[P_T(t) - \frac{P_L(t)}{\eta_{inv}}\right] \times \eta_{batt} \qquad (3.38)$$

where, η_{inv} and η_{batt} are efficiency of inverter and battery respectively while, $P_L(t)$ and σ are load demand and self-discharging rate respectively. Whereas, $P_T(t)$ is total power generated by renewable sources at time *t* given as:

$$P_T(t) = N_{pv}P_{pv} + N_{wt}P_{wt} \qquad (3.39)$$

where, $N_{pv}\ and\ N_{wt}$ are number of PV panel and wind turbine respectively while, $P_{pv}\ and\ P_{wt}$ are power output from PV panel and wind turbine respectively.

However, when the power output from renewable sources is insufficient to meet load demand the battery goes through discharge process. The nominal capacity of the battery and charge quantity at this period can be modeled respectively as follows:

$$C_{Batt}\ (Wh) = \frac{P_L(t) \times AD}{\eta_{batt} \times \eta_{inv} \times DOD} \qquad (3.40)$$

$$C_B(t) = C_B(t-1).(1-\sigma) + \left[\frac{P_L(t)}{\eta_{inv}} - P_T(t)\right]/\eta_{batt} \qquad (3.41)$$

where DOD and AD are the depth of discharge and autonomy days of the battery.

AD is the ratio of the battery bank size to the electric load. HOMER calculates the battery bank autonomy using following equation:

$$AD = \frac{N_{batt}\, V_{nom} C_{nom} \left(1 - \frac{SOC_{min}}{100}\right)(24h/d)}{L_{avg}\ (1000Wh/kWh)} \qquad (3.42)$$

where, N_{batt} is the number of battery in the battery bank, V_{nom} is nominal voltage of a single battery (V), C_{nom} is nominal capacity of single battery (Ah) and L_{avg} is average primary load (kW/d).

During the discharging process, the discharge efficiency of the battery is equal to the 1, while it varies between (0.65-0.85) during charging period depending on charging current (L. Olatomiwa, 2016). At any time *t*, the battery charge capacity is subjected to the following constraints:

$$SOC_{min} \leq C_B(t) \leq SOC_{max} \qquad (3.43)$$

At this point, the maximum charge quantity of battery bank (SOC_{max}) takes the value of nominal capacity of the battery bank C_{Batt} and minimum state of charge (SOC_{min}) of battery is determined by DOD as follows:

$$SOC_{min} = (1 - DOD)C_{batt} \qquad (3.44)$$

It is important to note that the life of the battery can be prolonged if DOD is set within the range (30-50)% depending on the manufacturer's specifications (L. Olatomiwa, 2016).

In this study, Trojan IND17-6V lead acid battery is considered that has a nominal voltage of 6V with maximum capacity 1231 Ah. The life throughput of each battery is considered 9300 kWh while each string of battery consists of 40 batteries. The round-trip efficiency (%), capacity ratio (k), rate constant (c), maximum charge rate (A/Ah), maximum charge and discharge current (A) are considered 81, 0.478, 0.133, 1, 155 and 208 respectively.

3.5.5 Bi-directional converter

A bi-directional converter (AC to DC and/or DC to AC) is included in the hybrid system design to maintain proper energy flow between DC to AC bus. A system converter from HOMER tool is used in this study. The capital, replacement and O & M costs of the converter are considered $890/kW, $800/kW and 10/yr. respectively. The life time of the converter is considered 15 years. On the other hand, the efficiency of the bidirectional converter is considered 90 and 85 % when it works as inverter and rectifier respectively.

3.5.6 Technical constraints

In HOMER, technical and economic constraints are such pre-defined and pre-determined conditions that must be fulfilled to ensure the realistic and optimal design of the system. Some predefined technical and economic constraints are the maximum allowable renewable fraction, annual capacity shortage, and unmet electric load, and in this study, their value was considered 100%, 0.1%, and 0% respectively. The outputs of solar and the wind were reserved 30% and 50% respectively because of an unpredictable nature of solar radiation and the wind speed. The carbon dioxide penalty cost was taken as zero. The control parameters of the hybrid system were economic minimization, cycle charging, allow diesel off operation, multiple generator operations, and system with two types of wind turbine allow.

3.5.7 Economic constraints

The inflation rate in Malaysia was 2.1% in 2015 and 2016 (Bank Negara Malaysia, 2016). Thus, the discount and inflation rate for this study were considered 8 % and 2 % respectively. These economic parameters needed to compute CRF presented in equation 2.6. The lifetime of the project was considered 25 years with 0.1 percent annual capacity shortage. The system cost in HOMER was simulated in US dollars ($USD). At the time of this research work, USD 1 was 4.20 Malaysian Ringgit. HOMER does not

use nominal interest rate in the computations but the real interest rate which is computed from nominal interest rate (Ramli et al., 2015).

3.5.8 Control strategy

In HOMER, how the diesel generator and the battery in a hybrid system will behave is defined by control strategy set by the designer which is termed as dispatch strategy. There are two types of dispatch strategy in HOMER namely load following and cycle charging. In load following strategy, the generator will follow the peak load demand which means that a generator will produce sufficient power only to serve the load not to charge the battery bank. On the other hand, in cycle charging strategy, a generator always runs its maximum capacity when it needs to run. After meeting the load demand, extra power charges the battery bank. The load following strategy is good for the hybrid system where load demand per day is small whereas, cycle charging strategy is good for the hybrid system where load demand per day is large. Both control strategy can be used in a single design of the hybrid system and in this case, HOMER will determine which strategy is suitable and cost-effective and it categorizes the system based on the result. In this study, cycle charging is used as dispatching the power between the generator and the battery bank. Thus, both renewable power output and diesel generator charge the battery after meeting load.

3.5.9 Summary of techno-economic parameters for systems components

In the previous section 3.5.1-3.5.5, different technical and economic parameters for the system components briefly described. In Table 3.8, the technical and economic parameters for all components/equipment of the proposed hybrid system is summarized.

Table 3.8: Summary of technical and economic parameters for the design of HRES

PV			**Wind Turbine**	
Factors	**Value**		**Factors**	**Value**
Size (step size 100kW)	0-1000kW		Model	EWT DW 52/54
Capital cost	$2000/kW		Size considered	0-10

Replacement cost	$2000/kW		Nominal output	250kW
O & M cost	$10/kW/year		Capital cost (CC)	$375,000/unit
Temperature coefficient	-0.5/℃		Replacement cost	$262,500/unit (70% of CC)
Derating factor	80%		O & M cost	$7,500/year (2% of CC)
Operation temperature	47℃		Cut in wind speed	2.5 m/s
Battery			Rated wind speed	7.5/8 m/s
Factors	**Value**		Cut out wind speed	25 m/s
Model	IND 17		Life time	20 years
Nominal voltage	6 Volt		Hub height	50m
Capacity	1,231Ah		**Diesel Generator**	
Capital cost	$1,200/unit		**Factors**	**Value**
Replacement cost	$1,170/unit		Brand name	Cummins
O & M cost	$10/year.		Size (step size 50kW)	0-1000 kW (Generator 1)
String size (40/string)	0-10		Size (step size 50kW)	0-500 kW (Generator 2 & 3)
Life throughput per battery	9300kWh		Capital cost	$220/kW
Bi-directional Converter			Replacement cost	$200/kW
Factors	**Value**		O & M cost	$0.03/hr.
Size (step size 100kW)	0-1000kW		Minimum running hours	15,000hr.
Capital cost	$890/kW		Minimum load ratio	25%
Replacement cost	$800/kW		-	-
O & M cost	$10/kW/year		-	-
Lifetime	15 years		-	-
Efficiency	95%		-	-

3.6 Sensitivity analysis

A sensitivity analysis is important to extrapolate the effect of the uncertainty of renewable resources, economic conditions and much more in the project life time. In this study, the sensitivity variables were chosen as solar radiation, wind speed and diesel price to understand the effect on the cost of energy (COE), and they were varied

by ±30% from annual scaled average value. The sensitivity values for each variable is presented in Table 3.9.

Table 3. 9: Sensitivity variables in the selected project

Sensitivity variables	**Percentage of input variation from base value**						
	-30	-20	-10	0	+10	+20	+30
Solar radiation (kWh/m^2/d)	3.647	4.168	4.689	5.21	5.731	6.252	6.773
Wind speed (m/s)	2.611	2.984	3.357	3.73	4.103	4.476	4.849
Diesel price ($)	0.56	0.64	0.72	0.80	0.88	0.96	1.04

3.7 Summary

In this chapter, the entire methodologies of this research are presented. Firstly, the methodologies to compute wind power density from measured data and from standard deviation and power density method using Weibull distribution was discussed followed by the development of soft computing methodologies, including ANFIS (adaptive neuro-fuzzy inference system), ANFIS-PSO (particle swarm optimization), ANFIS-GA (genetic algorithm) and ANFIS-DE (differential evolution). In the proposed hybrid methodologies, the optimization algorithms like PSO, GA, and DE are used to minimize the prediction errors. Thereafter, different popular statistical error metrics such as mean absolute percentage error (MAPE), mean absolute bias error (MABE), relative root mean square error (RMSE) and coefficient of determination (R^2) were presented to measure prediction accuracy. After that, site description, data collection, resource assessment, and load estimation for the selected resort facilities were conducted. Renewable resource assessment is one of the most important steps to measure the feasibility of a renewable power generation system for any particular location. Furthermore, discussed in this chapter, is the methodologies for designing, modeling and techno-economic specifications of different hybrid system components like PV, wind turbine, diesel generator, battery, and converter which were designed in the hybrid optimization model for electric renewable (HOMER) software tool. Different technical, controlling and economic parameters also discussed here. Finally, this chapter

concludes with the sensitivity analysis method that was performed in HOMER to understand the impact of variation of different input parameters like solar radiation, wind speed, and diesel price.

CHAPTER 4: RESULT AND DISCUSSION

4.1 Introduction

In this chapter, prediction results from the proposed hybrid ANFIS models are analyzed and discussed, followed by the wind speed extrapolation capabilities of the proposed soft computing methodologies for the locations where measured wind data is not available. After that, this chapter presents a detailed techno-economic performance analysis of the proposed and modeled hybrid RE system in Tioman Island. Finally, a detailed sensitivity analysis on wind speed, solar radiation and diesel price has been conducted to see how these meteorological variables affect the performance of the proposed hybrid system.

4.2 Wind power density prediction

In this dissertation, hybrid ANFIS (ANFIS-PSO, ANFIS-GA, ANFIS-DE) and standalone ANFIS models were used to predict monthly wind power density (W/m^2) of Mersing, the nearest coastal city of Pulau Tioman. The distance between the meteorological station at Mersing and Pulau Tioman is 32km (Basir Khan et al., 2016b). Thereafter, the prediction capability and accuracy of the developed models were justified by predicting monthly wind power density (W/m^2) of three additional cities named Kuala Terengganu, Pulau Langkawi, and Bayan Lepas. The above-mentioned models were trained and tested with different data size. Table 4.1 and 4.2 show the descriptive values of input and output parameters respectively such as maximum (Max.), minimum (Min.), standard deviation (St Dev.) and ranges for different underlying locations.

Table 4.1: Descriptive statistical parameters of input (wind speed, m/s) for different locations.

Parameters	Locations			
	Mersing	Kuala Terengganu	Pulau Langkawi	Bayan Lepas
Max.	6.05	4.50	5.35	4.80
Min.	2.15	1.84	1.72	2.12
St dev.	0.87	0.57	0.72	0.52
Range	3.91	2.66	3.63	2.68

Table 4.2: Descriptive statistical parameters of measured WPD (W/m^2) for different locations.

Parameters	Locations			
	Mersing	Kuala Terengganu	Pulau Langkawi	Bayan Lepas
Max.	152.85	90.35	104.50	78.31
Min.	6.44	4.49	4.07	6.66
St dev.	33.80	17.75	17.28	13.73
Range	146.41	100.43	71.66	85.86

On the other hand, Fig 4.1 shows visual presentation of wind speed at 50m hub height for the study locations. It can be found from Fig. 4.1 that the maximum wind speed prevails in Mersing, followed by Bayan Lepas, Pulau Langkawi, and Kuala Terengganu.

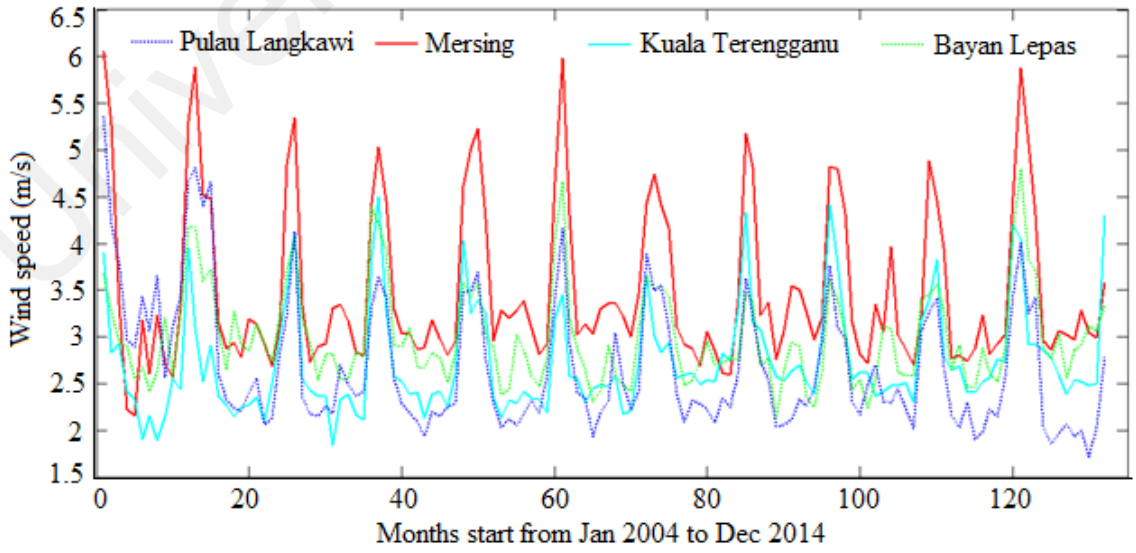

Figure 4. 1: Visual presentation of wind speed at 50m hub height of underlying locations.

However, the wind speed in Malaysia and several islands in the South China Sea is subjected to two major and two transitional climate conditions including the NEM (northeast monsoon), SWM (southwest monsoon), FIM (first inter monsoon) and the SIM (second inter monsoon). In NEM and SWM season, the wind speed is affected by northeasterly and southwesterly wind respectively. The SWM season usually begins in May and typically lasts up to three or four months. On the other hand, the NEM season usually occurs in November and ends in February or March of the next year. The two inter-monsoon periods happen between the southwest and northeast monsoon seasons. These generally take place in March to April, which is the FIM (first inter-monsoon), and from September to October, namely the SIM (second inter-monsoon) (Basir Khan et al., 2015). As mention earlier, the probability density function (PDF) determines the probability of the wind at a given velocity V and cumulative distribution function (CDF) of the wind speed indicates the probability that the wind velocity is equal to or lower than V or within a given wind speed range, i.e. they are used to characterize the wind velocity in Weibull distribution. In this study, the PDF and CDF of wind speed for the underlying locations are computed and plotted based on the equations (3.1-3.7) presented in section 3.3.1, which are shown in Figures (4.2-4.9).

From Figures. (4.2-4.3), it is observed that the wind speed range greater or equal to 3 m/s have the frequencies of about 94.49%, 89.15%, 88.74% and 85.98% for Mersing in NEM, SWM, FIM and SIM seasons respectively during the period of 2004-2014.

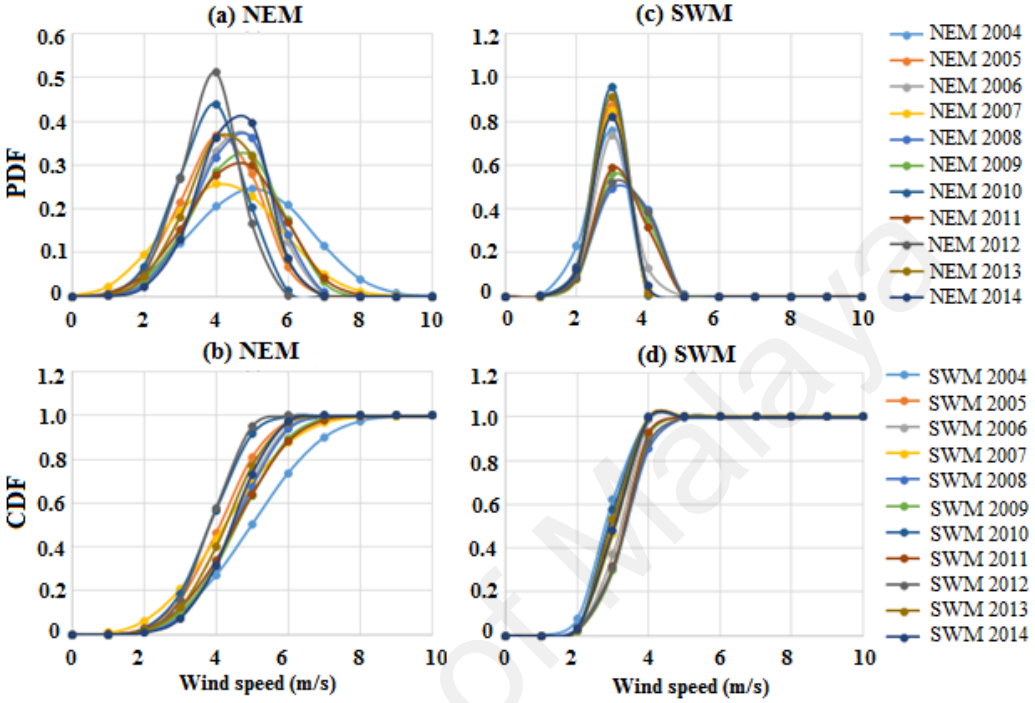

Figure 4. 2: (a) PDF, (b) CDF in NEM and (c) PDF, (d) CDF of wind speed in SWM for Mersing during 2004-14.

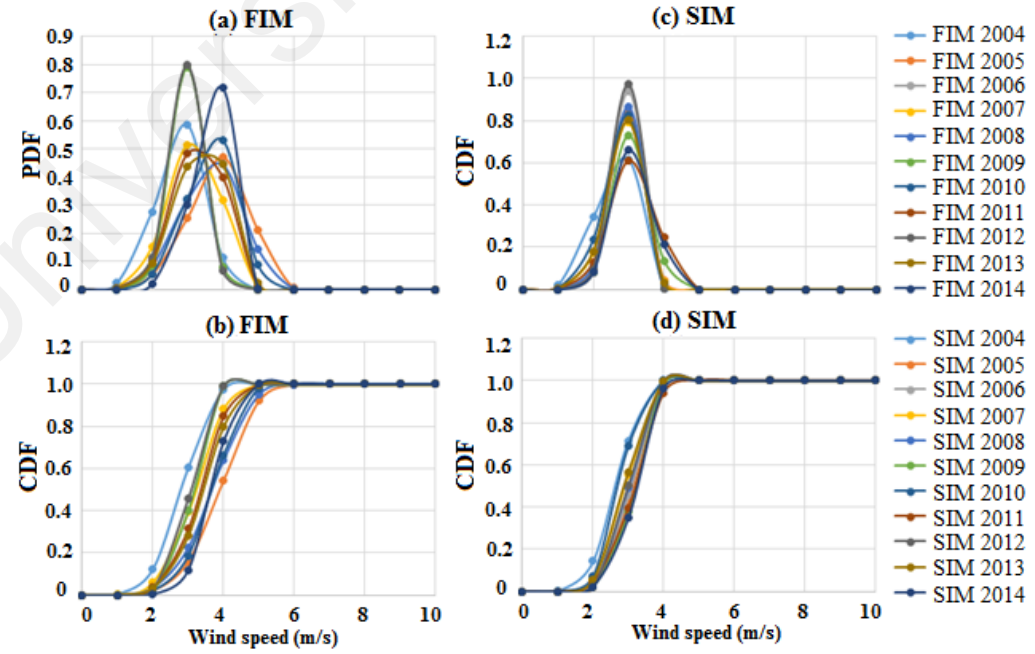

Figure 4. 3: (a) PDF, (b) CDF in FIM and (c) PDF, (d) CDF of wind speed in SIM for Mersing during 2004-14.

On the other hand, in Pulau Langkawi, the wind speed range greater or equal to 3 m/s have the frequencies of about 79.46%, 30.94%, 61.65% and 35.92% in NEM, SWM, FIM, and SIM respectively during 2004-2014 which is observed in Figures. (4.4-4.5).

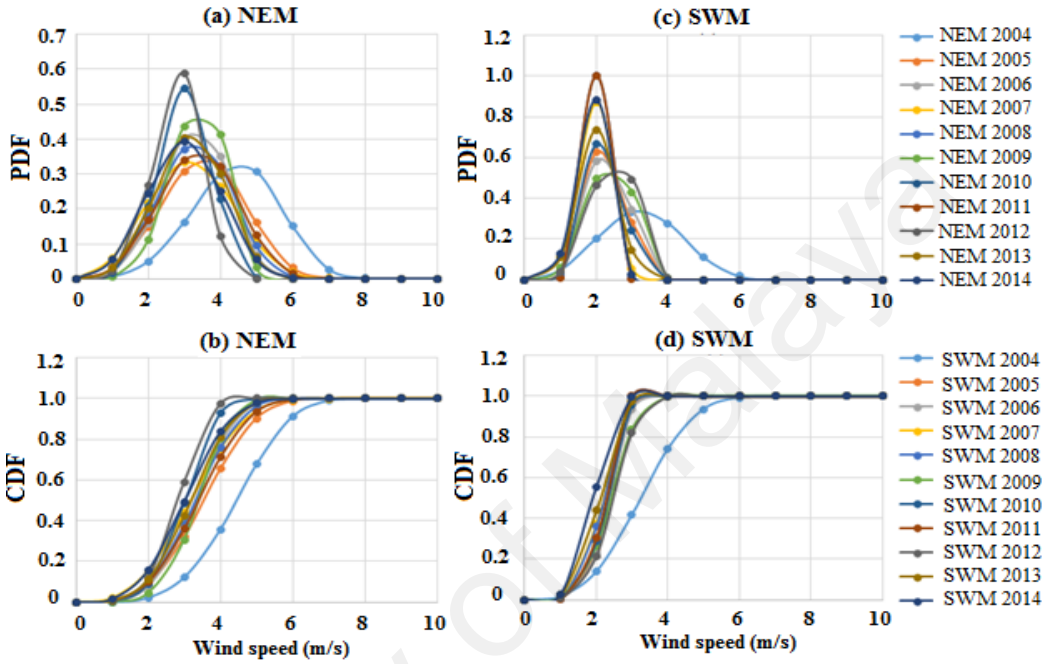

Figure 4. 4: (a) PDF, (b) CDF in NEM and (c) PDF, (d) CDF of wind speed in SWM for Pulau Langkawi during 2004-14.

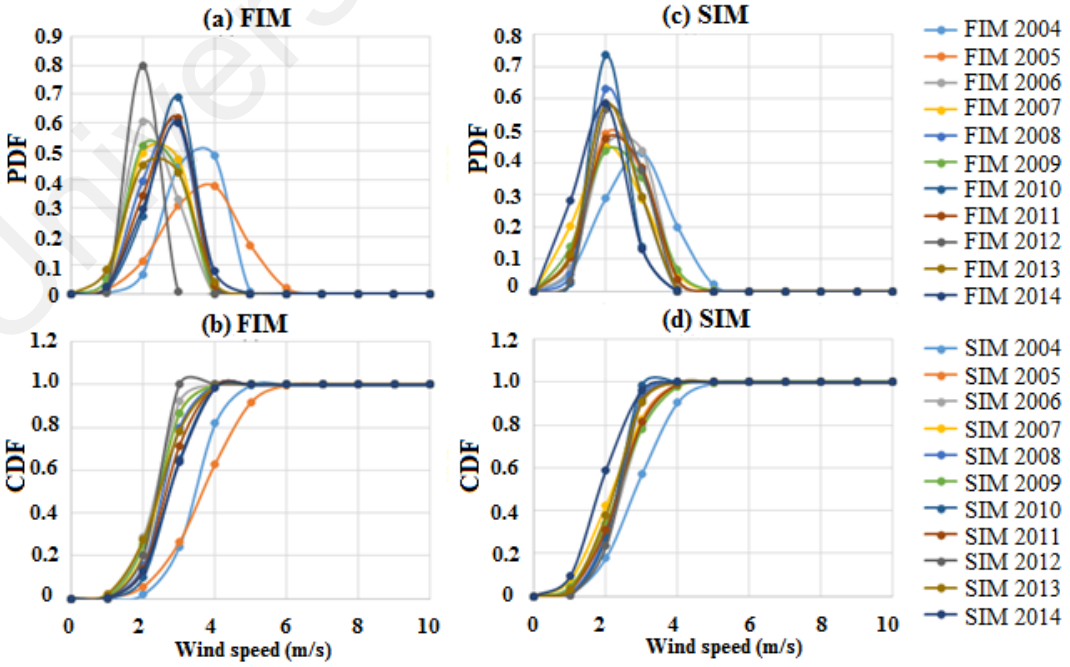

Figure 4. 5: (a) PDF, (b) CDF in FIM and (c) PDF, (d) CDF of wind speed in SIM for Pulau Langkawi during 2004-14.

From Figures (4.6-4.7), the wind speed range greater or equal to 3 m/s were found to be 85.29%, 64.09%, 80.70% and 63.98% in Bayan Lepas during the NEM, SWM, FIM, and SIM respectively.

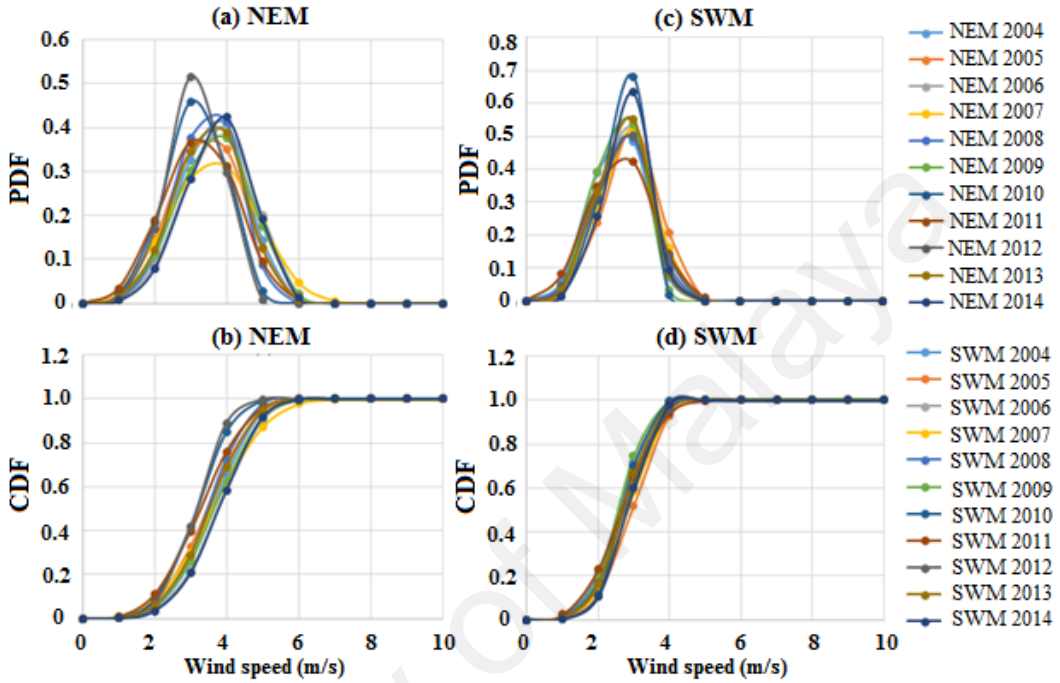

Figure 4. 6: (a) PDF, (b) CDF in NEM and (c) PDF, (d) CDF of wind speed in SWM for Bayan Lepas during 2004-14.

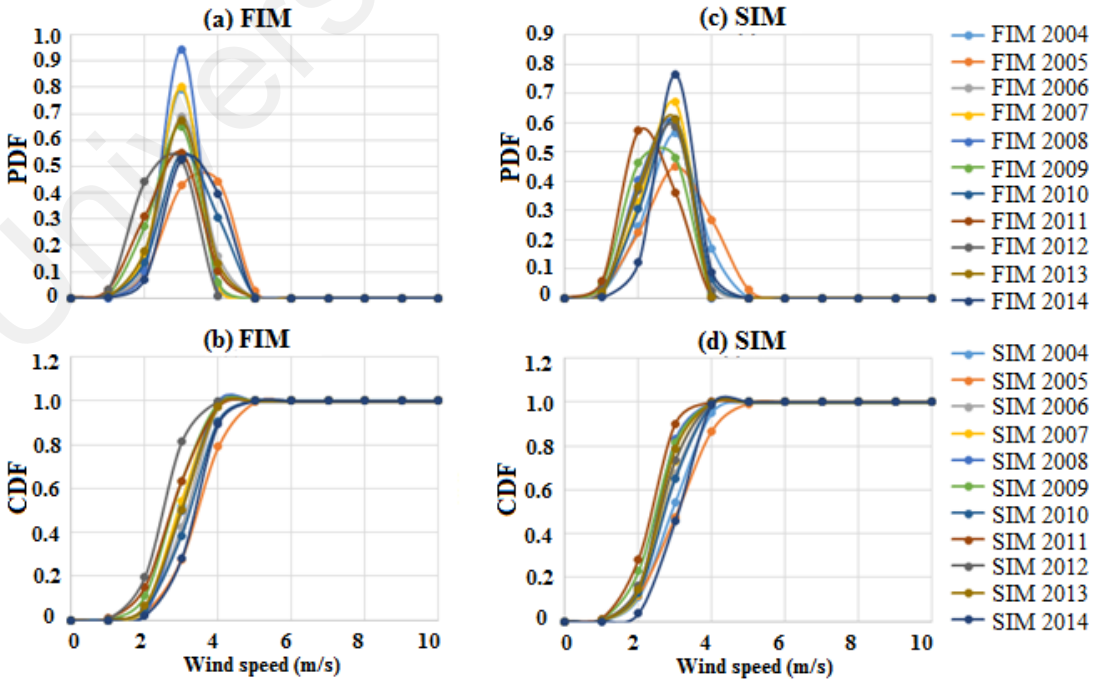

Figure 4. 7: (a) PDF, (b) CDF in FIM and (c) PDF, (d) CDF of wind speed in SIM for Bayan Lepas during 2004-14.

It is observed in Figurs (4.8-4.9) that these frequencies were 74.79%, 36.93%, 72.07% and 36.10% for Kuala Terengganu during the NEM, SWM, FIM, and SIM respectively.

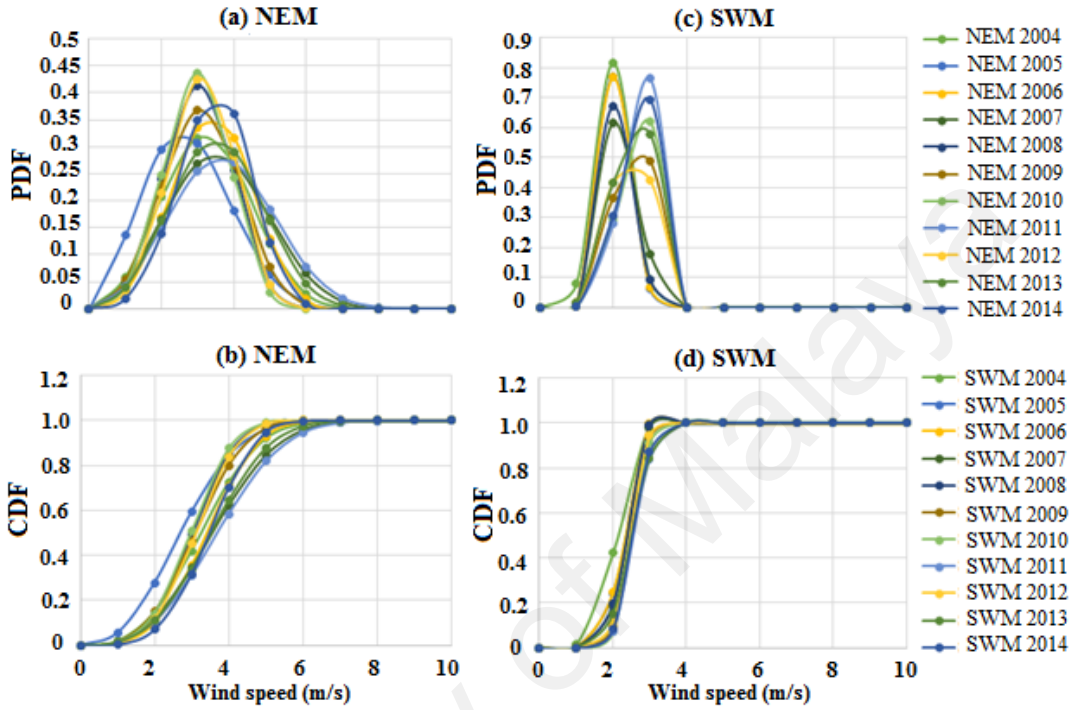

Figure 4. 8: (a) PDF, (b) CDF in NEM and (c) PDF, (d) CDF of wind speed in SWM for Kuala Terengganu during 2004-14.

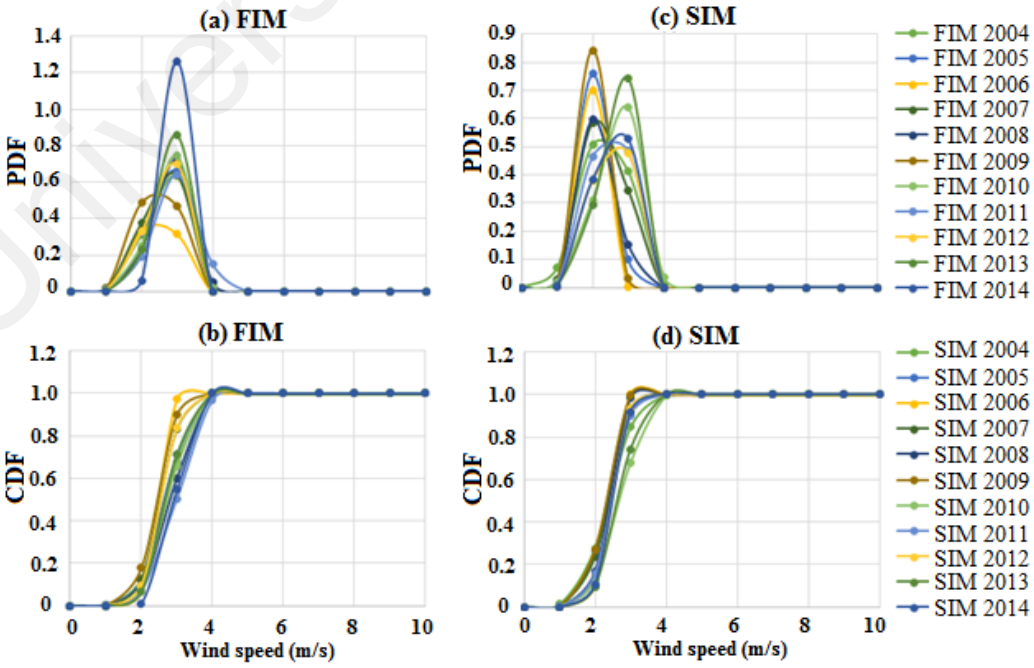

Figure 4. 9: (a) PDF, (b) CDF in FIM and (c) PDF, (d) CDF of wind speed in SIM for Kuala Terengganu during 2004-14.

Overall, it is found from Figs. (4.2-4.9) that the NEM season is the windiest season for all underlying locations whereas, the wind speed characteristics in the SWM, FIM, and SIM is more or less similar. It is important to note that most unstable wind speed prevails in SWM season for all study locations.

However, as described that the proposed soft computing models were trained and tested with different training and testing data set. The data size used for the training and testing the prediction models are defined as P and Q respectively. Based on the literature, the percentage of training data must be higher than the testing data for effective learning of the system before the system can produce a good result. The developed models were trained and validated with several data segments such as P=80%, Q=20%; P=70%, Q=30% and P=60%, Q=40% for training and testing respectively. The percentage of data selected for training and testing has been carefully tested based on the minimal error obtained in the statistical indicator. It is important to mention that no specific rules were considered to choose the data size for training and testing the models. Application of different training and testing data size on the prediction models helps to observe the error metrics and to choose best data size providing the minimum error in the prediction.

Table 4.3 presents the error metrics such as MAPE, MABE, RMSE obtained while training the prediction models with the input-output data set for Mersing, Langkawi, Bayan Lepas, and Kuala Terengganu. The data set consists of P=105 (80%) and Q=27 (30%) observations during the period of Jan. 2004 to Sep. 2012 and Oct. 2012 to Dec.2014 when training and testing the models respectively. In this study, the performance of the prediction models is categorized based on the smallest RMSE. The error metrices presented in result and discussion part in tables (4.3-4.8) are not from any single simulation. Usually, the error of prediction would not be same every time it run, more or less the error varies from one run/simulation to other (slightly). Thus, the

predictions models were run many times, especially as long as the models does not provide stable output, and after the stabilization, the average error metrics of all stable simulations were listed in results.

Table 4. 3: A Statistical model comparison in training the models when first 80% data applied on prediction models.

Locations	Rank	Prediction models	Training			
			RMSE	MAPE (%)	MABE	R^2
Mersing	1	ANFIS-PSO	4.96	5.14	2.61	0.9781
	2	ANFIS-GA	5.41	5.77	2.63	0.9756
	3	ANFIS-DE	5.50	9.70	3.03	0.9749
	4	ANFIS	5.82	10.88	3.07	0.9728
Pulau Langkawi	1	ANFIS-GA	3.13	10.17	1.89	0.9709
	2	ANFIS-PSO	3.16	10.96	1.90	0.9703
	3	ANFIS	3.26	11.70	1.96	0.9684
	4	ANFIS-DE	3.30	10.10	1.90	0.9676
Bayan Lepas	1	ANFIS-PSO	2.14	7.88	1.65	0.9762
	2	ANFIS	2.28	9.06	1.74	0.9709
	3	ANFIS-GA	2.34	8.52	1.72	0.9692
	4	ANFIS-DE	2.54	9.04	1.83	0.9638
Kuala Terengganu	1	ANFIS-PSO	3.73	8.90	1.91	0.9523
	2	ANFIS-GA	4.0	10.30	2.19	0.9449
	3	ANFIS	4.03	14.57	2.29	0.9448
	4	ANFIS-DE	4.37	18.30	2.88	0.9392

It can be observed from Table 4.3 that ANFIS-PSO model has lowest RMSE, MAPE and MABE in the training stage for the data set of Mersing, Bayan Lepas, and Kuala Terengganu whereas, ANFIS-GA ranks in the first for the data set of Pulau Langkawi. The RMSE, MAPE, and MABE performance metrics, when testing data set of different underlying locations is applied to the predictions models, are summarized in Table 4.4. It can be observed from Table 4.4 that the ANFIS-GA model ranks in the first for the data sets of Mersing and Kuala Terengganu. On the other hand, ANFIS-PSO model provides the smallest error metrics for the data set of Pulau Langkawi and Bayan Lepas.

Table 4. 4: A Statistical model comparison in testing the models when rest 20% data applied on prediction models.

Locations	Rank	Prediction models	Training			
			RMSE	MAPE (%)	MABE	R^2
Mersing	1	ANFIS-GA	5.04	5.25	2.52	0.9701
	2	ANFIS-PSO	5.10	5.88	2.67	0.9691
	3	ANFIS	5.14	6.65	2.74	0.9690
	4	ANFIS-DE	5.56	9.22	3.26	0.9636
Pulau Langkawi	1	ANFIS-PSO	1.53	11.11	1.21	0.9774
	2	ANFIS-DE	1.59	13.07	1.19	0.9775
	3	ANFIS-GA	1.72	10.27	1.23	0.9737
	4	ANFIS	2.17	23.07	1.79	0.9578
Bayan Lepas	1	ANFIS-PSO	2.37	8.17	1.82	0.9749
	2	ANFIS	2.49	9.02	1.92	0.9720
	3	ANFIS-GA	2.75	7.27	1.83	0.9659
	4	ANFIS-DE	2.81	8.84	1.96	0.9643
Kuala Terengganu	1	ANFIS-GA	4.79	13.65	3.06	0.9412
	2	ANFIS-PSO	4.92	10.77	3.54	0.9456
	3	ANFIS-DE	5.01	21.67	3.70	0.9355
	4	ANFIS	5.37	12.97	3.15	0.9261

It is important to mention that sometimes ANFIS model provides better performance than the hybrid ANFIS models but does not provide best model performance for any of the underlying locations. For instance, ANFIS shows second and third best performance for the data set of Bayan Lepas and Mersing respectively when testing the prediction models.

The R^2 is the correlation between the measured and predicted WPD, which has the highest value of one. A pronounced observation of R^2 from Table 4.3 and 4.4 reveals that a very good correlation between measured and predicted WPD obtained when training and testing the prediction models using the data set from Mersing, Pulau Langkawi, and Bayan Lepas. On the other hand, the measured and predicted WPD of Kuala Terengganu suffer comparatively lower correlation when training and testing the prediction models.

Furthermore, the performance of the developed prediction models is compared to different training and testing data size to illustrate the effect of data size on the prediction accuracy. Tables (4.5-4.8) summarize the RMSE, MABE, MAPE, and R^2 when input-output data sets of Mersing, Pulau Langkawi, Bayan Lepas, and Kuala Terengganu respectively are applied to the prediction models. In this case, training and testing data set consists of P=92 (70%) and Q=40 (30%) observations during the period of Jan. 2004 to Aug. 2011 and Sep. 2011 to Dec.2014 respectively. Again, to choose the best data size that will provide the optimal error in WPD prediction, all the developed models were trained and tested with another input-output data size, which consists of P=80 (60%) and Q=52 (40%) observations during the period of Jan. 2004 to Aug. 2010 and Sep. 2010 to Dec.2014 respectively. Tables (4.5-4.8) also summarize the RMSE, MABE, MAPE, and R^2 when training and testing the prediction models with this data size.

Table 4. 6: Effect of data size for the prediction wind power density of Mersing.

Data Size	Training						Testing					
	Rank	Prediction models	RMSE	MABE	MAPE (%)	R^2	Rank	Prediction models	RMSE (W)	MABE (W)	MAPE (%)	R^2
70% training 30% testing	1	ANFIS-PSO	5.23	2.64	6.88	0.9786	1	ANFIS-PSO	5.37	2.75	5.95	0.9663
	2	ANFIS-GA	5.36	2.92	9.45	0.9712	2	ANFIS-GA	5.46	2.89	6.53	0.9651
	3	ANFIS	5.39	2.92	10.28	0.9767	3	ANFIS	5.55	2.94	7.06	0.9640
	4	ANFIS-DE	5.52	2.81	7.84	0.9756	4	ANFIS-DE	5.72	2.84	5.68	0.9617
60% training 40% testing	1	ANFIS-PSO	5.41	2.82	6.40	0.9780	1	ANFIS-PSO	5.22	2.79	6.40	0.9662
	2	ANFIS-GA	5.59	3.33	8.95	0.9765	2	ANFIS-DE	5.33	3.58	11.56	0.9652
	3	ANFIS	5.82	3.13	12.46	0.9745	3	ANFIS-GA	5.46	3.34	8.95	0.9634
	4	ANFIS-DE	6.21	4.29	11.56	0.9709	4	ANFIS	5.48	3.12	7.55	0.9632

Table 4. 5: Effect of data size for the prediction wind power density of Bayan Lepas.

Data Size	Training						Testing					
	Rank	Prediction models	RMSE	MABE	MAPE (%)	R^2	Rank	Prediction models	RMSE (W)	MABE (W)	MAPE (%)	R^2
70% training 30% testing	1	ANFIS-PSO	2.17	1.64	7.85	0.9748	1	ANFIS-PSO	2.54	1.74	7.83	0.9684
	2	ANFIS-GA	2.22	1.69	7.99	0.9740	2	ANFIS-GA	2.62	1.78	7.67	0.9584
	3	ANFIS	2.24	1.72	8.95	0.9698	3	ANFIS	2.73	1.93	9.95	0.9541
	4	ANFIS-DE	2.38	1.73	7.98	0.9738	4	ANFIS-DE	2.80	1.87	8.25	0.9577
60% training 40% testing	1	ANFIS-PSO	2.18	1.56	7.29	0.9770	1	ANFIS	2.65	1.96	11.67	0.9441
	2	ANFIS	2.25	1.73	8.35	0.9756	2	ANFIS-PSO	2.74	1.98	11.14	0.9409
	3	ANFIS-GA	2.46	1.77	7.71	0.9707	3	ANFIS-DE	2.77	2.18	11.76	0.9398
	4	ANFIS-DE	3.34	2.34	10.23	0.9461	4	ANFIS-GA	3.38	2.0	9.39	0.9252

Table 4. 7: Effect of data size for the prediction wind power density of Pulau Langkawi.

Data Size	Training						Testing					
	Rank	Prediction models	RMSE	MABE	MAPE (%)	R^2	Rank	Prediction models	RMSE (W)	MABE (W)	MAPE (%)	R^2
70% training 30% testing	1	ANFIS-PSO	3.29	1.92	10.28	0.9707	1	ANFIS-PSO	1.69	1.38	12.28	0.9717
	2	ANFIS-GA	3.34	1.92	10.09	0.9698	2	ANFIS-GA	1.71	1.31	11.89	0.9707
	3	ANFIS	3.38	2.03	11.60	0.9690	3	ANFIS-DE	1.88	1.44	11.55	0.9650
	4	ANFIS-DE	3.43	2.21	13.08	0.9682	4	ANFIS	2.23	1.84	20.39	0.9508
60% training 40% testing	1	ANFIS	3.45	2.14	11.64	0.9705	1	ANFIS-GA	2.04	1.64	18.18	0.9572
	2	ANFIS-GA	3.58	2.19	12.61	0.9668	2	ANFIS	2.20	1.66	17.19	0.9501
	3	ANFIS-DE	4.06	3.04	19.24	0.9591	3	ANFIS-PSO	2.37	1.68	13.91	0.9421
	4	ANFIS-PSO	4.15	2.55	11.60	0.9572	4	ANFIS-DE	3.23	2.68	26.17	0.8921

Table 4. 8: Effect of data size for the prediction wind power density of Kaula Terengganu.

Data Size	Training						Testing					
	Rank	Prediction models	RMSE	MABE	MAPE (%)	R^2	Rank	Prediction models	RMSE (W)	MABE (W)	MAPE (%)	R^2
70% training 30% testing	1	ANFIS	4.07	2.28	12.61	0.9407	1	ANFIS-PSO	4.15	2.72	12.74	0.9436
	2	ANFIS-PSO	4.15	2.32	11.61	0.9385	2	ANFIS-DE	4.24	2.50	13.07	0.9531
	3	ANFIS-GA	4.32	2.33	12.40	0.9421	3	ANFIS	4.61	2.68	11.83	0.9448
	4	ANFIS-DE	4.39	2.37	12.06	0.9307	4	ANFIS-GA	5.16	2.78	11.95	0.9307
60% training 40% testing	1	ANFIS-PSO	3.99	2.05	10.06	0.9438	1	ANFIS-PSO	4.58	2.85	12.43	0.9405
	2	ANFIS-GA	4.06	2.36	13.13	0.9415	2	ANFIS	4.73	3.27	16.18	0.9307
	3	ANFIS	4.11	2.23	12.85	0.9401	3	ANFIS-DE	4.92	3.74	24.15	0.9363
	4	ANFIS-DE	4.70	3.04	21.10	0.9217	4	ANFIS-GA	4.94	3.64	19.35	0.9312

A profound observation on Tables (4.3-4.8) reveals that:

i. For WPD prediction of Mersing, ANFIS-PSO is the best model when training the models and the value of RMSE obtained are 4.96, 5.23 and 5.41 for the data size P=105, Q=27; P=92, Q=40, and P=80, Q=52 respectively. On the other hand, when testing the prediction models, ANFIS-GA is the best for the data size P=105, Q=27 and having RMSE of 5.04 whereas, ANFIS-PSO is the best model when data size P=92, Q=40, and P=80, Q=52 resulting the RMSE of 5.37 and 5.22 respectively.

ii. For WPD prediction of Bayan Lepas, ANFIS-PSO shows the best performance for all above data size when training the prediction models. In this case, the computed values of RMSE are 2.14, 2.17 and 2.18 when the training data sizes are of P=105, Q=27; P=92, Q=40, and P=80, Q=52 respectively. Then again, ANFIS-PSO shows the best performance for a testing data size of P=105, Q=27 and P=92, Q=40 resulting RMSE of 2.37 and 2.54 respectively. It is not surprising that ANFIS model has the best accuracy when testing data size of P=80, Q=52 and having RMSE of 2.65.

iii. For WPD prediction of Pulau Langkawi, ANFIS-GA and ANFIS-PSO show the best performance in training and testing the models respectively with data size of P=105, Q=27, which results in RMSE of 3.13 and 1.53 in training and testing respectively. In case of the data size P=92 and Q=40, ANFIS-PSO ranks in first both training and validation with RMSE of 3.29 and 1.69 respectively. For the training and testing data size P=80, Q=52; ANFIS and ANFIS-GA model show optimal RMSE, which are 3.45 and 2.04 in training and testing respectively.

iv. For WPD prediction of Kuala Terengganu, ANFIS-PSO and ANFIS-GA show the best performance in training and testing the models respectively with data size of P=105, Q=27, which results in RMSE of 3.73 and 4.79 respectively. For

the data size P=92, Q=40; ANFIS model shows optimal RMSE, which is 3.45 in training stage and ANFIS-PSO presents optimal RMSE of 2.23 in the testing stage. In case of data size P=80 and Q=52, ANFIS-PSO ranks in first both training and validation of the prediction models with RMSE of 3.99 and 4.58 respectively.

Based on the above discussion, it is clear that P=105, Q=27 (first 80% for training and rest 20% for testing) data size applied to the prediction models provides minimal error for WPD prediction of all underlying locations. For this data size, overall ANFIS-PSO and ANFIS-GA showed a higher correlation between measured and predicted WPD all locations both in training and the testing stages.

On the other hand, when P=92, Q=40 (first 70% for training and rest 30% for testing) data set are applied to the prediction models, ANFIS-PSO shows the best performance in both training and testing stages for predicting WPD of Mersing, Pulau Langkawi, and Bayan Lepas. However, when predicting WPD of Kuala Terengganu, ANFIS-PSO ranks second in training and first in the testing stage. It is important to mention that P=80, Q=52 data size shows the largest error for predicting WPD of all underlying locations, and therefore, this study does not want to use P=80, Q=52 (first 60% for training and rest 40% for testing) data set for model performance justification.

However, both ANFIS-PSO and ANFIS-GA seem to be able to provide an overall good performance both in training and testing stages. Therefore, hybrid ANFIS, especially ANFIS-PSO and ANFIS-GA can be suggested for practical utilization in WPD prediction for the locations having similar wind resource conditions.

Figures (4.10-4.13) depict the visual presentation of the measured and predicted WPD when testing the ANFIS-PSO and ANFIS-GA models using the data from

Mersing, Bayan Lepas, Pulau Langkawi, and Kuala Terengganu respectively with best data size i.e. P=105, Q=27 (first 80% for training and rest 20% for testing) data.

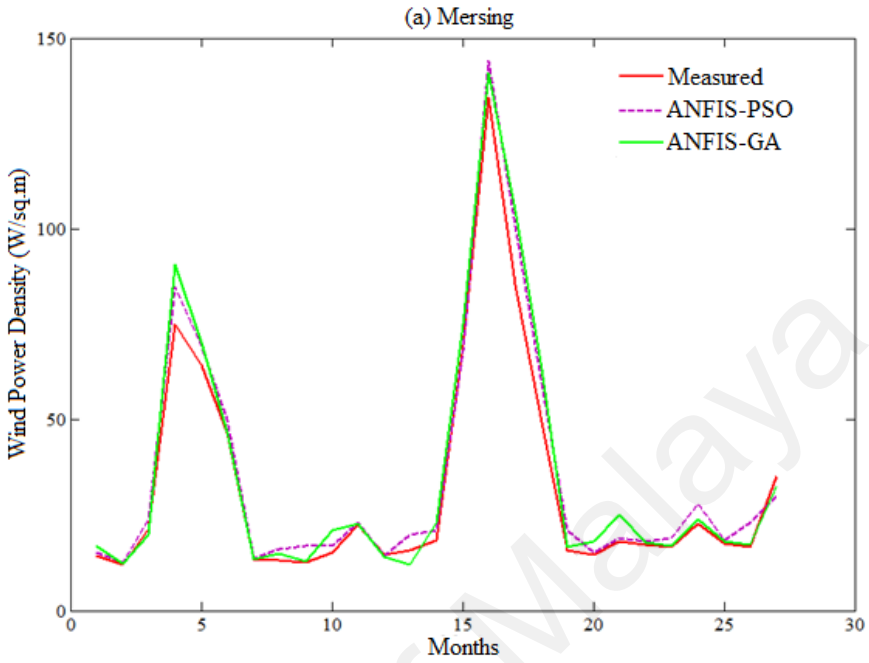

Figure 4. 10: Comparison of WPD prediction of the proposed methods when testing with measured WPD value for Mersing.

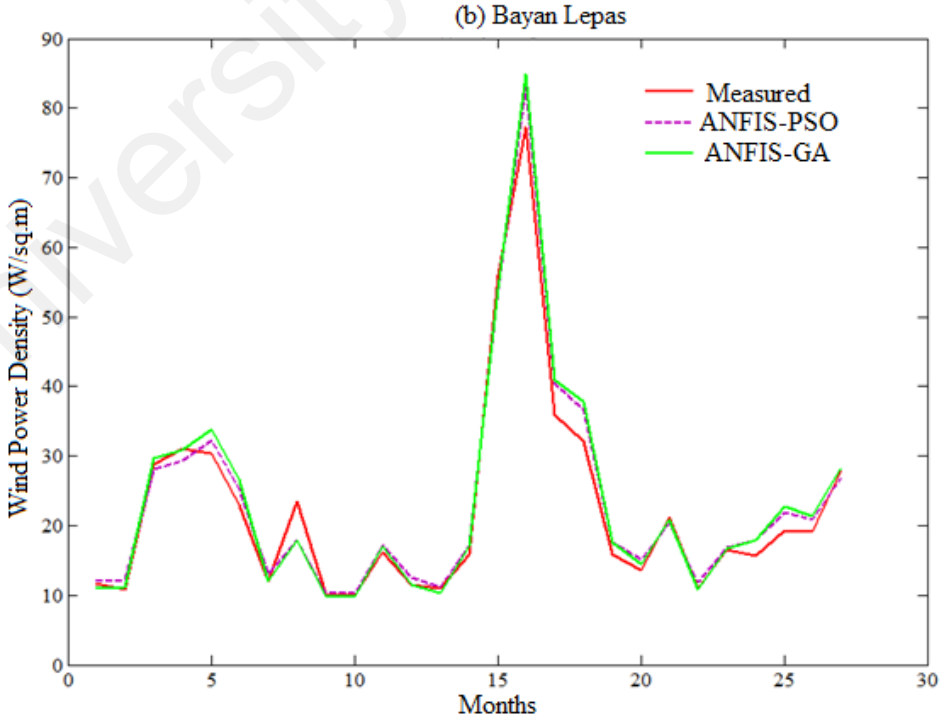

Figure 4. 11: Comparison of WPD prediction of the proposed methods when testing with measured WPD value for Bayan Lepas

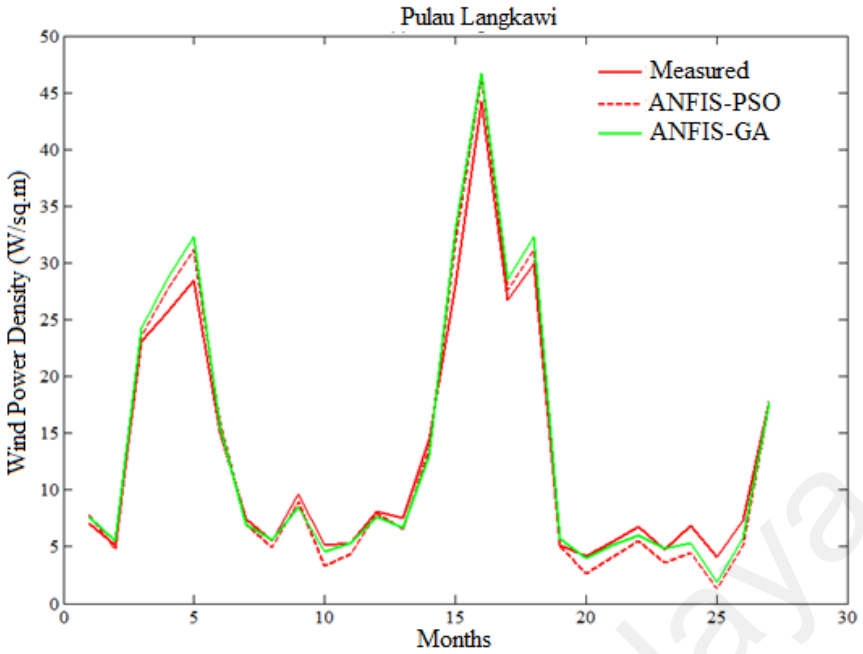

Figure 4. 12: Comparison of WPD prediction of the proposed method with measured value for Pulau Langkawi.

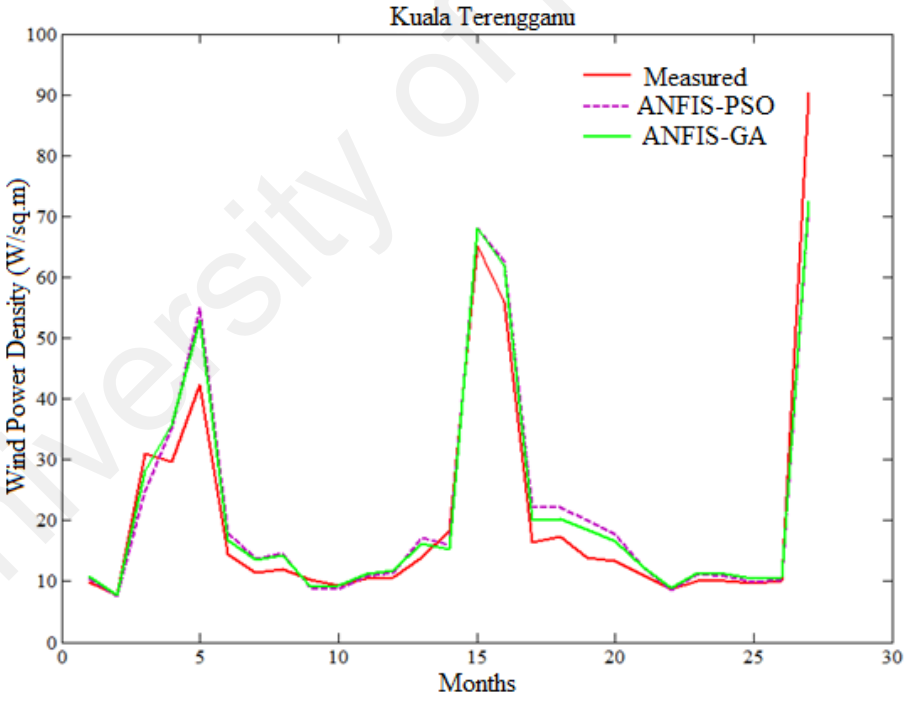

Figure 4. 13: Comparison of WPD prediction of the proposed methods with measured value for Kuala Terengganu.

The Figure 4.14 shows the error distribution of WPD prediction using ANFIS-PSO and ANFIS-GA for underlying locations. According to the definition of relative percentage error (RPE) presented in (Mohammadi et al., 2015; Shamshirband et al., 2016), the RPE falls in an interval of -10% to 10% can be considered as acceptable. The computed value of RPE presented in the Figure 4.14 is obtained from the proposed ANFIS-PSO and ANFIS-GA when 27 months testing data set of underlying locations applied to the models. It can be observed that most of the wind power values obtained via the proposed ANFIS-PSO and ANFIS-GA model fall within the range of -5% up to 5%. In case of Mersing and Kuala Terengganu, only one prediction RPE falls outside (-10% to 10%) range for both ANFIS-PSO and ANFIS-GA.

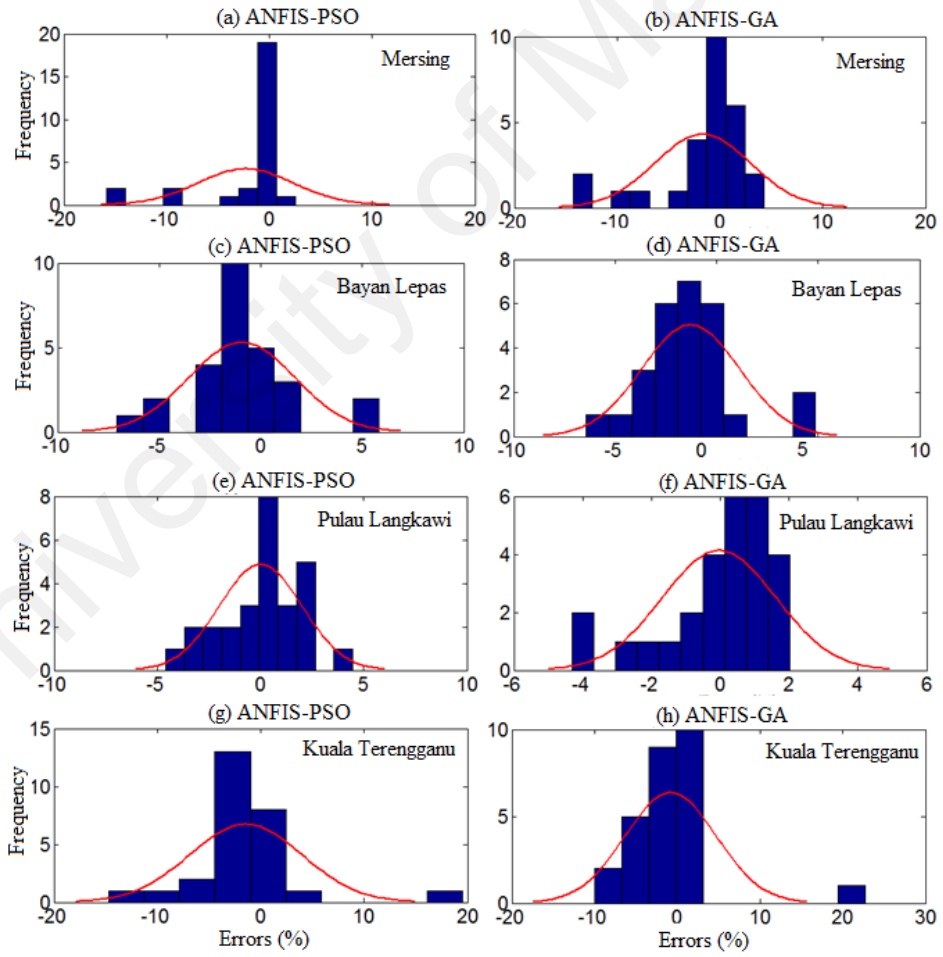

Figure 4. 14: Error distribution when testing ANFIS-PSO and ANFIS-GA for (a, b) Mersing, (c, d) Bayan Lepas (e, f) Pulau Langkawi, (g, h) Kuala Terengganu.

Based on the above discussion, the performance of ANFIS-PSO can be considered the best among other the models. The Figures 4.15 and 4.16 show the visual presentation of regression analysis of the measured and predicted WPD computed from ANFIS-PSO for all underlying locations when P=105, Q=27. The Figure 4.15 shows the correlation between actual and predicted WPD obtained from the ANFIS-PSO method in the training stage. The correlation coefficient (R^2) is the agreement between measured and predicted values, which has the highest value of one. The R^2 obtained when training proposed the ANFIS-PSO model are 0.9781, 0.9703, 0.9762 and 0.9523 for Mersing, Pulau Langkawi, Bayan Lepas and Kuala Terengganu respectively, which indicates a very high and adequate prediction performance of ANFIS-PSO model.

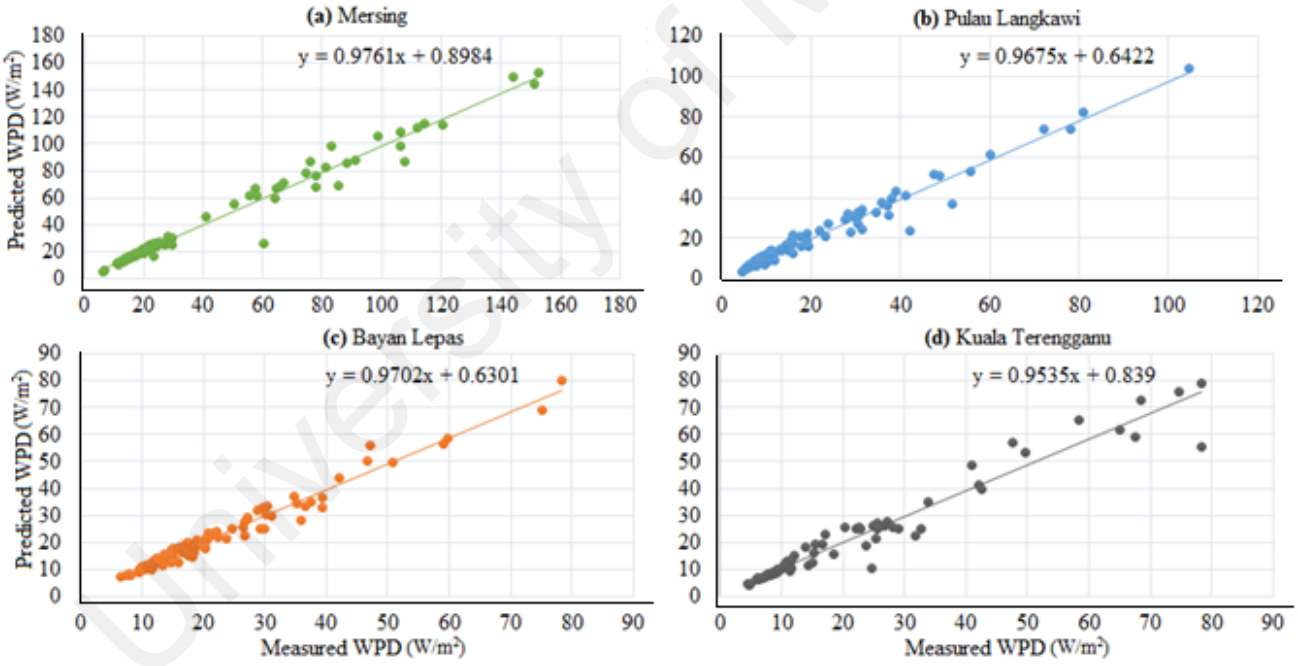

Figure 4. 15: Measured versus predicted WPD when training ANFIS-PSO model with data size P=105, Q=27 (a) Mersing, (b) Pulau Langkawi, (c) Bayan Lepas and (d) Kuala Terengganu.

Again, the linear regression analysis presented in Figure 4.16 shows the correlation between actual and predicted WPD obtained from ANFIS-PSO when testing the prediction models with data from different underlying locations. The R^2 obtained while testing the proposed ANFIS-PSO model for Mersing, Pulau Langkawi, Bayan Lepas

and Kuala Terengganu are 0.9691, 0.9774, 0.9749 and 0.9456 respectively, which supports that ANFIS-PSO has a high precision for the prediction of WPD.

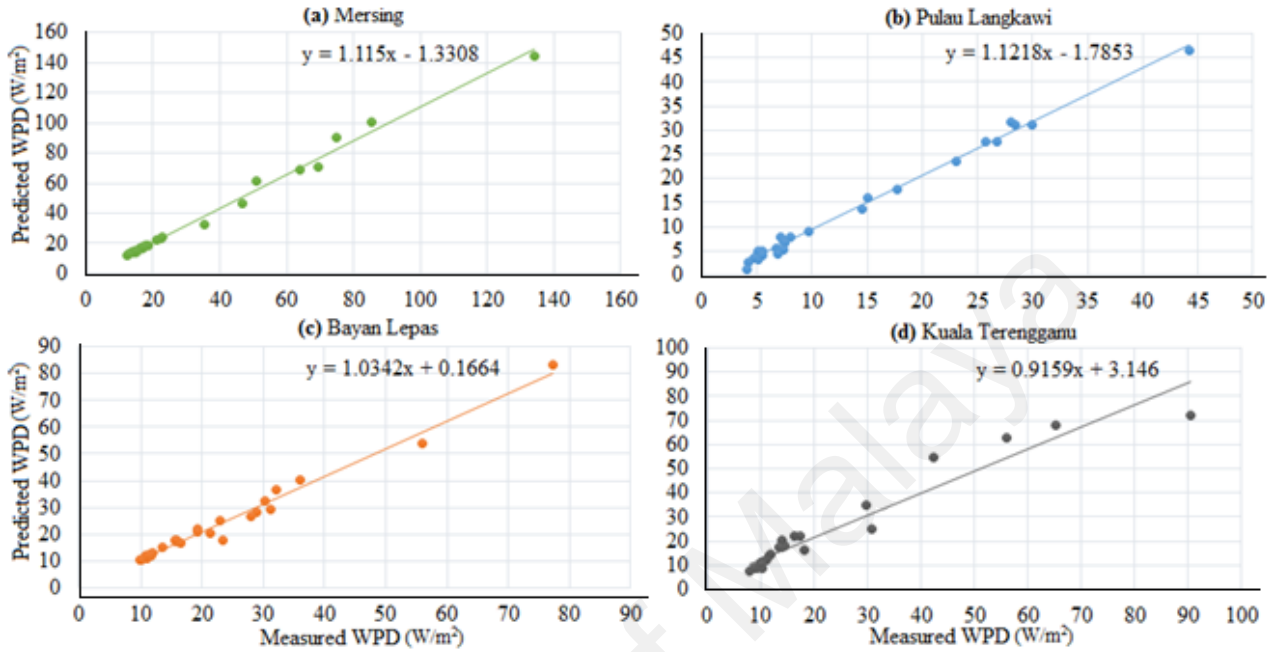

Figure 4. 16: Measured versus predicted WPD when testing ANFIS-PSO model with data size P=105, Q=27 (a) Mersing, (b) Pulau Langkawi, (c) Bayan Lepas and (d) Kuala Terengganu.

4.2 Extrapolation capabilities of the proposed models

Measured wind speed data are not available for many locations in Malaysia, including remote islands (less than 200 km^2) and decentralized places to identify possible wind energy applications. In this dissertation, extrapolation capabilities of the wind speed of the proposed hybrid ANFIS models have been examined for a location in Tioman Island having latitude 2° 48' 30" N and longitude 104° 8' 29" E, where measured wind data are not available. And then, the result is compared with the measured wind data at Mersing station (latitude 2° 27' N and longitude 103° 50' E) which is the nearby station having similar climate conditions. As the study location does not have any actual measured meteorological data, the daily average solar radiation ($kWh/m^2/day$), daily average air temperature, maximum and minimum air temperature, air pressure, relative humidity and altitude data were collected from NASA surface meteorology and solar energy database for the whole year of 2004 for the prediction of daily average wind speed (m/s). The Figures 4.17 and 4.18 show the prediction of daily average wind speed for Tioman Island using ANFIS-PSO and ANFIS-GA respectively, which are compared with measured wind speed at Mersing meteorological station that was measured at 50m above the sea level in 2004.

From error analysis, it was found that the MAPE, MABE and RMSE for ANFIS-PSO were 31.56%, 0.9672% and 0.5644 respectively whereas, they were found to be 32.21%, 0.9872% and 0.5349 for ANFIS-GA respectively. It can be observed from the figures that the wind characteristics in Tioman Island, obtained with the proposed ANFI-PSO and ANFIS-GA, is not exactly similar with the measured wind at Mersing in many cases. However, it is important to take note that the performance of the prediction models can be justified accurately when measured wind data in Tioman Island will be available for comparison. Thus, measuring real time wind data and short and long-term wind speed forecasting can be a potential future study for this climate zone.

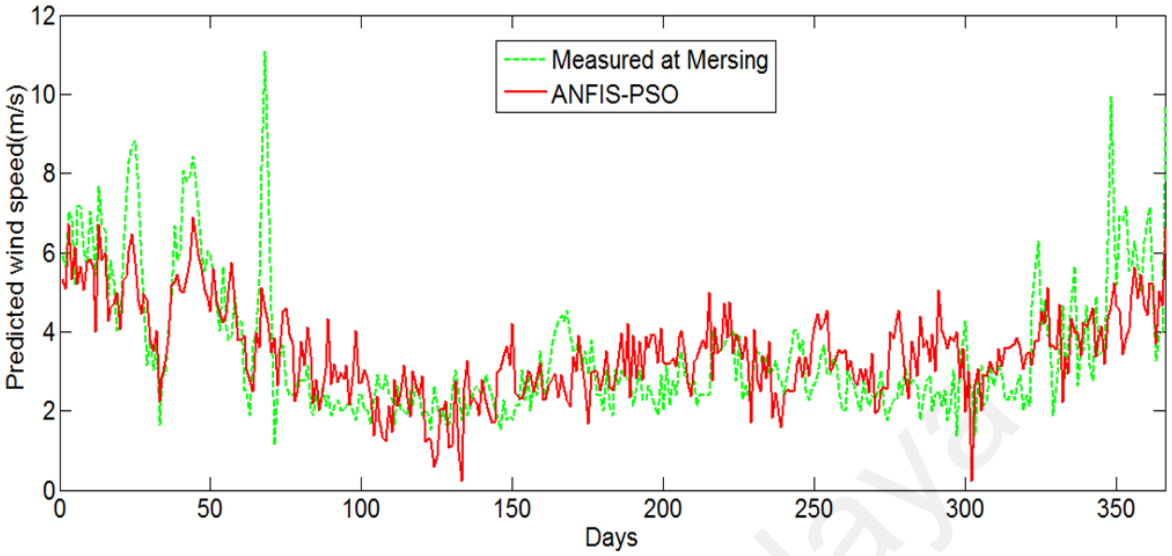

Figure 4. 17: Extrapolation of daily average wind speed for Tioman Island using the proposed ANFIS-PSO model.

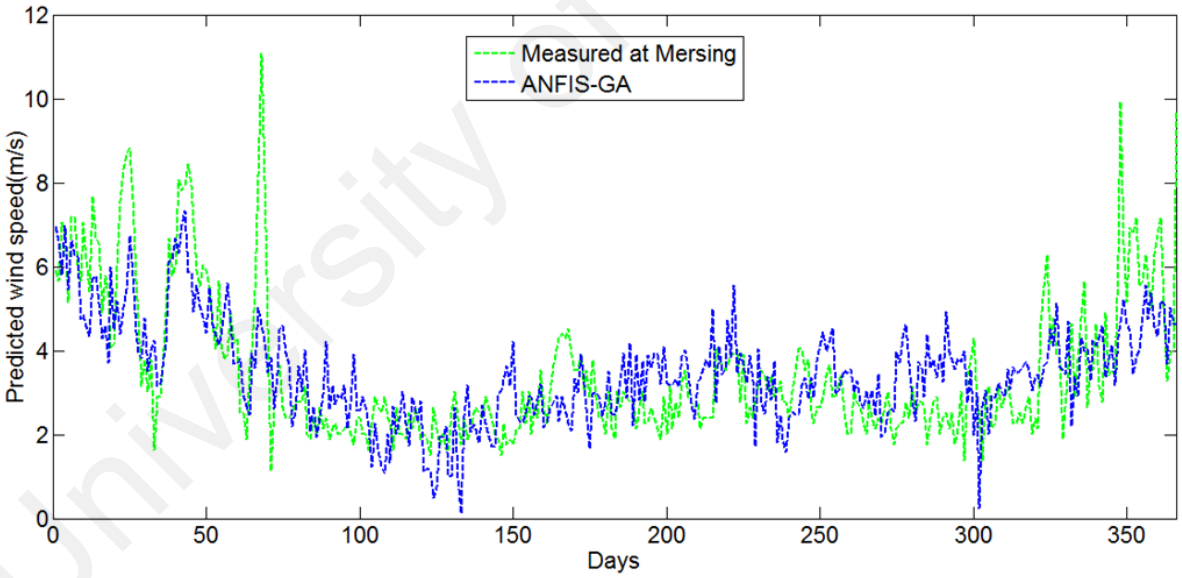

Figure 4. 18: Extrapolation of daily average wind speed for Tioman Island using the proposed ANFIS-GA model.

4.3 Techno-economic performance analysis of proposed HRES

An optimal combination of HRES has been modeled in HOMER with a large number of hourly simulations. HOMER simulates all possible combinations according to the input parameters and sorts the optimization result from lowest NPC to highest NPC. The optimization results in the categorized form are shown in Table 4.9, which includes the optimal system configurations, NPC, RF, COE, dispatch strategy, and excess electricity per year. The maximum allowable annual capacity shortage for all simulations was considered to be 1 percent. Moreover, the obtained yearly unmet electric load in all feasible systems were negligible and cycle charging is considered to be the best dispatch strategy for all hybrid systems.

It can be observed from Tables 4.9 that the best optimized HRES comprised of 700kW PV module, 5 wind turbines, 3 diesel generators and 240 units of the battery. This system resulted in the COE of $0.279/kWh, NPC of $17.15millions, a renewable fraction (RF) of 41.6%, and excess electricity (EE) of 16.2% of total electrical production. The third best-optimized system is the wind-diesel-battery system. This configuration has an RF of 37.6 % with seven wind turbine contributing about 51.65% of total electrical production and the NPC is close to the best optimization system. It can be noticed that the system in rank 6 has EE of 3.4 % of total production per year with $0.028 higher COE than rank 1. However, the size of PV in this rank is 1000kW, which needs almost double the land area than rank 1, also this system will increase the dependency on diesel generators. And notably, this system has RF of 21.7 % which is almost half that of rank 1. Additionally, this system will increase the carbon footprint.

Table 4. 9: Optimized hybrid renewable system sorted by the NPC.

Rank	PV (kW)	Wind	GEN 1(kW)	GEN 2(kW)	GEN 3(kW)	Batt	Conv (kW)	Disp	COE ($/kWh)	NPC (million $)	RF (%)	EE (%)
1	700	5	400	200	100	240	600	CC	0.279	17.1552	41.6	16.2
2	700	5	500	0	200	280	700	CC	0.286	17.5750	41.4	15.9
3	0	7	400	200	100	320	700	CC	0.287	17.6771	37.6	17.9
4	0	7	500	200	0	320	700	CC	0.296	18.2007	36.2	18.2
5	800	5	600	0	0	320	700	CC	0.306	18.7898	41.4	17.8
6	1000	0	500	200	100	160	500	CC	0.307	18.8516	21.7	3.4
7	1000	0	600	0	200	240	500	CC	0.316	19.4232	21.0	3.3
8	0	7	600	0	0	320	800	CC	0.316	19.4288	35.7	18.8
9	1000	0	0	200	500	240	500	CC	0.317	19.4726	20.5	3.3
10	1000	0	700	0	0	320	700	CC	0.336	20.6613	20.4	2.5
11	0	0	400	200	300	160	400	CC	0.343	21.0944	0	0
12	0	0	500	300	0	160	400	CC	0.354	21.7353	0	0
13	0	0	700	0	0	240	400	CC	0.385	23.6165	0	0

Table 4.10 shows the running hours of diesel generators and the percentage of contributions by individual system components in terms of power generation whereas, Table 4.11 shows a number of harmful emissions including CO_2, CO, unburned hydrocarbon (UHC), particulate matter (PM), sulfur dioxide (SO_2) and nitrogen oxide (NO) in each optimized system.

Table 4. 10: Performance of system components in different optimization result.

Rank	Running hours of DG in a year				Percentage of individual power generation				
	GEN 1	GEN 2	GEN 3		PV	Wind	GEN 1	GEN 2	GEN 3
1	4127	4057	4070		16.20	37.65	27.12	12.96	6.07
2	4407	0	3703		16.16	37.56	35.01	0	11.26
3	4685	3837	3856		0	51.65	30.37	12.17	5.81
4	4857	3698	0		0	51.08	37.86	11.06	0
5	5828	0	0		18.08	36.37	45.06	0	0
6	5178	3804	4230		27.21	0	50.39	14.58	7.82
7	5378	0	3536		27.02	0	60.18	0	12.80
8	6380	0	0		0	50.92	49.08	0	0
9	0	5311	5617		26.94	0	0	19.54	53.52
10	6112	0	0		26.86	0	73.14	0	0
11	5955	4661	5121		0	0	49.25	19.24	31.52
12	7077	4964	0		0	0	71.76	28.24	0
13	8756	0	0		0	0	100	0	0

Table 4. 11: Harmful emissions from different system type.

Rank	Emissions (kg/year)					
	CO_2	CO	UHC	PM	SO_2	NO
1	2,571,131	6346.5	702.99	478.43	5163.3	56,630
2	2,600,885	6419.9	711.13	483.96	5223.0	57,285
3	2,736,751	6755.3	748.28	509.24	5495.9	60,278
4	2,820,157	6961.2	771.08	524.76	5663.4	62,115
5	2,755,103	6800.6	753.30	512.66	5532.7	60,682
6	3,426,989	8459.0	937.0	637.68	6882.0	75,481
7	3,495,995	8629.4	955.87	650.52	7020.6	77,001
8	3,020,503	7455.7	825.86	562.04	6065.7	66,528
9	3,487,326	8608.0	953.5	648.91	7003.2	76,810
10	3,612,237	8916.3	987.65	672.15	7254.0	79,561
11	5,432,244	10,940.0	1211.9	824.74	8900.7	97,622
12	5,518,589	11,153.0	1235.0	840.80	9074.1	99,523
13	5,829,111	11,920.0	1320.4	898.58	9697.7	1,06,363

It can be observed that the system in ranks (11-13) is made up of a diesel-battery system configuration that has much more harmful emissions than of the best-optimized hybrid system. Not only this but also the COE and NPC are much higher compared to

the best case. Therefore, the system in rank 1 is considered as the best off-grid system configuration to supply reliable electricity to the resort.

Figure 4.19 shows the monthly electric power generated by each system components in the best optimized standalone PV-wind-diesel-battery hybrid system. It can be found that the wind turbines contribute highest in the NEM season. On the other hand, the contribution of diesel generators is higher than other system components in the SWM, FIM and SIM seasons due to comparatively low wind speed. The selected PV panel can harvest about 81 MW per month all over the year. Therefore, the diesel-RE hybrid system is considered a more reliable power supply option to the resort than 100% RE system.

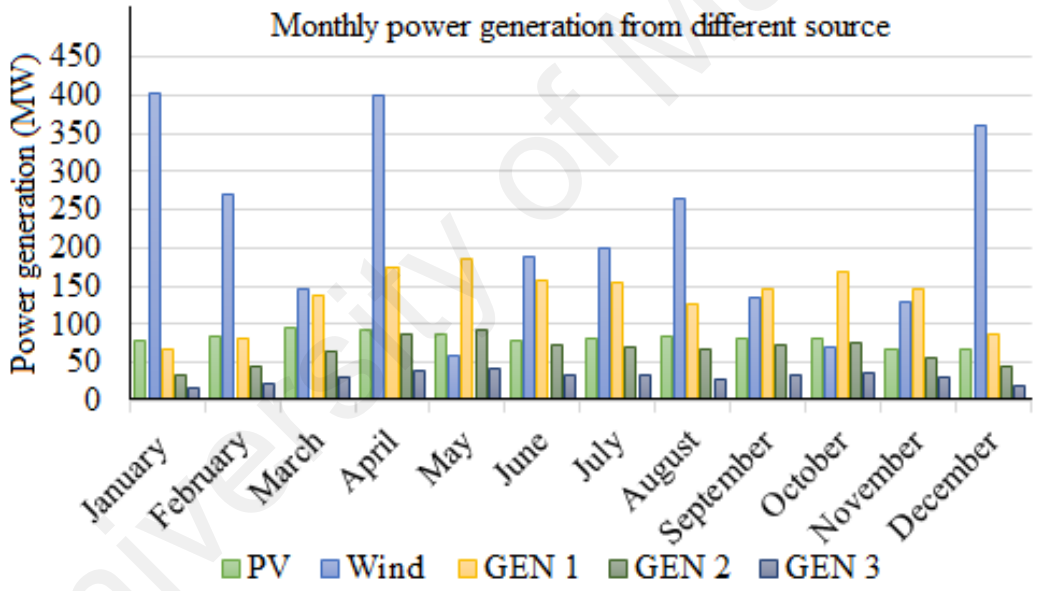

Figure 4. 19: Monthly electrical power generation in the best HRES by each system components.

Figure 4.20 shows the nominal cash flow of 25 years' project life time, which is the NPC by cost type. It can be seen from Figure 4.20 that the initial capital cost of PV, wind turbine, batteries, converter, and generators is around $4.2 million. Notably, $10.1 million of total NPC ($17.15 million) is gulped up by fuel cost of diesel generators only.

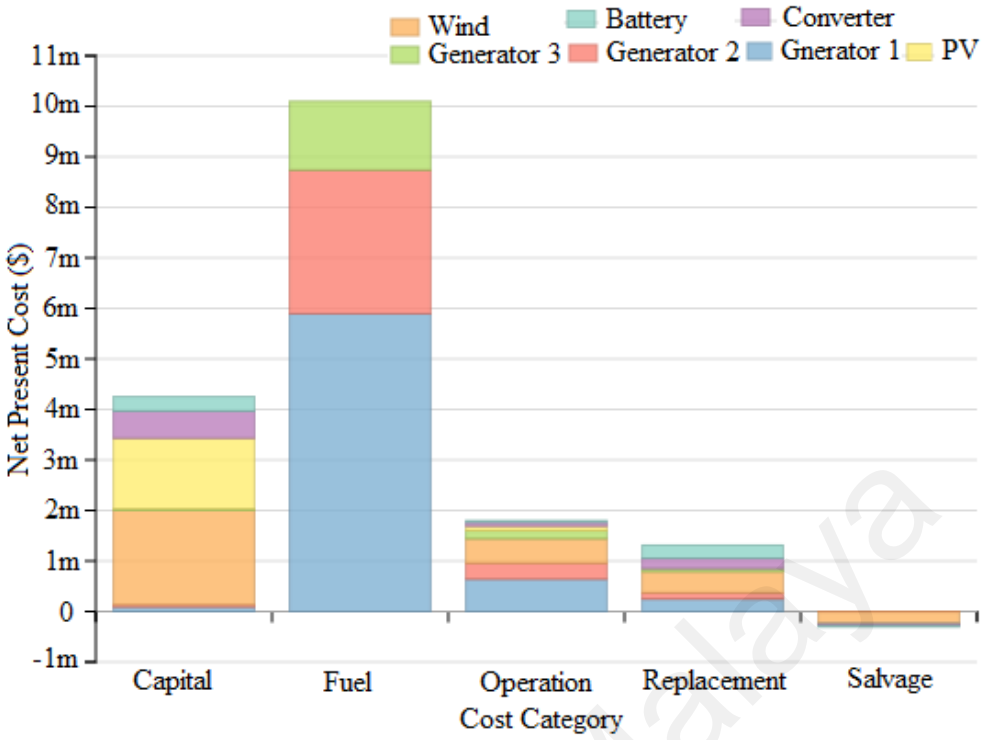

Figure 4. 20: Summary of nominal cash flow for the best optimized HRES.

Figures 4.21 and 4.22 respectively show the monthly excess energy and the battery state of charge in different months of the year in the best optimized HRES. It can be noted from Figure 4.21 that the amount of excess electricity is much higher in the months of January, February, and December than other months of the year due to high wind speed usually experienced in these months. Consequently, the red color of the Figure 4.22 reveals that the batteries are over charging during the months of January, February, March, August, November, and December because of excess electricity experienced in these months. The batteries can be damaged or lifetime can be shortened due to overcharging. The high contribution of wind turbines in NEM season is responsible for this surplus electricity and consequently responsible for over charging of the batteries. Therefore, this excess electricity can be dumped for the safe operation of the system components.

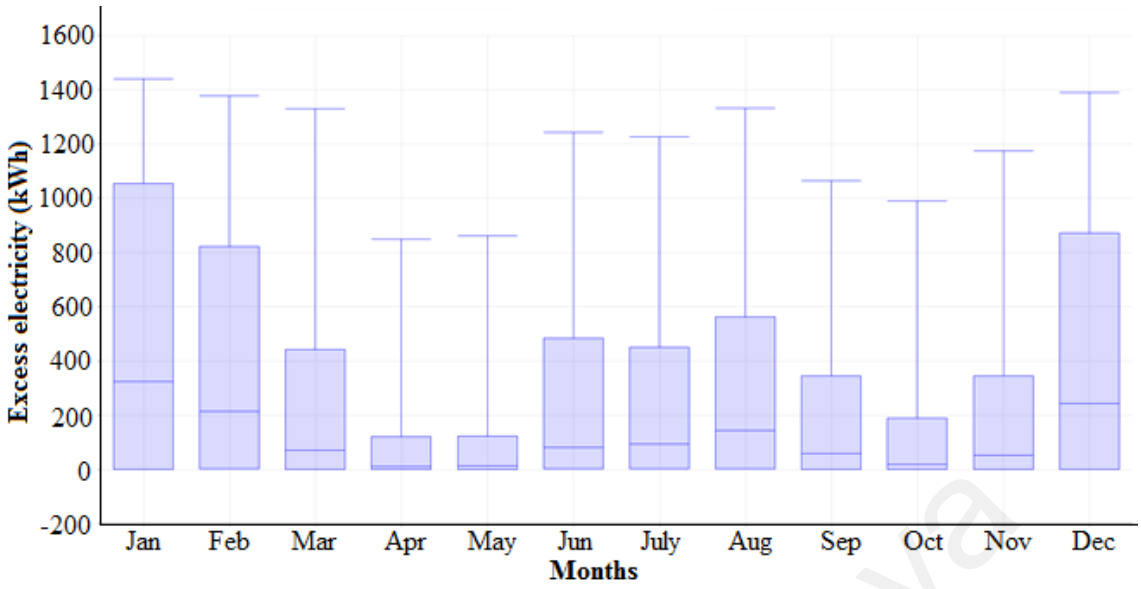

Figure 4. 21: Monthly excess electricity production by the best-optimized system.

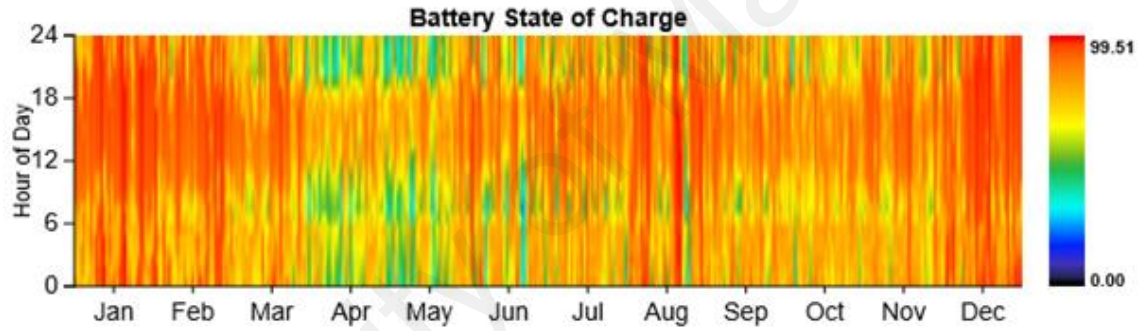

Figure 4. 22: SOC of battery in a different month of a year.

4.4 Sensitivity analysis

To understand the uncertainty of the model in terms of COE, a sensitivity analysis was carried out. The sensitivity variables were wind speed, solar radiation and diesel price. The variables were varied ± 30% from their scaled average value. The scaled yearly average solar irradiance and wind speed for Tioman Island were 5.21 kWh/m^2/day and 3.73 m/s respectively whereas, base case diesel price was $0.8/L. Figure 4.23 shows the sensitivity result. It can be observed from the figure that solar radiation variation does not affect the COE significantly. On the other hand, COE is greatly affected by the variation of diesel price and the wind speed. The COE varies from $0.229/kWh to $0.329/kWh when diesel price shifts from $0.56/L to $1.04/L. The

second dominant factor wind speed was varied from 2.611 m/s to 4.849 m/s that resulted in COE declining from $0.324 kWh to $0.241/kWh.

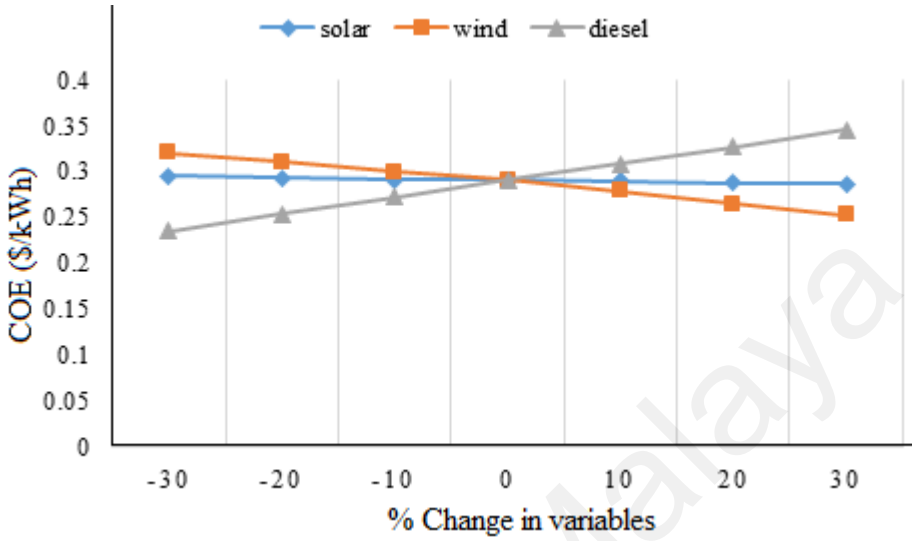

Figure 4. 23: Sensitivity result of the system with variable wind speed, solar radiation and diesel fuel price.

4.5 Summary

In this chapter, the entire result of this dissertation is presented and discussed. Firstly, the prediction result of wind power density using the proposed ANFIS (adaptive neuro-fuzzy inference system), ANFIS-PSO (particle swarm optimization), ANFIS-GA (genetic algorithm) and ANFIS-DE (differential evolution) is presented. Different statistical error metrics such as mean absolute bias error (MABE), mean absolute percentage error (MAPE), root mean square error (RMSE) and coefficient of determination (R^2) are used to find prediction accuracy. Among them, ANFIS-PSO and ANFIS-GA perform an overall good performance both in training and testing stages. After that, wind speed extrapolation capability using ANFIS-PSO and ANFIS-GA is presented for Tioman Island. The extrapolation result is compared with measured wind speed data collected from Mersing station. Also, discussed in this chapter, is the techno-economic performance of the proposed hybrid renewable energy system which was designed in hybrid optimization model for electric renewable (HOMER) software tool.

The best optimized HRES is comprised of 700kW PV, 5 wind turbines, 3 generators and 240 units of the battery. This system results in the COE of $0.279/kWh, NPC of $17.15millions, a renewable fraction (RF) of 41.6%. Finally, this chapter concludes with the sensitivity analysis method that was performed in HOMER to understand the impact of variation of different input parameters like solar radiation, wind speed, and diesel price.

CHAPTER 5: CONCLUSIONS

5.1 Conclusions

In Malaysia, electricity generation alone emitted 36,925,190 ton of CO_2 in 2002, and it is projected that it would be 107,318,707 ton in 2020 (Mahlia, 2002). This amount of CO_2 emission from power sector solely is a great threat to a developing country like Malaysia. Therefore, a stand-alone hybrid renewable energy system (HRES) can be cost effective, reliable and environmentally friendly solution in providing electricity access to the tourist facilities and rural community in these islands. In this dissertation, a HRES has been designed and analyzed the techno-economic performance for a large resort center located in a decentralized and rural island named Pulau Tioman in the South China Sea, Malaysia. Besides, in this dissertation, an efficient soft computing technique based on the hybrid ANFIS (adaptive neuro-fuzzy inference system) prediction models namely ANFIS-PSO, ANFIS-GA, ANFIS-DE and standalone ANFIS have been developed to predict monthly wind power density (WPD) for the nearest coastal city of Pulau Tioman named Mersing and again the capacity and accuracy of proposed prediction models are justified by predicting monthly WPD of three additional cities named Kuala Terengganu, Bayan Lepas, and Pulau Langkawi. Also, in this dissertation, extrapolation capabilities of the wind speed of the proposed hybrid ANFIS models have been examined very briefly for a location in Tioman Island having latitude 2° 48' 30" N and longitude 104° 8' 29" E, where measured wind data are not available.

The most significant advantage of hybrid ANFIS is that PSO/GA/DE tune the membership functions of the ANFIS model to ensure minimum error. The prediction models were trained and tested using the wind speed data collected from meteorological stations of the underlying locations and measured wind power density. Moreover, different training and testing data size were applied to the prediction models to obtain best data size that provides an optimal error. The first 80% data for training and

remaining 20% data for testing provide the optimal error in WPD prediction. Based on the result from best data size, there is no model that performed uniformly superior to other for all locations in both training and testing stages. Overall, ANFIS-PSO and ANFIS-GA out-performed ANFIS standalone and ANFIS-DE. Therefore, the results and analysis confirmed that the proposed hybrid ANFIS, especially ANFIS-PSO and ANFIS-GA have the excellent capability to predict the WPD with higher accuracy and precision. The result of the wind data extrapolation also reveals that the proposed ANFIS-PSO and ANFIS-GA show a good result in case of the wind speed data extrapolation for Tioman Island but wind characteristics between Tioman Island and Mersing station is not similar many cases.

On the other hand, the results analysis of the proposed HRES shows that the best-optimized system is made up of a 700kW PV, 5 wind turbine, 240 batteries, 3 units of diesel generator and a bi-directional converter of 600 kW. The selected wind turbine for the site has low cut in wind speed of 2-3 m/s. The turbine gives the rated power of 250kW at the wind speed of 7-8 m/s. The COE, NPC, and RF of the optimized system were \$0.279/kWh, \$17.15m, 41.6% respectively. The proposed HRES ensures a significant reduction in CO_2 and other GHG emissions and economic viability in terms of the COE and NPC. Importantly, there are more than twelve small islands in the South China Sea that surround Pulau Tioman and have more or less same climate conditions as Pulau Tioman. Thus, this analysis can represent any of the off-grid hybrid RE systems for a large resort center located on these islands, especially the optimized system in rank 3. The hybrid system in rank 3, consists of wind-diesel-battery, is more suitable for these small islands because a 700 kW PV panel in rank 1 might not be suitable for the small area of these small islands. Moreover, the analyzed hybrid energy system might be applicable to the different areas of the world where the climate conditions are same as the analyzed area.

5.2 Recommendations

In view of the above findings, the following are recommended:

- The remote and rural islands (normally less than 200 km^2) in the South China Sea, Malaysia do not have any meteorological stations. Consequently, the renewable energy resources assessment, especially solar and the wind based on real data cannot be accomplished. The researchers usually use data either from NASA surface meteorology or from the nearest meteorological stations. Thus, the government of Malaysia should establish meteorological stations in some of the major islands like Pulau Tioman that will help more accurate feasibility study and performance evaluation of the hybrid renewable energy system.
- The implementation of the proposed hybrid renewable energy system needs high capital cost, which is considered as a major barrier to investing by such a rural resort facility owner. On the other hand, the remote islands in the South China Sea, Malaysia are the great places of tourist attraction. Thus, the government of Malaysia should come forward to intensify financial solutions that can ease capital cost barriers.

5.3 Suggestions for future work

In this research, an optimal configuration of PV-wind-diesel-battery hybrid system, including optimal design, technical and economic performance evaluation for a rural and decentralized resort facilities located in Pulau Tioman, Malaysia has been conducted. Although various analysis has been carried out in this study to ensure the achievement of the set of objectives, therefore, the following are suggested for further studies:

- The government of Malaysia, TNB, SEB and individual researchers have explored many small hydro potentials in different remote places in Malaysia,

still, the potential sites of micro and mini hydro in many remote and rural islands in the South China Sea, Malaysia are not properly investigated. To identify all the potential sites of small hydro in such remote islands can be a good future research work.

- In conjunction with solar and the wind; small hydro, biomass and fuel cell based hybrid system can be a smart power supply option to such tourist facilities. Therefore, more study needs to consider that will measure the performance of the hybrid renewable system having solar, wind, small hydro, and biomass.
- Although the Sustainable Energy Development Authority (SEDA), Malaysia has determined the appropriate feed in tariff (FiT) rate for selling renewable electricity to the national grid, there is no particular research on the appropriate off-FiT value. Thus, demand side management and to identify the appropriate off-FiT value to sell per unit of renewable electricity to the local mini grid and individual load need to be investigated.
- The hybrid system needs sophisticated and complex control, power and energy management. More advance research on the power and energy management of a hybrid ac-dc micro-grid system with optimal selection of battery and super capacitor as energy storage device can be conducted to expand the current research.

REFERENCES

Aagreh, Y., & Al-Ghzawi, A. (2013). Feasibility of utilizing renewable energy systems for a small hotel in Ajloun city, Jordan. Applied Energy, 103, 25-31.

Abdilahi, A. M., Mohd Yatim, A. H., Mustafa, M. W., Khalaf, O. T., Shumran, A. F., & Mohamed Nor, F. (2014). Feasibility study of renewable energy-based microgrid system in Somaliland′s urban centers. Renewable and Sustainable Energy Reviews, 40, 1048-1059.

Adaramola, M. S. (2014). Viability of grid-connected solar PV energy system in Jos, Nigeria. International Journal of Electrical Power & Energy Systems, 61, 64-69.

Adaramola, M. S., Paul, S. S., & Oyewola, O. M. (2014). Assessment of decentralized hybrid PV solar-diesel power system for applications in Northern part of Nigeria. Energy for Sustainable Development, 19, 72-82.

Admuthe, L., & Apte, S. (2009). Computational model using ANFIS and GA: Application for textile spinning process. 2nd IEEE International Conference on Computer Science and Information Technology, 2009, pp. 110-114.

Ajayi, O. O., Ohijeagbon, O. D., Mercy, O., & Ameh, A. (2016). Potential and econometrics analysis of standalone RE facility for rural community utilization and embedded generation in North-East, Nigeria. Sustainable Cities and Society, 21, 66-77.

Akdağ, S. A., & Dinler, A. (2009). A new method to estimate Weibull parameters for wind energy applications. Energy Conversion and Management, 50(7), 1761-1766.

Akorede, M. F., Rashid, M. I. M., Sulaiman, M. H., Mohamed, N. B., & Ab Ghani, S. B. (2013). Appraising the viability of wind energy conversion system in the Peninsular Malaysia. Energy Conversion and Management, 76, 801-810.

Anwari, M., Rashid, M. I. M., Muhyiddin, H. T. M., & Ali, A. R. M. (2012, 3-5 July 2012). An evaluation of hybrid wind/diesel energy potential in Pemanggil Island Malaysia. International Conference on Power Engineering and Renewable Energy (ICPERE), 2012, pp. 1-5.

Aquila, G., Rocha, L. C. S., Rotela Junior, P., Pamplona, E. d. O., Queiroz, A. R. d., & Paiva, A. P. d. (2016). Wind power generation: An impact analysis of incentive strategies for cleaner energy provision in Brazil. Journal of Cleaner Production, 137, 1100-1108.

Arslan, O. (2010). Technoeconomic analysis of electricity generation from wind energy in Kutahya, Turkey. Energy, 35(1), 120-131.

Ashourian, M. H., Cherati, S. M., Mohd Zin, A. A., Niknam, N., Mokhtar, A. S., & Anwari, M. (2013). Optimal green energy management for island resorts in Malaysia. Renewable Energy, 51, 36-45.

Ata, R. (2015). Artificial neural networks applications in wind energy systems: a review. Renewable and Sustainable Energy Reviews, 49, 534-562.

Azad, H. B. (2015). Techno Economic Analysis of Stand-Alone Hybrid Renewable Energy System. LAP LAMBERT Academic Publishing, Germany.

Bahramara, S., Moghaddam, M. P., & Haghifam, M. R. (2016). Optimal planning of hybrid renewable energy systems using HOMER: A review. Renewable and Sustainable Energy Reviews, 62, 609-620.

Bajpai, P., & Dash, V. (2012). Hybrid renewable energy systems for power generation in stand-alone applications: a review. Renewable and Sustainable Energy Reviews, 16(5), 2926-2939.

BNM. (2016). Bank Negara Malaysia: Interest rate in Malaysia. http://www.tradingeconomics.com/malaysia/interest-rate. (Accessed on 12.03.2016).

Bashir, Z., & El-Hawary, M. (2009). Applying wavelets to short-term load forecasting using PSO-based neural networks. IEEE transactions on power systems, 24(1), 20-27.

Basir Khan, M. R., Jidin, R., & Pasupuleti, J. (2016a). Data from renewable energy assessments for resort islands in the South China Sea. Data in Brief, 6, 117-120.

Basir Khan, M. R., Jidin, R., & Pasupuleti, J. (2016b). Energy audit data for a resort island in the South China Sea. Data in Brief, 6, 489-491.

Basir Khan, M. R., Jidin, R., Pasupuleti, J., & Shaaya, S. A. (2015). Optimal combination of solar, wind, micro-hydro and diesel systems based on actual seasonal load profiles for a resort island in the South China Sea. Energy, 82, 80-97.

Berjaya Tioman Resort. (2015). Retrieved from http://www.berjayahotel.com/tioman. (Accessed on 20.12.2016).

Bilgili, M., Sahin, B., & Yasar, A. (2007). Application of artificial neural networks for the wind speed prediction of target station using reference stations data. Renewable Energy, 32(14), 2350-2360.

Borhanazad, H., Mekhilef, S., Gounder Ganapathy, V., Modiri-Delshad, M., & Mirtaheri, A. (2014). Optimization of micro-grid system using MOPSO. Renewable Energy, 71, 295-306.

Borhanazad, H., Mekhilef, S., Saidur, R., & Boroumandjazi, G. (2013). Potential application of renewable energy for rural electrification in Malaysia. Renewable Energy, 59, 210-219.

Borowy, B. S., & Salameh, Z. M. (1996). Methodology for optimally sizing the combination of a battery bank and PV array in a wind/PV hybrid system. IEEE Transactions on Energy Conversion, 11(2), 367-375.

Charfi, S., Atieh, A., & Chaabene, M. (2016). Modeling and cost analysis for different PV/battery/diesel operating options driving a load in Tunisia, Jordan and KSA. Sustainable Cities and Society, 25, 49-56.

Chedid, R., & Rahman, S. (1997). Unit sizing and control of hybrid wind-solar power systems. IEEE Transactions on Energy Conversion, 12(1), 79-85.

Chong, W. T., Gwani, M., Shamshirband, S., Muzammil, W. K., Tan, C. J., Fazlizan, A., Wong, K. H. (2016). Application of adaptive neuro-fuzzy methodology for performance investigation of a power-augmented vertical axis wind turbine. Energy, 102, 630-636.

Dai, K., Bergot, A., Liang, C., Xiang, W.-N., & Huang, Z. (2015). Environmental issues associated with wind energy–A review. Renewable Energy, 75, 911-921.

Dalton, G. J., Lockington, D. A., & Baldock, T. E. (2008). Feasibility analysis of stand-alone renewable energy supply options for a large hotel. Renewable Energy, 33(7), 1475-1490.

Dalton, G. J., Lockington, D. A., & Baldock, T. E. (2009a). Case study feasibility analysis of renewable energy supply options for small to medium-sized tourist accommodations. Renewable Energy, 34(4), 1134-1144.

Dalton, G. J., Lockington, D. A., & Baldock, T. E. (2009b). Feasibility analysis of renewable energy supply options for a grid-connected large hotel. Renewable Energy, 34(4), 955-964.

Darus, Z. M., Hashim, N. A., Manan, S. A., Rahman, M. A. A., Maulud, K. A., & Karim, O. A. (2009). The development of hybrid integrated renewable energy system (wind and solar) for sustainable living at Perhentian Island, Malaysia. European Journal of Social Sciences, 9(4), 557-563.

Demiroren, A., & Yilmaz, U. (2010). Analysis of change in electric energy cost with using renewable energy sources in Gökceada, Turkey: An island example. Renewable and Sustainable Energy Reviews, 14(1), 323-333.

Diaf, S., Belhamel, M., Haddadi, M., & Louche, A. (2008). Technical and economic assessment of hybrid photovoltaic/wind system with battery storage in Corsica island. Energy Policy, 36(2), 743-754.

Diaf, S., Diaf, D., Belhamel, M., Haddadi, M., & Louche, A. (2007). A methodology for optimal sizing of autonomous hybrid PV/wind system. Energy Policy, 35(11), 5708-5718.

Dihrab, S. S., & Sopian, K. (2010). Electricity generation of hybrid PV/wind systems in Iraq. Renewable Energy, 35(6), 1303-1307.

Eberhart, R. C., & Kennedy, J. (1995). A new optimizer using particle swarm theory. Proceedings of the Sixth International Symposium on Micro Machine and Human Science , 1995, pp. 39-43.

El-Hefnawi, S. H. (1998). Photovoltaic diesel-generator hybrid power system sizing. Renewable Energy, 13(1), 33-40.

Fadaeenejad, M., Radzi, M. A. M., AbKadir, M. Z. A., & Hizam, H. (2014). Assessment of hybrid renewable power sources for rural electrification in Malaysia. Renewable and Sustainable Energy Reviews, 30, 299-305.

Fyrippis, I., Axaopoulos, P. J., & Panayiotou, G. (2010). Wind energy potential assessment in Naxos Island, Greece. Applied Energy, 87(2), 577-586.

Gnana Sheela, K., & Deepa, S. N. (2013). Neural network based hybrid computing model for wind speed prediction. Neurocomputing, 122, 425-429.

Goater, D. A. (May 2014). Intermittent Electricity Generation. Retrieved from http://researchbriefings.files.parliament.uk/documents/POST-PN-464/POST-PN-464.pdf. (Accessed on 20.02.2016).

Green, R., & Vasilakos, N. (2010). Market behavior with large amounts of intermittent generation. Energy Policy, 38(7), 3211-3220.

Güler, Ö., Akdağ, S. A., & Dinçsoy, M. E. (2013). Feasibility analysis of medium-sized hotel's electrical energy consumption with hybrid systems. Sustainable Cities and Society, 9, 15-22.

GWEC. (2012). Global Wind Energy Council: Wind & Climate. Retrieved from http://gwec.net/wp-content/uploads/2012/06/Wind-climate-fact-sheet-low-res.pdf. (Accessed on 25.06.2016).

GWEC. (2015). Global wind report (annual market update 2015). Retrieved from http://www.gwec.net/publications/global-wind-report-2/global-wind-report-2014-annual-market-update/.(Accessed on 25.06.2016).

Hegerty, B., Hung, C., & Kasprak, K. (2009). A comparative study on differential evolution and genetic algorithms for some combinatorial problems. In Proceedings of 8th Mexican International Conference on Artificial Intelligence, 2009, pp. 9-13.

Heydari, A., & Askarzadeh, A. (2016). Optimization of a biomass-based photovoltaic power plant for an off-grid application subject to loss of power supply probability concept. Applied Energy, 165, 601-611.

Hiendro, A., Kurnianto, R., Rajagukguk, M., & Simanjuntak, Y. M. (2013). Techno-economic analysis of photovoltaic/wind hybrid system for onshore/remote area in Indonesia. Energy, 59, 652-657.

Himri, Y., Boudghene Stambouli, A., Draoui, B., & Himri, S. (2008). Techno-economical study of hybrid power system for a remote village in Algeria. Energy, 33(7), 1128-1136.

Ho, L.-W. (2016). Wind energy in Malaysia: Past, present and future. Renewable and Sustainable Energy Reviews, 53, 279-295.

Hoen, B., Wiser, R., Cappers, P., Thayer, M., & Sethi, G. (2011). Wind energy facilities and residential properties: the effect of proximity and view on sales prices. Journal of Real Estate Research, 33(3), 279-316.

Huang, J., & McElroy, M. B. (2015). A 32-year perspective on the origin of wind energy in a warming climate. Renewable Energy, 77, 482-492.

Hussein, I., & Raman, N. (2010). Reconnaissance studies of micro hydro potential in Malaysia. Proceedings of the International Conference on Energy and Sustainable Development: Issues and Strategies (ESD), 2010, pp. 1-10.

IEA. (2015). International Energy Agency-Trends 2015 in photovoltaic applications, Executive summary. Available at http://www.iea-pvps.org/fileadmin/dam/public/report/national/IEA-PVPS-Trends 2015-Executive Summary-Final.pdf. (Accessed on. 1.10.16).

IEA. (2016). International Energy Agency: Key World Energy Statistics, 2016. Retrieved from https://www.iea.org/publications/freepublications/publication/KeyWorld2016.pdf. (Accessed on 7.10.2016).

Islam, M. R., Saidur, R., & Rahim, N. A. (2011). Assessment of wind energy potentiality at Kudat and Labuan, Malaysia using Weibull distribution function. Energy, 36(2), 985-992.

Ismail, M. S., Moghavvemi, M., & Mahlia, T. M. I. (2013). Techno-economic analysis of an optimized photovoltaic and diesel generator hybrid power system for remote houses in a tropical climate. Energy Conversion and Management, 69, 163-173.

Izadyar, N., Ong, H. C., Chong, W. T., Mojumder, J. C., & Leong, K. (2016). Investigation of potential hybrid renewable energy at various rural areas in Malaysia. Journal of Cleaner Production, 139, 61-73.

Izadyar, N., Ong, H. C., Chong, W. T., Mojumder, J. C., & Leong, K. Y. (2016). Investigation of potential hybrid renewable energy at various rural areas in Malaysia. Journal of Cleaner Production, 139, 61-73.

Jang, J.-S. (1993). ANFIS: adaptive-network-based fuzzy inference system. IEEE transactions on systems, man, and cybernetics, 23(3), 665-685.

Jensen, C. U., Panduro, T. E., & Lundhede, T. H. (2014). The vindication of Don Quixote: The impact of noise and visual pollution from wind turbines. Land Economics, 90(4), 668-682.

Jowder, F. A. (2009). Wind power analysis and site matching of wind turbine generators in Kingdom of Bahrain. Applied Energy, 86(4), 538-545.

Juang, C.-F. (2010). Combination of Particle Swarm and Ant Colony Optimization Algorithms for Fuzzy Systems Design. INTECH Open Access Publisher.

Jung, J., & Broadwater, R. P. (2014). Current status and future advances for wind speed and power forecasting. Renewable and Sustainable Energy Reviews, 31, 762-777.

Justus, C. G. (1978). Winds and wind system performance. Research supported by the National Science Foundation and Energy Research and Development Administration. Philadelphia, Pa., Franklin Institute Press, 1978. p.120.

Karaki, S., Chedid, R., & Ramadan, R. (1999). Probabilistic performance assessment of autonomous solar-wind energy conversion systems. IEEE Transactions on Energy Conversion, 14(3), 766-772.

Kellogg, W., Nehrir, M., Venkataramanan, G., & Gerez, V. (1998). Generation unit sizing and cost analysis for stand-alone wind, photovoltaic, and hybrid wind/PV systems. IEEE Transactions on Energy Conversion, 13(1), 70-75.

Khairul, A. A. A. (2014). Experience in Developing Solar Hybrid System for Rural Electrification in Malaysia. Retrieved from https://energypedia.info/images/a/aa/Solar_Hybrid_System_for_Rural_Electrification_in_Malaysia.pdf. (Accessed on 25.12.2015).

Khan, M. R. B., Jidin, R., Pasupuleti, J., & Shaaya, S. A. (2014, 1-3 Dec. 2014). Micro-hydropower potential assessment and generation volatility due to seasonal climate. IEEE International Conference on Power and Energy (PECon), 2014, pp. 371-376.

Lambert, T., Gilman, P., & Lilienthal, P. (2006). Micropower system modeling with HOMER. Integration of alternative sources of energy, 1(15), 379-418.

Li, Y., He, Y., Su, Y., & Shu, L. (2016). Forecasting the daily power output of a grid-connected photovoltaic system based on multivariate adaptive regression splines. Applied Energy, 180, 392-401.

List of major environmental issues affecting communities in Malaysia. (2012). Retrieved from http://peoplesdocumentary.files.wordpress.com/2012/07/list-of-major-environmental-issues-jpeg.pdf. (Accessed on 25.03.2016).

Mahlia, T. M. I. (2002). Emissions from electricity generation in Malaysia. Renewable Energy, 27(2), 293-300.

Malik, A. Q. (2011). Assessment of the potential of renewables for Brunei Darussalam. Renewable and Sustainable Energy Reviews, 15(1), 427-437.

Manwell, J. F., McGowan, J. G., & Rogers, A. L. (2010). Wind energy explained: theory, design and application: John Wiley & Sons.

Mathew, S. (2006). Wind energy: fundamentals, resource analysis and economics (Vol. 1): Springer.

Mekhilef, S., Safari, A., Mustaffa, W. E. S., Saidur, R., Omar, R., & Younis, M. A. A. (2012). Solar energy in Malaysia: Current state and prospects. Renewable and Sustainable Energy Reviews, 16(1), 386-396.

Mitchell, M. (1998). An introduction to genetic algorithms: MIT Press Cambridge, MA, USA.

Mohamed, M. H. (2016). Reduction of the generated aero-acoustics noise of a vertical axis wind turbine using CFD (Computational Fluid Dynamics) techniques. Energy, 96, 531-544.

Mohammadi, K., Alavi, O., Mostafaeipour, A., Goudarzi, N., & Jalilvand, M. (2016). Assessing different parameters estimation methods of Weibull distribution to compute wind power density. Energy Conversion and Management, 108, 322-335.

Mohammadi, K., & Mostafaeipour, A. (2013). Using different methods for comprehensive study of wind turbine utilization in Zarrineh, Iran. Energy Conversion and Management, 65, 463-470.

Mohammadi, K., Shamshirband, S., Yee, P. L., Petković, D., Zamani, M., & Ch, S. (2015). Predicting the wind power density based upon extreme learning machine. Energy, 86, 232-239.

Muda, A., Omar, C., Ponrahono, Z., Shamsuddin, K., Chung, D., & Gambaris, A. (2011). Tioman as international tourism island: In perspective of planning development, management and guidelines. Contemporary Environmental Quality Management in Malaysia and Selected Countries. UPM Press, Malaysia.

Nandi, S. K., & Ghosh, H. R. (2010). Techno-economical analysis of off-grid hybrid systems at Kutubdia Island, Bangladesh. Energy Policy, 38(2), 976-980.

NASA surface meteorology and solar energy data base. (2016). https://eosweb.larc.nasa.gov/cgi-bin/sse/sse.cgi? (Accessed 12.01.2016).

NEB. (2014). National Energy Balance 2014- Malaysia Energy Information Hub. Retrieved from http://meih.st.gov.my. (Accessed 15.01.2016).

Nehrir, M., Wang, C., Strunz, K., Aki, H., Ramakumar, R., Bing, J., . . . Salameh, Z. (2011). A review of hybrid renewable/alternative energy systems for electric power generation: Configurations, control, and applications. Sustainable Energy, IEEE Transactions on, 2(4), 392-403.

Ngan, M. S., & Tan, C. W. (2012). Assessment of economic viability for PV/wind/diesel hybrid energy system in southern Peninsular Malaysia. Renewable and Sustainable Energy Reviews, 16(1), 634-647.

Nikolić, V., Petković, D., Shamshirband, S., & Ćojbašić, Ž. (2015). Adaptive neuro-fuzzy estimation of diffuser effects on wind turbine performance. Energy, 89, 324-333.

Ohunakin, O., Adaramola, M., & Oyewola, O. (2011). Wind energy evaluation for electricity generation using WECS in seven selected locations in Nigeria. Applied Energy, 88(9), 3197-3206.

Olatomiwa, L. (2016). Optimal Planning and Design of Hybrid Renewable Energy System for Rural Healthcare Facilities. PhD Thesis, University of Malaya, Malaysia.

Olatomiwa, L., Mekhilef, S., Huda, A., & Ohunakin, O. S. (2015). Economic evaluation of hybrid energy systems for rural electrification in six geo-political zones of Nigeria. Renewable Energy, 83, 435-446.

Olatomiwa, L., Mekhilef, S., Huda, A., & Sanusi, K. (2015). Techno-economic analysis of hybrid PV–diesel–battery and PV–wind–diesel–battery power systems for mobile BTS: the way forward for rural development. Energy Science & Engineering, 3(4), 271-285.

Olatomiwa, L., Mekhilef, S., Huda, A. S. N., & Ohunakin, O. S. (2015). Economic evaluation of hybrid energy systems for rural electrification in six geo-political zones of Nigeria. Renewable Energy, 83, 435-446.

Olatomiwa, L., Mekhilef, S., & Ohunakin, O. S. (2016). Hybrid renewable power supply for rural health clinics (RHC) in six geo-political zones of Nigeria. Sustainable Energy Technologies and Assessments, 13, 1-12.

Ould Bilal, B., Sambou, V., Ndiaye, P. A., Kébé, C. M. F., & Ndongo, M. (2010). Optimal design of a hybrid solar–wind-battery system using the minimization of the annualized cost system and the minimization of the loss of power supply probability (LPSP). Renewable Energy, 35(10), 2388-2390.

Park, E., & Kwon, S. J. (2016). Towards a Sustainable Island: Independent optimal renewable power generation systems at Gadeokdo Island in South Korea. Sustainable Cities and Society, 23, 114-118.

Peng, H., Liu, F., & Yang, X. (2013). A hybrid strategy of short term wind power prediction. Renewable Energy, 50, 590-595.

Petković, D. (2015). Adaptive neuro-fuzzy approach for estimation of wind speed distribution. International Journal of Electrical Power & Energy Systems, 73, 389-392.

Petković, D., Pavlović, N. T., & Ćojbašić, Ž. (2016). Wind farm efficiency by adaptive neuro-fuzzy strategy. International Journal of Electrical Power & Energy Systems, 81, 215-221.

Phuangpornpitak, N., & Kumar, S. (2011). User acceptance of diesel/PV hybrid system in an island community. Renewable Energy, 36(1), 125-131.

Pousinho, H. M. I., Mendes, V. M. F., & Catalão, J. P. S. (2011). A hybrid PSO–ANFIS approach for short-term wind power prediction in Portugal. Energy Conversion and Management, 52(1), 397-402.

Qazi, A., Fayaz, H., Wadi, A., Raj, R. G., Rahim, N. A., & Khan, W. A. (2015). The artificial neural network for solar radiation prediction and designing solar systems: a systematic literature review. Journal of Cleaner Production, 104, 1-12.

Rahman, M. M., Khan, M. M.-U.-H., Ullah, M. A., Zhang, X., & Kumar, A. (2016). A hybrid renewable energy system for a North American off-grid community. Energy, 97, 151-160.

Ramadan, H. (2017). Wind energy farm sizing and resource assessment for optimal energy yield in Sinai Peninsula, Egypt. Journal of Cleaner Production, 161, 1283-1293.

Raman, N., Hussein, I., & Palanisamy, K. (2009, 7-8 Dec. 2009). Micro hydro potential in West Malaysia. 3rd IEEE International Conference on Energy and Environment, 2009, pp. 348-359.

Ramasamy, P., Chandel, S. S., & Yadav, A. K. (2015). Wind speed prediction in the mountainous region of India using an artificial neural network model. Renewable Energy, 80, 338-347.

Ramli, M. A. M., Hiendro, A., & Al-Turki, Y. A. (2016). Techno-economic energy analysis of wind/solar hybrid system: Case study for western coastal area of Saudi Arabia. Renewable Energy, 91, 374-385.

Ramli, M. A. M., Hiendro, A., & Twaha, S. (2015). Economic analysis of PV/diesel hybrid system with flywheel energy storage. Renewable Energy, 78, 398-405.

REN21. (2016). Renewables 2015 Global Status Report (978-3-9815934-6-4). Retrieved from http://www.ren21.net/wp-content/uploads/2015/07/REN12-GSR2015_Onlinebook_low1.pdf. (Accessed on 25.05.2016).

RMK11. (2016-2020). Eleven Malaysia Plan (RMK11) 2016-2020. Retrieved from http://www.pmo.gov.my/dokumenattached/RMK/RMK11_E.pdf. (Accessed on 12.07.2016).

Rogers, A. L., Manwell, J. F., & Wright, S. (2006). Wind turbine acoustic noise. Renewable Energy Research Laboratory, Amherst: University of Massachusetts.

Saidur, R., Rahim, N., Ping, H., Jahirul, M., Mekhilef, S., & Masjuki, H. (2009). Energy and emission analysis for industrial motors in Malaysia. Energy Policy, 37(9), 3650-3658.

Shaahid, S. M., Al-Hadhrami, L. M., & Rahman, M. K. (2014). Potential of Establishment of Wind Farms in Western Province of Saudi Arabia. Energy Procedia, 52, 497-505.

Shaahid, S. M., Al-Hadhrami, L. M., & Rahman, M. K. (2014). Review of economic assessment of hybrid photovoltaic-diesel-battery power systems for residential loads for different provinces of Saudi Arabia. Renewable and Sustainable Energy Reviews, 31, 174-181.

Shaahid, S. M., & El-Amin, I. (2009). Techno-economic evaluation of off-grid hybrid photovoltaic–diesel–battery power systems for rural electrification in Saudi Arabia—A way forward for sustainable development. Renewable and Sustainable Energy Reviews, 13(3), 625-633.

Shadmand, M. B., & Balog, R. S. (2014). Multi-objective optimization and design of photovoltaic-wind hybrid system for community smart DC microgrid. IEEE Transactions on Smart Grid, 5(5), 2635-2643.

Shamshirband, S., Keivani, A., Mohammadi, K., Lee, M., Hamid, S. H. A., & Petkovic, D. (2016). Assessing the proficiency of adaptive neuro-fuzzy system to estimate wind power density: Case study of Aligoodarz, Iran. Renewable and Sustainable Energy Reviews, 59, 429-435.

Shezan, S. A., Julai, S., Kibria, M. A., Ullah, K. R., Saidur, R., Chong, W. T., & Akikur, R. K. (2016). Performance analysis of an off-grid wind-PV (photovoltaic)-diesel-battery hybrid energy system feasible for remote areas. Journal of Cleaner Production, 125, 121-132.

Shezan, S. A., Saidur, R., Ullah, K., Hossain, A., Chong, W., & Julai, S. (2015). Feasibility analysis of a hybrid off-grid wind–DG-battery energy system for the eco-tourism remote areas. Clean Technologies and Environmental Policy, 17(8), 2417-2430.

Shoorehdeli, M. A., Teshnehlab, M., Sedigh, A. K., & Khanesar, M. A. (2009). Identification using ANFIS with intelligent hybrid stable learning algorithm approaches and stability analysis of training methods. Applied Soft Computing, 9(2), 833-850.

Simons, P. J., & Cheung, W. M. (2016). Development of a quantitative analysis system for greener and economically sustainable wind farms. Journal of Cleaner Production, 133, 886-898.

Sinha, S., & Chandel, S. S. (2014). Review of software tools for hybrid renewable energy systems. Renewable and Sustainable Energy Reviews, 32, 192-205.

Sinha, S., & Chandel, S. S. (2015a). Prospects of solar photovoltaic–micro-wind based hybrid power systems in western Himalayan state of Himachal Pradesh in India. Energy Conversion and Management, 105, 1340-1351.

Sinha, S., & Chandel, S. S. (2015b). Review of recent trends in optimization techniques for solar photovoltaic–wind based hybrid energy systems. Renewable and Sustainable Energy Reviews, 50, 755-769.

Sopian, K., Othman, M. Y., & Rahman, M. A. A. (2005). Performance of a photovoltaic diesel hybrid system in Malaysia. ISESCO Sci Technol Vision, 1, pp.37-39.

Stocker, T., Qin, D., Plattner, G., Tignor, M., Allen, S., Boschung, J., . . . Midgley, P. (2013). Technical summary for policymakers in climate change 2013: the physical science basis, contribution of working group I to the fifth assessment report of the intergovernmental panel on climate change, pp. 33-115. Cambridge University Press, Cambridge, New York, USA.

Storn, R., & Price, K. (1997). Differential evolution–a simple and efficient heuristic for global optimization over continuous spaces. Journal of global optimization, 11(4), 341-359.

Thakagi, H., & Sugeno, M. (1983). Derivation of control rules from human operator's control action. Proc of the IFAC Sysmp. on Fuzzy Information, Knowledge Representation and Decision Analisis, pp.55-60.

TNBES. (2016). TNB Energy Services. Retrieved from http://tnbes.com.my/achievement-awards/ (Accessed on 20.02.2016).

Uddin, M. S., & Kumar, S. (2014). Energy, emissions and environmental impact analysis of wind turbine using life cycle assessment technique. Journal of Cleaner Production, 69, 153-164.

Wang, C. (2006). Modeling and control of hybrid wind/photovoltaic/fuel cell distributed generation systems. Doctoral dissertation, Montana State University-Bozeman, College of Engineering.

Wang, J., & Yang, F. (2013). Optimal capacity allocation of standalone wind/solar/battery hybrid power system based on improved particle swarm optimisation algorithm. IET Renewable Power Generation, 7(5), 443-448.

Wang, L., & Singh, C. (2009). Multicriteria design of hybrid power generation systems based on a modified particle swarm optimization algorithm. IEEE Transactions on Energy Conversion, 24(1), 163-172.

Xydis, G. (2015). A wind energy integration analysis using wind resource assessment as a decision tool for promoting sustainable energy utilization in agriculture. Journal of Cleaner Production, 96, 476-485.

Zhou, W., Lou, C., Li, Z., Lu, L., & Yang, H. (2010). Current status of research on optimum sizing of stand-alone hybrid solar–wind power generation systems. Applied Energy, 87(2), 380-389.

.

LIST OF PUBLICATIONS AND PAPERS PRESENTED

Journals

1. **Hossain, M.,** Mekhilef, S., & Olatomiwa, L. (2017). Performance evaluation of a stand-alone PV-wind-diesel-battery hybrid system feasible for a large resort center in South China Sea, Malaysia. **Published in "Sustainable Cities and Society"**(Elsevier). ISSN:2210-6707, vol. 28, pp. 358-366, 1// 2017. (ISI cited journal, Tier-2, Impact factor 1.777).

2. Hossain, M., Mekhilef, S., et al., (2017). Application of extreme learning machine for short term output power forecasting of three grid-connected PV systems. **Published in "Journal of Cleaner Production"** (Elsevier). ISSN: 0959-6526, 167, 395-405. (ISI cited journal, Tier-1, Impact factor 5.715).

3. **M. Hossain**, S. Mekhilef, F. Afifi and L.M. Halabi, "Application of the Hybrid ANFIS models for monthly wind power density prediction," **PLOS ONE**, Got minor correction and submitted, currently, under review, ISI cited journal, Tier-1, Impact factor 2.81.

4. **M. Hossain**, S. Mekhilef, and L. Olatomiwa, "Hydro power in Malaysia: Current status and future prospects," **Energy Strategy Reviews** (Elsevier), Under Review, ISI cited journal, Tier-1, Impact factor 1.89.

5. **M. Hossain** and S. Mekhilef, "Techno-economic evaluation of solar hybrid mini grid system for rural electrification in Malaysia". (Final draft stage).

APPENDIX A

Table A. 1: Monthly average solar radiation and the wind speed of the Islands located in the South China Sea surrounding Tioman Island (NASA surface meteorology and solar energy data base, 2016).

Months	Solar radiation (kWh/m^2/day)			Wind speed (m/s) at 50m	
	Pulau Aur, Pemanggil, Sibu, Tinggi, Tioman, Dayang and Pulau Tulai.	Pulau Babi Besar, Harimau, Tengah, Seri Buat and Pulau Sembilang.		Pulau Aur, Pemanggil, Sibu, Tinggi, Tioman, Dayang and Pulau Tulai.	Pulau Babi Besar, Harimau, Tengah, Seri Buat and Pulau Sembilang.
January	4.78	4.12		5.36	4.35
February	5.76	4.97		4.55	3.73
March	5.99	5.02		3.44	2.97
April	6.10	5.08		2.38	1.94
May	5.55	4.84		2.60	2.12
June	5.22	4.66		3.82	3.23
July	5.14	4.61		3.85	3.24
August	5.30	4.70		4.32	3.55
September	5.36	4.83		3.38	2.72
October	5.05	4.70		2.74	2.18
November	4.23	4.05		3.32	2.87
December	4.04	3.62		5.04	4.19

Table A. 2: Monthly average ambient temperature and clearness index of the Islands located in the South China Sea surrounding Tioman Island (NASA surface meteorology and solar energy data base, 2016).

Months	Ambient temperature (°C)			Clearness index	
	Pulau Aur, Pemanggil, Sibu, Tinggi, Tioman, Dayang and Pulau Tulai.	Pulau Babi Besar, Harimau, Tengah, Seri Buat, and Pulau Sembilang.		Pulau Aur, Pemanggil, Sibu, Tinggi, Tioman, Dayang and Pulau Tulai	Pulau Babi Besar, Harimau, Tengah, Seri Buat and Pulau Sembilang.
January	25.83	25.49		0.49	0.42
February	25.84	25.70		0.56	0.49
March	26.24	26.11		0.57	0.48
April	26.84	26.51		0.59	0.49
May	27.18	26.61		0.56	0.49
June	27.13	26.34		0.55	0.49
July	26.90	26.03		0.53	0.48
August	26.83	26.04		0.53	0.47
September	26.75	26.07		0.52	0.47
October	26.75	26.29		0.49	0.46
November	26.52	26.12		0.43	0.41
December	26.15	25.74		0.42	0.38

APPENDIX B

Table B. 1: Monthly average wind speed, Weibull parameters and measured wind power density for Mersing.

		Jan	Feb	Mar	Apr	May	Jun	July	Aug	Sep	Oct	Nov	Dec
2004	V (m/s)	6.05	5.27	3.34	2.23	2.15	3.18	2.60	3.23	2.72	2.57	3.32	5.31
	k	4.52	3.45	1.62	7.98	6.11	4.77	7.34	6.47	5.68	4.66	3.13	3.14
	c	6.63	5.87	3.73	2.36	2.32	3.48	2.77	3.47	2.94	2.81	3.71	5.93
	P/A (W/m²)	152.85	111.71	60.26	6.85	6.44	21.98	11.03	21.57	13.13	11.63	29.65	120.64
2005	V (m/s)	5.88	4.52	4.47	3.14	2.87	2.94	2.79	3.19	3.13	2.93	2.69	3.13
	k	3.66	3.93	2.38	8.15	8.30	6.10	5.48	10.17	7.28	8.38	5.45	4.65
	c	6.52	4.99	5.05	3.33	3.04	3.16	3.02	3.35	3.34	3.10	2.92	3.43
	P/A (W/m²)	151.04	66.96	85.54	19.28	14.65	16.38	14.22	19.79	19.39	15.56	12.98	21.22
2006	V (m/s)	4.84	5.34	3.34	2.72	2.90	2.93	3.30	3.35	3.17	2.84	2.80	4.44
	k	3.18	3.57	3.64	11.81	8.30	6.69	8.63	6.46	8.51	8.51	10.55	2.70
	c	5.41	5.93	3.70	2.84	3.07	3.14	3.49	3.59	3.36	3.00	2.93	4.99
	P/A (W/m²)	91.32	114.40	27.40	12.20	15.04	16.00	22.24	24.00	19.69	14.11	13.29	78.06
2007	V (m/s)	5.03	4.46	3.30	3.03	3.03	2.87	2.89	3.18	2.98	2.81	2.96	4.61
	k	2.89	3.75	4.86	5.30	7.69	9.65	5.29	7.70	7.90	5.34	2.85	3.21
	c	5.64	4.94	3.60	3.29	3.23	3.02	3.14	3.38	3.16	3.04	3.33	5.15
	P/A (W/m²)	106.22	65.78	24.44	18.82	17.41	14.41	16.11	20.07	16.43	14.76	23.57	78.06
2008	V (m/s)	5.02	5.23	4.27	2.96	3.28	3.20	3.28	3.39	3.09	2.81	2.93	4.66
	k	5.51	3.59	3.07	6.58	4.81	7.62	4.71	5.65	5.57	9.59	6.91	3.79
	c	5.44	5.80	4.78	3.17	3.58	3.41	3.59	3.66	3.35	2.96	3.14	5.15
	P/A (W/m²)	83.21	106.16	63.99	16.45	24.12	20.58	24.35	25.57	19.49	13.62	16.00	74.55
2009	V (m/s)	5.98	4.31	3.02	3.13	3.04	3.31	3.36	3.36	3.22	3.00	3.46	4.43
	k	4.99	4.46	7.81	7.56	6.09	8.08	6.80	5.89	7.89	6.95	4.33	3.72
	c	6.52	4.73	3.21	3.34	3.27	3.51	3.59	3.63	3.42	3.21	3.80	4.90
	P/A (W/m²)	144.06	55.74	17.15	19.29	18.12	22.52	24.07	24.73	20.79	17.12	29.17	64.70
2010	V (m/s)	4.74	4.42	4.17	3.11	2.92	2.87	2.69	3.05	2.86	2.62	2.59	3.41
	k	3.41	5.14	4.57	7.00	7.63	7.47	9.44	7.04	7.82	5.82	6.42	4.42
	c	5.27	4.80	4.56	3.32	3.11	3.06	2.83	3.26	3.04	2.83	2.78	3.74
	P/A (W/m²)	80.95	57.59	50.39	18.95	15.59	14.81	11.92	17.96	14.58	11.77	11.14	27.67
2011	V (m/s)	5.17	4.82	3.23	3.37	2.77	3.07	3.55	3.50	3.27	2.97	3.20	4.82
	k	4.17	4.93	6.02	5.18	8.96	6.03	7.26	4.70	5.94	6.12	4.75	2.39
	c	5.69	5.25	3.48	3.66	2.92	3.30	3.79	3.83	3.53	3.20	3.49	5.44
	P/A (W/m²)	98.51	75.89	21.76	25.55	12.99	18.68	28.11	29.43	22.90	17.08	22.34	107.80
2012	V (m/s)	4.80	4.32	3.16	2.81	2.72	3.35	3.06	3.96	3.02	2.86	2.70	3.21
	k	3.12	4.08	4.79	9.63	7.60	6.93	4.57	5.45	6.15	10.62	8.75	6.52
	c	5.37	4.76	3.45	2.96	2.89	3.58	3.35	4.29	3.25	3.00	2.85	3.45
	P/A (W/m²)	88.44	57.82	21.68	13.55	12.54	23.69	20.01	41.02	17.86	14.23	12.08	21.19
2013	V (m/s)	4.88	4.47	3.95	2.77	2.80	2.74	2.87	3.24	2.81	2.92	3.02	4.49
	k	6.15	4.07	3.71	7.34	10.26	8.99	6.19	5.41	5.73	7.53	5.31	3.46
	c	5.25	4.93	4.38	2.96	2.94	2.89	3.09	3.51	3.04	3.11	3.28	5.00
	P/A (W/m²)	74.91	64.15	46.64	13.38	13.30	12.65	15.24	22.50	14.55	15.67	18.45	69.58
2014	V (m/s)	5.88	5.08	4.30	2.96	2.87	3.07	3.02	2.97	3.28	3.04	2.99	3.58
	k	5.21	5.70	6.54	9.69	7.53	7.54	7.18	6.72	6.58	7.66	8.08	3.39
	c	6.39	5.49	4.62	3.12	3.05	3.26	3.22	3.18	3.52	3.24	3.18	3.98
	P/A (W/m²)	134.41	85.46	50.87	15.90	14.78	18.07	17.34	16.78	22.69	17.64	16.68	35.28

Table B. 2: Monthly average wind speed, Weibull parameters and measured wind power density for Kuala Terengganu.

		Jan	Feb	Mar	Apr	May	Jun	July	Aug	Sep	Oct	Nov	Dec
2004	V (m/s)	3.90	2.83	2.93	2.41	2.33	1.90	2.15	1.89	2.15	2.55	2.44	3.95
	k	3.09	3.52	1.94	8.46	6.38	3.80	4.99	5.41	5.72	2.92	3.32	2.10
	c	4.36	3.15	3.30	2.56	2.50	2.11	2.34	2.05	2.32	2.86	2.72	4.46
	P/A (W/m²)	47.67	16.61	31.88	8.64	8.11	5.06	6.65	4.49	6.51	14.29	11.40	67.66
2005	V (m/s)	3.10	2.52	2.90	2.36	2.26	2.14	2.25	2.27	2.35	2.09	2.50	3.03
	k	2.54	3.80	2.35	8.71	7.16	7.26	6.46	8.28	8.92	4.48	1.67	2.04
	c	3.50	2.78	3.28	2.49	2.42	2.29	2.42	2.41	2.48	2.29	2.79	3.42
	P/A (W/m²)	28.12	11.53	25.37	8.03	7.34	6.20	7.32	7.32	8.03	6.32	24.60	32.78
2006	V (m/s)	3.47	4.12	2.55	2.42	2.36	2.37	1.84	2.33	2.38	2.16	2.11	3.85
	k	2.37	2.88	8.53	10.50	7.01	9.52	3.46	8.80	12.78	6.84	7.12	1.70
	c	3.92	4.62	2.70	2.54	2.53	2.49	2.05	2.46	2.48	2.31	2.25	4.32
	P/A (W/m²)	42.08	58.46	10.36	8.68	8.36	8.17	4.63	7.84	8.16	6.45	5.97	78.45
2007	V (m/s)	4.50	3.28	2.58	2.52	2.39	2.40	2.14	2.38	2.42	2.24	2.60	4.02
	k	2.84	3.53	5.60	7.25	7.79	6.41	7.06	8.04	5.95	5.40	3.08	2.19
	c	5.05	3.64	2.79	2.68	2.54	2.58	2.28	2.53	2.61	2.43	2.91	4.54
	P/A (W/m²)	78.32	25.66	11.39	10.06	8.50	8.90	6.17	8.42	9.24	7.47	15.06	64.95
2008	V (m/s)	3.25	3.39	3.25	2.35	2.13	2.32	2.29	2.41	2.34	2.34	2.19	3.20
	k	3.48	2.86	4.07	7.73	4.77	9.74	7.94	8.29	7.70	7.81	5.30	2.80
	c	3.62	3.81	3.58	2.50	2.33	2.44	2.43	2.56	2.49	2.48	2.38	3.59
	P/A (W/m²)	26.80	33.84	24.85	7.99	6.55	7.64	7.52	8.73	8.07	7.98	7.10	29.04
2009	V (m/s)	3.46	2.58	2.55	2.30	2.44	2.49	2.47	2.59	2.18	2.20	2.71	3.67
	k	2.26	5.34	5.84	6.30	7.40	11.14	6.17	7.93	5.92	8.63	2.63	2.97
	c	3.90	2.80	2.76	2.48	2.60	2.60	2.65	2.76	2.35	2.33	3.05	4.11
	P/A (W/m²)	42.54	10.85	10.95	7.88	9.21	9.36	9.68	10.93	6.72	6.62	18.55	40.92
2010	V (m/s)	3.01	2.84	2.94	2.56	2.59	2.61	2.49	2.54	2.52	2.82	2.74	3.29
	k	3.17	4.41	5.35	6.84	10.07	9.83	7.71	6.89	8.10	2.41	3.90	3.54
	c	3.37	3.11	3.19	2.74	2.72	2.75	2.65	2.71	2.67	3.18	3.02	3.66
	P/A (W/m²)	22.23	15.60	17.11	10.67	10.63	10.94	9.70	10.37	9.93	23.85	15.34	27.27
2011	V (m/s)	4.32	3.16	3.07	2.80	2.58	2.53	2.64	2.70	2.52	2.38	3.01	4.41
	k	2.90	3.64	3.52	7.55	7.50	7.26	7.74	8.72	6.94	5.87	2.57	2.76
	c	4.85	3.50	3.41	2.98	2.75	2.70	2.81	2.85	2.69	2.57	3.39	4.96
	P/A (W/m²)	68.58	22.75	22.55	13.81	10.73	10.23	11.51	12.13	10.09	8.80	25.66	74.65
2012	V (m/s)	3.79	3.05	2.55	2.62	2.61	2.36	2.41	2.48	2.48	2.51	2.30	3.17
	k	2.65	3.72	6.83	7.36	7.28	7.23	7.85	9.03	8.23	7.86	6.59	2.55
	c	4.27	3.37	2.73	2.80	2.79	2.52	2.56	2.62	2.63	2.67	2.47	3.58
	P/A (W/m²)	49.69	20.30	10.50	11.43	11.27	8.40	8.79	9.39	9.50	9.89	7.80	30.91
2013	V (m/s)	3.39	3.83	2.79	2.65	2.68	2.40	2.41	2.52	2.56	2.76	2.73	4.20
	k	3.62	3.37	5.62	8.80	8.72	3.88	5.13	6.19	6.85	5.89	2.94	2.74
	c	3.76	4.27	3.01	2.80	2.84	2.65	2.62	2.72	2.74	2.98	3.06	4.72
	P/A (W/m²)	29.63	42.30	14.42	11.50	11.95	10.19	9.34	10.37	10.66	13.86	18.25	65.10
2014	V (m/s)	4.05	2.92	2.92	2.86	2.78	2.59	2.39	2.54	2.52	2.48	2.50	4.30
	k	3.10	4.53	4.91	16.18	8.55	6.87	6.61	9.35	8.21	7.09	6.42	2.00
	c	4.53	3.20	3.18	2.95	2.94	2.78	2.56	2.68	2.68	2.65	2.68	4.86
	P/A (W/m²)	55.91	16.40	17.29	13.91	13.35	11.10	8.67	10.10	10.06	9.66	10.04	90.35

Table B. 3: Monthly average wind speed, Weibull parameters and measured wind power density for Pulau Langkawi.

		Jan	Feb	Mar	Apr	May	Jun	July	Aug	Sep	Oct	Nov	Dec
2004	V (m/s)	5.35	4.19	3.81	2.97	2.88	3.43	3.06	3.65	2.56	3.09	3.45	4.66
	k	4.69	3.26	3.93	8.65	6.03	2.67	1.81	2.22	4.85	2.26	4.80	4.03
	c	5.85	4.68	4.21	3.14	3.11	3.86	3.45	4.12	2.80	3.49	3.77	5.14
	P/A (W/m^2)	104.50	55.83	41.28	15.93	15.61	37.50	42.11	51.68	11.23	31.29	28.29	72.13
2005	V (m/s)	4.81	4.40	4.66	2.59	2.32	2.24	2.20	2.39	2.56	2.06	2.13	2.84
	k	3.93	3.89	3.45	4.74	5.20	7.36	5.47	4.93	2.88	4.43	3.25	3.03
	c	5.32	4.87	5.18	2.83	2.52	2.38	2.39	2.61	2.87	2.26	2.38	3.18
	P/A (W/m^2)	80.93	60.09	78.22	11.05	8.47	7.09	7.18	9.48	15.05	6.13	7.83	19.02
2006	V (m/s)	3.23	4.13	2.35	2.18	2.15	2.25	2.18	2.70	2.49	2.37	2.42	3.33
	k	2.68	3.95	2.54	7.42	7.06	6.85	6.24	2.73	3.86	4.20	6.54	3.64
	c	3.63	4.56	2.65	2.32	2.30	2.41	2.34	3.03	2.75	2.60	2.60	3.70
	P/A (W/m^2)	30.38	48.76	11.53	6.47	6.36	7.35	6.76	17.93	11.73	9.73	9.12	27.78
2007	V (m/s)	3.64	3.43	2.55	2.29	2.19	2.09	1.93	2.19	2.15	2.25	2.29	3.48
	k	3.40	3.31	5.38	5.21	5.11	6.49	8.05	4.14	2.50	3.16	2.58	3.00
	c	4.05	3.82	2.76	2.49	2.38	2.24	2.05	2.42	2.42	2.51	2.58	3.89
	P/A (W/m^2)	36.95	30.64	11.13	8.15	7.11	5.88	4.49	7.72	9.66	9.72	11.95	34.54
2008	V (m/s)	3.49	3.69	2.77	2.29	2.03	2.12	2.05	2.18	2.32	2.18	2.59	3.41
	k	4.03	3.70	3.71	7.40	8.17	4.72	6.41	8.82	3.77	6.40	3.59	3.64
	c	3.85	4.09	3.07	2.44	2.15	2.32	2.20	2.30	2.57	2.34	2.87	3.78
	P/A (W/m^2)	30.51	35.83	16.04	7.46	5.21	6.77	5.55	6.39	9.49	6.71	13.32	29.63
2009	V (m/s)	4.16	2.94	2.39	2.36	1.93	2.19	2.32	3.05	2.50	2.22	2.41	3.89
	k	5.59	4.03	5.17	4.39	6.67	4.86	3.76	2.30	2.44	3.94	5.57	5.45
	c	4.51	3.24	2.60	2.59	2.07	2.39	2.57	3.44	2.81	2.45	2.61	4.22
	P/A (W/m^2)	47.48	17.46	9.24	9.36	4.64	7.31	9.54	28.99	16.03	8.07	9.35	39.11
2010	V (m/s)	3.49	3.55	3.08	2.38	2.09	2.33	2.28	2.22	2.08	2.34	2.25	2.62
	k	3.91	3.92	3.84	7.40	10.10	3.29	3.98	4.82	8.70	3.82	7.18	4.05
	c	3.86	3.92	3.41	2.54	2.20	2.59	2.51	2.43	2.20	2.59	2.40	2.89
	P/A (W/m^2)	31.03	31.55	22.06	8.37	5.62	10.43	8.84	7.68	5.57	9.64	7.23	13.08
2011	V (m/s)	3.63	3.23	2.74	2.54	2.03	2.06	2.12	2.33	2.26	2.45	2.93	3.77
	k	3.39	3.99	4.60	5.73	9.64	8.31	7.57	6.08	3.02	4.37	2.63	4.24
	c	4.04	3.56	3.00	2.74	2.14	2.19	2.25	2.51	2.53	2.68	3.30	4.15
	P/A (W/m^2)	36.99	23.73	14.23	10.77	5.18	5.47	5.97	8.30	10.23	10.45	23.36	37.90
2012	V (m/s)	3.09	2.99	2.31	2.17	2.49	2.70	2.31	2.29	2.45	2.23	2.02	3.07
	k	3.77	3.93	8.48	9.11	5.08	2.61	5.34	6.36	4.08	6.98	8.35	3.23
	c	3.42	3.31	2.44	2.29	2.71	3.04	2.50	2.46	2.70	2.38	2.14	3.42
	P/A (W/m^2)	21.93	19.16	7.62	6.30	10.43	19.38	8.24	7.75	10.79	7.09	5.11	23.09
2013	V (m/s)	3.26	3.41	2.69	2.17	2.03	2.30	1.90	1.99	2.23	2.14	2.56	3.44
	k	3.74	3.78	3.57	4.14	5.58	3.37	3.86	5.36	4.21	3.68	3.05	4.66
	c	3.61	3.78	2.98	2.39	2.20	2.56	2.11	2.16	2.45	2.37	2.87	3.76
	P/A (W/m^2)	25.70	28.45	15.09	7.41	5.55	9.66	5.16	5.32	8.06	7.51	14.47	27.98
2014	V (m/s)	4.00	3.26	3.41	2.04	1.85	1.97	2.07	1.93	1.99	1.72	2.04	2.78
	k	4.55	3.21	3.69	6.09	5.56	4.46	3.80	5.78	3.01	3.38	2.94	2.96
	c	4.38	3.64	3.78	2.20	2.00	2.16	2.11	2.09	2.23	1.91	2.29	3.12
	P/A (W/m^2)	44.17	26.74	29.90	5.16	4.16	5.43	6.80	4.72	6.84	4.07	7.34	17.77

Table B. 4: Monthly average wind speed, Weibull parameters and measured wind power density for Bayan Lepas.

		Jan	Feb	Mar	Apr	May	Jun	July	Aug	Sep	Oct	Nov	Dec
2004	V (m/s)	3.67	3.28	2.94	2.89	2.55	2.67	2.41	2.62	3.20	2.58	3.26	4.17
	k	3.78	3.50	4.22	9.27	6.12	3.43	3.96	2.78	5.25	4.18	4.44	5.97
	c	4.06	3.64	3.23	3.05	2.75	2.97	2.66	2.94	3.48	2.83	3.57	4.49
	P/A (W/m^2)	37.48	26.43	18.32	14.90	10.75	15.04	10.13	16.00	22.19	12.15	24.57	47.14
2005	V (m/s)	4.17	3.60	3.72	3.07	2.65	3.27	2.92	2.86	3.13	2.93	2.73	3.26
	k	3.18	4.72	5.06	5.84	5.77	3.10	5.03	4.03	3.01	4.95	4.71	2.97
	c	4.66	3.93	4.05	3.32	2.86	3.66	3.18	3.15	3.51	3.19	2.98	3.65
	P/A (W/m^2)	58.98	30.43	34.79	18.84	12.23	29.96	17.02	17.11	26.72	16.98	14.13	29.20
2006	V (m/s)	3.71	4.06	3.19	2.94	2.55	2.81	2.82	2.54	2.54	2.84	2.78	4.40
	k	3.52	4.06	6.36	6.67	6.13	3.84	3.87	3.24	3.91	6.13	7.28	2.70
	c	4.12	4.47	3.42	3.15	2.74	3.11	3.12	2.83	2.81	3.06	2.97	4.94
	P/A (W/m^2)	39.31	46.76	20.83	16.26	10.70	16.74	16.53	13.44	12.08	14.92	13.60	75.16
2007	V (m/s)	4.21	3.91	2.91	2.89	3.09	2.67	2.67	2.83	2.77	2.51	2.85	3.59
	k	3.21	3.90	6.94	6.49	3.37	5.32	5.21	3.23	4.40	6.98	3.58	2.95
	c	4.70	4.32	3.12	3.10	3.44	2.90	2.90	3.16	3.04	2.68	3.16	4.02
	P/A (W/m^2)	59.66	42.19	15.71	15.57	23.72	12.70	12.81	18.59	15.03	10.00	17.99	39.33
2008	V (m/s)	3.43	3.58	3.01	2.90	2.38	2.44	3.02	2.85	2.58	2.47	2.77	4.04
	k	5.20	5.13	6.98	9.38	4.16	4.01	3.75	4.30	5.85	6.07	4.83	3.55
	c	3.73	3.89	3.22	3.05	2.62	2.69	3.34	3.14	2.79	2.66	3.02	4.49
	P/A (W/m^2)	27.18	29.63	17.41	14.97	9.74	10.55	20.39	16.69	11.30	9.80	14.74	50.85
2009	V (m/s)	4.66	3.20	2.87	2.66	2.30	2.43	2.90	2.60	2.48	2.41	3.09	3.65
	k	3.47	4.17	5.74	4.90	5.91	3.48	3.87	5.25	4.31	4.94	4.61	4.09
	c	5.18	3.52	3.10	2.90	2.48	2.70	3.21	2.82	2.73	2.63	3.38	4.02
	P/A (W/m^2)	78.31	21.75	15.51	12.82	7.97	11.54	18.12	11.70	11.04	9.54	20.66	35.11
2010	V (m/s)	3.49	3.55	3.43	2.88	2.48	2.54	2.73	2.95	2.70	2.72	2.78	2.75
	k	4.24	5.24	5.39	5.57	6.85	5.84	6.14	3.83	7.21	2.74	5.08	2.97
	c	3.84	3.86	3.72	3.11	2.66	2.75	2.94	3.26	2.88	3.06	3.02	3.09
	P/A (W/m^2)	30.15	28.77	27.10	15.68	9.73	10.82	13.27	19.01	12.40	18.28	14.51	17.65
2011	V (m/s)	3.47	3.38	2.69	2.77	2.12	2.64	2.94	2.90	2.35	2.25	2.63	3.60
	k	3.86	4.15	4.07	4.95	4.30	3.00	3.35	3.13	3.92	5.68	3.11	3.30
	c	3.83	3.72	2.96	3.02	2.33	2.96	3.28	3.24	2.60	2.43	2.94	4.01
	P/A (W/m^2)	31.21	26.70	14.05	14.55	6.66	15.67	20.12	20.21	9.49	7.47	14.77	36.71
2012	V (m/s)	3.39	3.02	2.43	2.54	2.22	2.54	3.11	3.09	2.63	2.58	2.58	3.40
	k	2.54	5.37	5.01	5.01	3.58	4.08	3.87	4.85	5.04	4.95	7.67	4.07
	c	3.82	3.28	2.65	2.76	2.47	2.80	3.44	3.37	2.86	2.81	2.75	3.75
	P/A (W/m^2)	35.94	17.58	9.73	11.07	8.23	11.92	22.34	20.25	12.33	11.65	10.86	28.84
2013	V (m/s)	3.45	3.56	3.27	2.64	2.91	2.46	2.46	2.88	2.60	2.52	2.88	4.13
	k	3.76	4.45	5.85	5.77	2.73	4.98	5.33	5.06	6.26	4.90	5.62	3.28
	c	3.82	3.90	3.53	2.85	3.27	2.68	2.67	3.13	2.80	2.75	3.11	4.60
	P/A (W/m^2)	31.11	30.34	22.96	12.00	23.45	10.05	9.92	16.15	11.43	10.91	15.82	55.92
2014	V (m/s)	4.80	3.82	3.71	2.90	2.76	3.04	2.57	2.86	2.91	3.11	3.06	3.34
	k	4.53	4.88	7.70	5.69	6.40	3.71	6.28	4.34	7.14	6.70	5.44	3.72
	c	5.26	4.17	3.95	3.13	2.96	3.36	2.76	3.14	3.11	3.34	3.32	3.70
	P/A (W/m^2)	77.24	35.92	32.10	15.86	13.52	21.25	10.92	16.55	15.69	19.35	19.17	28.03